IMPORTANCE OF PEPT1 IN THE ABSORPTION, TISSUE DISTRIBUTION AND DISPOSITION OF CEFADROXIL

By

María Mercedes Posada Henao

A dissertation submitted in partial fulfillment
of the requirements for the degree of
Doctor of Philosophy
(Pharmaceutical Sciences)
in the University of Michigan
2012

Doctoral Committee:

Professor David E. Smith, Chair
Professor Gordon Amidon
Professor Richard Keep
Associate Professor Duxin Sun

DEDICATION

To my parents with all my love

ACKNOWLEDGEMENTS

I would like to start by expressing my deepest gratitude to my research advisor Dr. David E. Smith for his full support and endless teaching. I am extremely grateful to him for the great personal, career, and scientific advice throughout the last 5 years.

Secondly, I would like to thank the members of my thesis committee, Dr. Gordon Amidon, Dr. Richard Keep, and Dr. Duxin Sun for their time and the enthusing scientific discussions throughout my doctoral studies.

Also, I could not be more grateful to Dr. Gus Rosania for giving me the opportunity to come to Michigan and believing in me. I am extremely grateful for his guidance and encouragement over the past seven and a half years, and especially for teaching me the importance of hard work and endurance.

I would like to express my appreciation to Dr. Mike Bolger, for his guidance with the absorption model and for all his help with my thesis. I would also like to thank Dr. Rose Feng for giving me an insight into clinical pharmacology, and the opportunity of working in a very enriching side project.

I would like thank to all the members of the Smith lab and previous Upjohn center, including Xiaomei Chen, Sheryl Flanagan, Yongjun Hu, Yeamin Huh, Dilara

Jappar, Ke Ma, Mohamed Kamal, Leslie Parsels, Josh Parsels, Shupei Wu, and Bei Yang who were always ready to help and share their knowledge with me.

I am also very grateful to all the professors and staff at the University of Michigan College of Pharmacy including Dean Frank Ascione, Gail Benninghoff, Pam Dombrowski, Cherie Dotson, Susan Fitzpatrick, Jeanne Getty, Pat Greely, Maria Herbel, L.D. Hieber, Antoinette Hoper, Mark Nelson, Peter Niedbala, Jenn Rohl, Pennie Rutan, Steven Schwendeman, and Pam Taylor for contributing in many ways to this amazing experience and making my day-to-day life at Michigan so much easier.

Also, I would like to convey my deepest appreciation to all my Michigan friends for their amazing companionship and support. I would like to specially say thank you to Chasity Andrews, Jamie Connarn, Amy Doty, Randall Hicks, Maya Lipert, Deanna Muddie, Theresa Nguyen, Vivien Nielsen, Emily Rabinsky, Sam Reinhold, Lilly Roy, Carlos Sierra, Kathleen Stringer, Ulrika Tehler, and Xinyuan Zhang. Sharing my time with you in Ann Arbor has been a wonderful experience that will always be imprinted in my heart.

I would also like to say thank you to Daniel Bueno, Ana Celis, Sandra Camacho, Diana Cardenas, Marta Fontanilla, Alejandro Gomez, Marianne Lauschus, Daniel Matiz, Miguel Morales, Juliana Postarini and Paulina Restrepo who despite the distance, have always been there to support me.

Finally, I would like to thank my parents, Carlos Esteban Posada and Marta Luz Henao, for their unconditional love, guidance, and encouragement.

TABLE OF CONTENTS

LIST OF FIGURES

LIST OF TABLES

ABREVIATIONS

ACAT model: Advanced compartmental absorption and transit model.

AIC : Akaike Information Criterion

ADME: Absorption, distribution, metabolism and excretion.

AUC: Area under the plasma concentration-time curve.

CEF: Cefadroxil

CL: Total clearance

C_{in}: Concentration of cefadroxil coming into the perfused segment.

C_{max}: Maximum concentration in plasma

C_{out}: Water flux-corrected concentration of cefadroxil coming out of the perfused segment.

C_w: Concentration at the intestinal wall

D: Diffusion coefficient

F: Fraction absorbed

GI tract: Gastrointestinal tract

Gly-Pro: Glycylproline

Gly-Sar: Glycylsarcosine

K_a: Absorption rate constant

K_{12}, K_{21}: Micro-rate constants of distribution

K_m: Michaelis-Menten constant

M&S: Modeling and simulation

MRP: Multidrug resistance associated protein

MRT: Mean residence time

NMN: n-Methyl nicotinamide

OCT: Organic cation transporter

OAT: Organic anion transporter

OATP2B1: Organic anion transporting polypeptide

P_{aq}: Aqueous permeability of cefadroxil

PBPK: Physiologically-based pharmacokinetic model

P_{eff}: Effective permeability

P-gp: P-glycoprotein

PHT1/2: peptide histidine transporters 1 and 2

PK: Pharmacokinetics

PEPT1: Peptide transporter 1

PEPT2: Peptide transporter 2

POT: Proton-coupled oligopeptide transporter

P_w: Permeability at the intestinal wall

T_{max}: Time at which the maximum concentration is observed

V_c: Volume of distribution in the central compartment

Vd_{ss}: Volume of distribution steady state

V_p: Volume of distribution in the peripheral compartment

V_{max}: Maximal uptake rate

ABSTRACT

Although PEPT1 is the most important pathway in the absorption of di- and tri-peptides in the small intestine, its *in vivo* relevance in the absorption, tissue distribution, and disposition of pharmacologically active compounds is still not well understood. Hence, we decided to study the role of PEPT1 in the following: 1) the intestinal permeability of cefadroxil, 2) the *in vivo* pharmacokinetics of cefadroxil, and finally 3) the *in silico* absorption and pharmacokinetics of cefadroxil using the advanced compartmental absorption and transit (ACAT) model built into Gastroplus®. Cefadroxil was chosen as a model drug to study PEPT1 because of its good metabolic stability and commercial availability as a radiolabeled compound. The findings show that PEPT1 was responsible for 90% of the effective permeability (P_{eff}) of cefadroxil. PEPT1 transport of cefadroxil in the jejunum of wild-type mice had a K_m of 3.8 mM and a V_{max} of 4.75 nmol/cm^2/s. Also, the P_{eff} in the duodenum, jejunum, and ileum were significantly higher in wild-type than in PEPT1 knockout mice, but not in colon where the P_{eff} was very low in both genotypes. After oral administration, the C_{max} and $AUC_{0\text{-}120}$ across all doses were lower in knockout mice than in wild-type animals. There was also an "apparent" linearity in the C_{max} and $AUC_{0\text{-}120}$ for both genotypes. However, the analysis of the intravenous data showed no difference in disposition between genotypes. The third specific aim was an effort to integrate the experimental results and to retrospectively model the absorption and pharmacokinetics of cefadroxil using an ACAT model. In the knockout mice, a good prediction of plasma concentration-time profiles was obtained for all doses

studied. In the wild-type mice, the plasma concentration-time profiles for the lower doses were reproduced. The model predicts saturation of the intestinal PEPT1 at higher concentrations in wild-type mice that was not seen experimentally, probably due to a simultaneous saturation of the active tubular secretion and reabsorption, resulting in an apparent linearity of the plasma concentration-time profiles as a function of dose. A physiologically-based pharmacokinetic model will need to be developed to take into account the saturation in cefadroxil renal clearance.

CHAPTER 1

INTRODUCTION AND RESEARCH OBJECTIVES

Proton-coupled oligopeptide transporters, also known as peptide transporters, are a family of membrane transport proteins present in a broad range of species, from bacteria to mammals. These proteins transport di- and tri-peptides—themselves products of protein degradation—and other peptide-like molecules across different membranes in the body. These transporters are usually located in the brush border membrane (apical side) of epithelial cells. They co-transport peptides and protons into the cell cytosol, down an inwardly-directed proton gradient and negative membrane potential.

Proton-coupled oligopeptide transporters have been found in many species. In humans four types have been cloned and identified: PEPT1, PEPT2, PHT1 and PHT2. The first two, PEPT1 and PEPT2, can transport di- and tri-peptides with different sequences and charges, but not single amino acids or peptides longer than 4 amino acid residues. The last two, PHT1 and PHT2, can transport histidine, along with some di- and tri-peptides.

PEPT1 is a high-capacity and low-affinity transporter, expressed predominantly in the small intestine, and to a lesser extent in the kidney, pancreas, and liver. PEPT2 is a high-affinity and low-capacity transporter expressed in the kidney, mammary gland epithelium, brain and choroid plexus, lungs, and enteric nervous system, but not in the intestinal epithelium.

Understanding the importance of PEPT1 contribution to the absorption, tissue distribution, and/or disposition of peptides and peptide–like drugs has been a goal of several research groups for the past 30 years. This transporter has been shown to be relevant in the *in vitro* uptake of di- and tri-peptides and certain peptide-like drugs, such as beta-lactam antibiotics, angiotensin-converting enzyme and renin inhibitors, and some anticancer drugs like bestatin. It also has been shown to be relevant in the absorption of di-peptides, such as Gly-Sar, though to date nobody has actually shown its relevance and contribution to the *in vivo* and *in situ* absorption, tissue distribution and disposition of pharmacologically relevant molecules.

When it comes to studying drug transport, Caco-2 cells are convenient, inexpensive, and ideal for screening and preliminary experiments. It is widely known that experimental results obtained with these cells do not always correlate with human ones due to the over or lack of expression of several transport proteins in these cells. On the other hand, *ex vivo* experiments give results that are closer to natural conditions, but still lack the intact blood and nerve supply. Finally, *in situ* and *in vivo* experiments require the most time and resources, but they best

resemble the real anatomical and physiological conditions, giving more precise results.

For drug delivery, peptide transporters, especially PEPT1, have been of great interest to researchers and pharmaceutical companies because of their broad substrate specificity. Recent research activities have applied pro-drug strategies to target this transporter to improve drug bioavailability after oral dosing. One example is L-Dopa-L-Phe, a prodrug of L-Dopa, which is effectively absorbed in the small intestine, and is used in the treatment of Parkinson's disease.

In the proposed study, cefadroxil has been chosen as a model drug to investigate the role of PEPT1 in drug absorption because it has several advantages. For example, it has been shown to be a substrate for PEPT1. Also, since this antibiotic is very stable, quantification strategies are less demanding. Cefadroxil is excreted unchanged in the urine; it is not hydrolyzed in the acidic environment of the stomach or degraded by intra- or extracellular enzymes. Moreover, cefadroxil is commercially available as a radiolabeled compound, allowing its detection and quantification in very small quantities of blood, body fluids, tissues and organs.

Due to its chemical structure and its high steric resemblance to physiological occurring tri-peptides, cefadroxil has a high affinity for PEPT1, allowing us to hypothesize that its absorption will be affected by the deletion of this protein. Different from other di- and tri-peptides previously used in PEPT1 research (e.g. Gly-Sar), cefadroxil is pharmaceutically relevant, since it has been widely used to treat several bacterial infections in the skin, urinary tract, and upper respiratory airways.

In order to better comprehend the transporter's contribution to the absorption, distribution and disposition of cefadroxil, it is necessary to compare the drug's behavior in systems where the transporter is present to those where the transporter is not. In our laboratory, viable PEPT1 knockout mice were developed and have been proven to be a useful tool for the study of this protein. Having PEPT1 knockout mice as an experimental tool provides a unique opportunity to study the importance of PEPT1 in the kinetics of cefadroxil oral absorption, as well as the kinetics of cefadroxil distribution and elimination from the body. In this project, I studied the contribution of PEPT1 in the absorption and pharmacokinetics of cefadroxil by doing the following:

1) Measuring the contribution of PEPT1 to the intestinal permeability of cefadroxil and the influence of pH, sodium, substrate concentration, and intestinal segment on drug uptake, using an *in situ* single-pass perfusion technique in wild type and PEPT1 knockout mice.

2) Determining the contribution of PEPT1 to the *in vivo* absorption, tissue distribution, and disposition of cefadroxil using wild type and PEPT1 knockout mice.

3) Establishing an *in silico* model of the absorption and pharmacokinetics of cefadroxil in wild type and PEPT1 knockout mice using an advanced compartmental absorption and transit (ACAT) model.

CHAPTER 2

BACKGROUND AND LITERATURE REVIEW

Anatomy and Physiology of the Small Intestine

The small intestine is the longest part of the gastrointestinal tract and is located between the stomach and the large intestine. It consists of 3 parts that look very similar to the naked eye, but differ at the microscopic level [1]. The first part of the small intestine is called the duodenum. In adult humans the duodenum is approximately 25 cm and has a pH between 1-2 at fasted conditions. The subsequent segment of the small intestine is called the jejunum. It is about 250 cm long and has an approximate pH of 6.5. The final part of the small intestine is called the ileum and, like the jejunum, but unlike the duodenum, is attached to the body by the mesentery. The ileum is between 200 and 400 cm long and has an approximate pH of 6.6 during fasting conditions [1].

The absorption of most nutrients and orally administered drugs takes part in the small intestine. This is mostly due to its vast surface area, given the arrangement of the intestinal wall [1] (Figure 2.1)The surface of the intestinal wall contains: 1) circular folds (plicae circularis), 2) small projections called villi, and 3) tiny projections called microvilli.

The circular folds form creases and ridges that do not disappear when the intestine is extended, and can be seen with the naked eye. Villi are microscopic structures that have a hair-like shape and measures around 0.5 to 1.5 mm in height depending on the intestinal segment. Each villus plays an important role in the exchange of nutrients and drugs because it contains a capillary network and a lymph vessel [1]. Microvilli are cytoplasmic protrusions or extensions of the plasma membrane on the apical (luminal) side of the intestinal columnar epithelial cells, also known as enterocytes or absorptive cells. It is because of these hair-like microstructures that the apical membrane is also known as the brush-border membrane. Each absorptive cell can have as many as 3000 of these structures in its apical membrane, and each one can be up to 1 μm in length [1, 2].

The intestinal wall is a thick barrier that consists of four broad concentric layers: 1) the mucosa, 2) the submucosa, 3) the muscularis externa, and 4) the serosa or adventitia [1, 2]. The mucosa faces the luminal side of the intestine and is composed of the simple columnar epithelium, the lamina propia, and the muscularis mucosae. The epithelium is a monolayer made up of 4 different types of cells: absorptive, goblet, APUD, and M cells. The absorptive cells are the most numerous ones in the epithelium and are located on the tips of the villi. The two principal

functions of these cells are to produce and secrete enzymes, and to absorb nutrients. The goblet cells produce and secrete mucus, and are also located on the tips of the villi. Both the absorptive and the goblet cells are generated from undifferentiated cells in the crypts of Lieberkuhn. They then differentiate and migrate to the tips of the villi. APUD cells, which stand for amine precursor uptake and decarboxylation cells, produce hormones that regulate different functions in the intestine, such as mobility and secretion. M cells, also known as microfold cells, specialize in sampling, phagocyting, and transporting antigens from the intestinal lumen. These last two types of cells are produced in the crypts of Lieberkuhn and do not migrate to the top of the villi [2].

The next sublayer of the mucosa, the lamina propia, is the connective tissue that holds the epithelium. It contains collagen fibers, elastic fibers, blood and lymph capillaries, and lymph cells. The blood and lymph vessels are located close to the epithelium to facilitate absorption [2].

The layer above the lamina propia is called the muscularis mucosae. This stratum consists of two thin layers of smooth muscle. The fibers of the internal layer are arranged in a circular manner, while those of the external layer are arranged longitudinally. Both of these layers are responsible for the contraction of the villi during digestion [1].

The submucosa is the tissue section above the muscularis mucosae. It has a rich and well-developed network of blood and capillary vessels, and is highly innervated with parasympathetic nerves. The submucosa of the duodenum has an

unusual type of gland, the Brunner's Glands. These duodenal glands produce mucous, epidermal growth factor, and bicarbonate rich fluid [1].

The muscularis externa is the outer most level of the intestine, and is responsible for peristaltic movements. It is composed of two layers of smooth muscle—i.e. an inner circular layer, and an outer longitudinal one—and a middle layer of nerve fibers [1].

As mentioned above the intestinal wall is highly perfused with blood vessels. The arterial blood that reaches the jejunum and the ileum comes from the superior mesenteric artery, while the venous blood is transported to the portal vein and eventually to the liver [2].

Absorption and Transport Mechanisms

Most of the absorption of electrolytes, nutrients, water and drugs occurs in the proximal segment of the small intestine, which is facilitated by its vast surface area. For a molecule to go from the lumen of the intestine to the lumen of the blood vessel it needs to go through several barriers, including the unstirred water layer in the lumen of the intestine, the apical and the basolateral membranes of the epithelial cells, the intercellular space, and the apical and basolateral membranes of the endothelial cells [1].

There are different pathways molecules can cross a cellular membrane, including the paracellular and transcellular routes. Transcellular refers to the traffic of molecules across the interior of a cell, while paracellular means the traffic in Probetween the cells. Transcellular transport includes passive diffusion, active and facilitated transport, and transcytocis [3] (Figure 2.2)

Different physicochemical and structural factors influence the route a molecule takes to reach the blood stream. Water and some small ions, like chloride and potassium, are transported via paracellular channels, a process driven by osmotic and electrochemical gradients [3].

Some molecules can passively diffuse through the membrane. Passive diffusion is a process that does not require energy because the movement of molecules is driven by a concentration and/or an electrochemical gradient [3]. In passive diffusion the transport of a solute across a membrane is a non-saturable

process. The rate of transport or flux is proportional to the solute concentration gradient, and can be described using Fick's first law of diffusion, according to the following equation:

$$\frac{dM}{dt} = \frac{AD(C_i - C_o)}{X} \tag{2.1}$$

where dM/dt is the rate of transport (μg/sec), A is the surface area of the membrane (cm^2), D is the diffusion coefficient (cm^2/sec), X is the thickness of the membrane (cm), and Ci-Co is the difference of solute concentration between the two sides separated by the membrane (μg/mL). The diffusion coefficient D is a parameter related to the lipophilicity and the size of the molecule, and to the viscosity of the membrane. Usually small lipophilic drugs can cross membranes easier than large hydrophilic ones [1, 3, 4].

Large hydrophilic molecules usually need the help of membrane transport proteins to get into the cytosol. There are two types of membrane transport proteins: transporters and channels. Channels form aqueous pores in the cell membrane, that allow small ions and water to go through it without binding to it[3]. Transporters are proteins that bind the solute and after a series of conformational changes, transfer it across the cell membrane. Some transporters, but no channels, can transport a solute against its concentration gradient or electrochemical gradient. This process is called active transport because it uses energy, e.g. from ATP hydrolysis, to pump molecules across the membrane [3] (Figure 2.3)

There are several types of transporters and they can be classified according to the source of energy that they use to move solutes. ATP-driven pumps use the

energy that results from the hydrolysis of ATP to move solutes uphill (against a concentration gradient) [3]. Coupled transporters combine the downhill transport of a molecule to the uphill transport of another. These can either be symporters, in which both molecules go in the same direction, or antiporters, in which they move in opposite ones. Na+ and H+ are some of the most utilized molecules by coupled transporters [3].

When proteins are ingested, they get degraded into oligopeptides by different types of enzymes. Once the products of the degradation of these proteins reach the small intestine, they get further cleaved by peptidases located in the brush border membrane and then get absorbed, mainly as di- and tripeptides [5]. Due to the hydrophilicity and the presence of charged groups, it has been shown that these peptides need a transporter protein to reach the cytosol of the enterocytes. This transporter has been identified as PEPT1. Di- and tri-peptides that reach the cytosol get further hydrolyzed into amino acids by intracellular peptidases, and are either used in the cell or get released by amino acid transporters in the basolateral membrane. Some peptide-like molecules do not undergo degradation and are potentially transported by still unknown peptide transporters in the basolateral membrane [6].

The interaction of a transporter and its substrate follows the Michaelis-Menten kinetics. The rate of transport (v) increases with the drug concentration, but it reaches a maximum, called V_{max}, when the transporter gets saturated [7] (Figure 2.3). The concentration at half of the maximum rate of transport (V_{max}) is called the Michaelis-Menten constant (K_m) and is a good indicator of the affinity of the

transporter for the substrate. A substrate with low K_m has a higher affinity for the transporter than one with a higher K_m [7].

$$v = -\frac{dA}{dt} = -V\frac{dC}{dt} = \frac{V_{max}C}{K_m + C} \tag{2.2}$$

Some compounds can competitively inhibit the protein without being transported by it, and are therefore called inhibitors. The affinity of the inhibitor for the transporter can be expressed by the inhibition constant K_i, and is usually calculated using IC_{50} of the competitive inhibitor and the concentration and K_m of the substrate as shown in equation 2.3 [7].

$$K_i = \frac{IC_{50}}{1 + \frac{[Substrate]}{K_m}} \tag{2.3}$$

Modeling and Simulation of Absorption Behavior

The prediction of the rate and extent of absorption and pharmacokinetics of orally dosed drugs is a task many research groups have pursued in the last few decades, however it is still a difficult venture. This task has been proven to be not easy due to the several factors that affect the absorption process. Those factors can be divided into 3 categories: 1) Physiological factors of the GI tract, 2) Physicochemical characteristics of the drug, and 3) Dosage form factors[8]. In the first category, one can find that several physiological aspects of the gastrointestinal tract may affect drug absorption, including and not limited to pH, transit time, blood flow, gastric emptying, membrane porosity, surface area of the GI tract, and absorption mechanisms. In the second category some of the most common factors that affect absorption are solubility, pKa, stability, lipophilicity, and salt form. From the dosage form stand point, one should consider if the drug is administered as a solution, suspension, capsule, tablet or as a sustained release form[8, 9] [10].

A variety of models are available for the prediction of absorption of drugs in the intestine, from very simple ones such as the mixing tank model, to the more complex ones, such as the advanced compartmental absorption and transit model (ACAT) developed by Simulations Plus (Figure 2.4)[9].

The ACAT model was developed based on the compartmental absorption model developed (CAT) by Yu and Amidon in 1996 [11]. The original CAT model divides the gastrointestinal tract into 7 segments, but doesn't take into account the

absorption of drugs in the stomach or colon. It also needs the measured drug's effective permeability [8]. The ACAT model used in Gastroplus® was developed by Simulations Plus model and divides the gastrointestinal tract into 9 compartments, in all of which absorption can occur. The ACAT defines one compartment for stomach, one for the duodenum, 2 compartments for the jejunum, 3 for the ileum, 1 for the ceacum, and finally 1 compartment for the ascending colon. Those 9 compartments are then sub-divided into the following 4 sub-compartments: unreleased drug, undissolved drug, dissolved drug, and the enterocyte [8]. The ACAT model uses a series of differential equations, around 80 of them, to describe the transfer of drug along the GI tract and across the different sub-compartments. Different from the CAT model, the ACAT model allows drug absorption in the stomach and colon, and also can predict *in silico* the effective permeability of different drugs based on their chemical structure using the ADMET prediction module[8]. The ACAT model also allows the addition of paracellular absorption through out the gastrointestinal tract. It also allows the incorporation of transporter and metabolism processes in the small intestine, colon and liver, by using Michaelis-Menten kinetics differential equations [8, 12, 13].

One of the most interesting features of the ACAT model is its ability to extrapolate *in vitro* and pre-clinical data in order to predict a drug's absorption behavior and its pharmacokinetics and establish first in human doses. Abuasal *et al* [14] published recently a paper about the successful prediction of human pharmacokinetics, from *in vitro* and rat *in situ and in vivo* data for a compound that was a substrate of CYP3A4 and P-gp [12-14].

Proton-coupled Oligopeptide Transporters

Peptide transporters are plasma membrane proteins that belong to the SoLute Carrier family 15 (SLC15). The SLC15 family is a phylogenetically conserved family comprised by four proton-dependent membrane transporters: SLC15A1 (PEPT1), SLC15A2 (PEPT2), SLC15A3 (PHT2), and SLC15A4 (PHT1) [15-17]. Peptide transporters have been identified in a wide variety of species, both in prokaryote and eukaryote organisms, where they have been reported to have similar structural features and functions. PEPT1 was the first member of the SLC15 family to be identified. First, it was cloned and characterized in the rabbit small intestine in 1994 by Fei *et al and* Boll *et al* [18, 19], and later found in mouse, rat, and human. Peptide transporters have been found to be highly homologous across different species, with around 90% amino acid identity between mammal species. [20] [21]. Though, there is only 50% amino acid identity between PEPT1 and PEPT2, and only 20% between PHT1 and PEPT2 [22].

PEPT1 is highly expressed in the apical border of the small intestinal epithelial cells. It is mainly located at the tip of the villi of the duodenum, the jejunum, and the ileum. In healthy patients PEPT1 is not expressed in the colon, but it has been found in the colon of patients with chronic diseases, such as Crohn's disease and ulcerative colitis (for references see Table 2.1). PEPT1 has also been found to a lesser extent in other organs of the healthy human body, such as the kidney, liver, and pancreas. In the kidney, PEPT1 has been found in the apical

membrane of epithelial cells in the S1 segment of the proximal tubule, where it reabsorbs a very small percentage of the di- and tripeptides from the urine back into the blood prolonging their half-life [21].

PEPT2 is expressed in different parts of the body, including the kidney, the lung, the enteric nervous system, the choroid plexus, astrocytes, cerebral cortex, and neurons (for more details see Table 2.1. Localization of peptide transporters.) [23-26]. In the kidney, PEPT2 is mostly expressed on the apical membrane of the epithelial cells in the S3 segments of the in proximal tubules, where it does most of the reabsorption of di-and tri-peptides and peptide-like drugs. PEPT2 is expressed on the apical membrane of the choroid plexus, where it has been shown to remove neuropeptides and peptide-like drugs from the cerebrospinal fluid (CSF)[27-30].

While PEPT1 is a low affinity and high capacity transporter, its isoform PEPT2 is a low capacity and high affinity one [31]. Peptide transporters can move substrates against a concentration gradient thanks to an inwardly directed proton gradient and a negative membrane potential [32]. The proton gradient is caused by the pH difference between the acidic microclimate (pH=6.6) at the brush border membrane of the intestine and the neutral cytoplasm (pH=7.35). This acidic micro-climate is maintained by the sodium hydrogen exchanger (NHE3), which is a transporter located in the apical membrane of the cell, and responsible for catalyzing the exchange of an exiting H+ and an incoming Na^+ [6, 33] (see Figure 2.5).

The movement of substrates involves the binding and co-transport of a proton, or two, from the intestinal lumen to the cell cytosol, the excretion of a proton back to the lumen via the sodium-proton exchanger (NHE3), and the efflux of

sodium to the blood by a sodium potassium exchanger in the basolateral membrane. This sodium potassium exchanger is a transporter that uses the energy generated by the hydrolysis of ATP to exchange 3 sodium ions for 2 potassium ions [3] [33] [6]. While mammalian peptide transporters PEPT1 and PEPT2 can transport almost all possible di- and tri-peptide combinations, and some peptide-like drugs, they cannot move single amino acids or oligopeptides with 4 or more amino acid residues [34] (Table 2.2).

Little is known about the other 2 members of the SLC15 family, the peptide/histidine transporters PHT1 and PHT2. These transporters, different from PEPT1 and PEPT2, can transport the amino acid L-histidine. Although it has been shown that they transport peptides, it is still unknown to what extent they can transport all di- and tripeptide combinations [35] [36].

Although the three dimensional structure of human PEPT1 has not been completely elucidated, some structural features have been proven to be key for substrate recognition and transport. This human protein contains 708 amino acid residues, and is predicted to have 12 putative transmembrane domains, with both the amino- and carboxy-termini facing the cytosolic side of the membrane [20]. It also has a large extracellular loop between the 9^{th} and 10^{th} transmembrane domain with several glycosilation points [20] (Figure 2.6).

Several studies with chimeric transporters have shown that the transmembrane domains TM1-TM4 and TM7-TM are relevant for substrate affinity and binding [37-39]. Mutational studies proved that the extracellular histidine H57

is involved in the binding of the proton, and tyrosines Y12, Y56, Y64, Y91, and Y167 play a key role in the binding and translocation of the substrate [40-42].

Although PEPT1 has a preference for compounds with no net charge, it can transport both positively and negatively charged molecules [43, 44]. The transport of molecules with zero net charge is optimal at the pH of the brush border microclimate (around 6.5), but the optimal pH for the transport of ionic species shifts up or down according to their net charge. Neutral and cationic species are transported in a 1:1 stoichiometry in relation to protons. Acidic peptides, like the ones containing aspartic or glutamic acid are moved in a 1:2 relation, where the second proton is attached to the peptide side chain [44-46].

Water plays an important role in the active transport of the differently charged peptides. It interacts with the charged amino acid residues, acting as a shield. It also fills void spaces in the transporter to allow a better docking of the peptide [47, 48].

Different authors have shown that certain features in the substrate are required for its ability to bind to the transporter, such as two oppositely charged groups separated by carbon backbone with a distance of 5.5 to 6.3 Angstrom, along with the presence of at least one L-enantiomer amino acid residue in the molecule [49].

The alpha-amino group and the peptide bond have been shown not to be necessary for binding to the transporter, although their presence in the substrate increases the affinity [50]. Another important feature that helps increase the

bonding affinity is the carbonyl oxygen in the peptide bond, since it binds to the substrate-binding domain by a hydrogen bond [51].

Competition and electrophysiological experiments have helped measure K_m constants for different compounds and identified some substrates and inhibitors of the PEPT1 transporter. Peptides that have 3 amino acid residues as L-enantiomers have a higher affinity than those with only two or just one [50]. Also, compounds in which the peptide bond has a trans conformation also have a higher affinity for PEPT1 [52]. Molecules that have hydrophobic side chains expel water from the binding pockets and therefore have a higher affinity for the protein, acting as inhibitors [53].

Pharmacological Importance of Peptide Transporters

As mentioned above, PEPT1 is a high-capacity and low-affinity peptide transporter capable of carrying all natural di- and tripeptides, and some peptide-like drugs [20] [19]. Some of these drugs include betalactam antibiotics like cephalexin and cefadroxil, antiviral drugs like valacyclovir and valgancyclovir, peptidomimetic anticancer compounds like bestatin, and inhibitors of the angiotensin-converting enzyme (ACE) like enalapril [54-60] (Figure 2.8).

For several years researchers have experimented with drug chemical structures to improve undesirable pharmaceutical and pharmacokinetic characteristics without diminishing their therapeutic capabilities [61]. Several approaches are available, and attaching moieties to molecules to improve their characteristics is a widely used technique. The modified drug, also known as prodrug, is then later converted to the active drug in the body usually by enzymes. Prodrugs can be design specifically to target specific membrane transporters or enzymes in order to control their uptake into certain tissues [61].

Designing a prodrug to target PEPT1 is a strategy that has been used with hydrophilic drugs to improve their permeability through the intestine. Since PEPT1 has high capacity and broad substrate specificity it has been used as a target for improving drug delivery. Drugs with low permeability can be modified into prodrugs that can by recognized and transported by PEPT1, improving then the drug's bioavailability. There are already numerous prodrugs in the market that are bound and transported by PEPT1. L-valacyclovir is the ester prodrug of acyclovir, an

antiviral drug with low permeability. In this case the prodrug has 3 to 5 times higher oral bioavailability than the original nucleoside [62].

Another successful case in target-designed prodrugs is the one involving α-methyl-dopa, an antihypertensive drug with low permeability in the intestine. By modifying the parent drug with peptidic moieties, like Phe-α-methyl-dopa, α-methyl-dopa-Phe, and p-Glu-L-Dopa-Pro its permeability and therefore its bioavailability increased significantly [63, 64].

Genetic Variation of PEPT1

Similar to metabolizing enzymes, transporters also have genetic polymorphisms that have been linked to important changes in the pharmacokinetics of drugs, and potentially significant consequences on their pharmacodynamics and toxicity. For example, genetic variations in p-glycoprotein have been associated with changes in the disposition of some of its substrates, such as digoxin [65] and fexofenadine [66]. Also, genetic variants of OATP-C and OAT3 have been implicated with changes in the disposition of pravastatin in humans [67].

Interestingly enough, three independent studies found that PEPT1 has well conserved substrate recognition and very few genetic polymorphisms that actually affect the uptake of its substrates [68-70]. For the study done by Zhang *et al* the 9 non-synonymous SNPs, and their relative frequencies, were: S117N (22.7%), G419A (6.8%), T451N (3.4%), V416L (1.1%), V450I (1.1%), R459C (1.1%), T114I (1.1%), V122M (1.1%), and P586L (1.1%) (see Figure 2.7). The latter two non-synonymous polymorphisms are located in the transmembrane domains, while the other seven are located in the extracellular loops. When the variants were transfected into HeLa cells and their transport capacity was tested using Gly-Sar, the results showed that none of the non-synonymous polymorphisms had reduced affinity for the substrate (i.e. significant changes in the K_m). The only significant difference was seen with the P586L variant, which showed reduced maximal uptake of Gly-Sar (V_{max} was 10-fold lower) [69].

In their second study, Anderle *et al* [70] show that, although the non-synonymous polymorphism F28Y has reduced Gly-Sar uptake (K_m is 3.5-fold higher)

when transfected into HeLa cells. They also showed its frequency is rare (0.002), and interestingly enough it was only detected in the African-American population.

Regulation of PEPT1

The expression level and function of PEPT1 can be regulated by a variety of factors, and several studies have reported changes in mRNA and protein levels both *in vivo* and *in vitro* under different conditions.

For example, fasting and type of diet are some of the most reported factors affecting the levels of PEPT1. For example, it has been shown that the expression of PEPT1 is subject to the influence of the diurnal rhythm, and that the amount of transporter is higher at night when the rats are awake and eating, than during the day when they are sleeping [71, 72]. Pan *et al* revealed that in rats PEPT1 levels were dependent on food intake and that its functionality was higher at 8pm than at 8am, which indicates that the levels of the protein were higher after a few hours of fasting [72, 73]. Also, Ferraris *et al* showed that RNA and protein levels of PEPT1 in rats increased after fasting for periods of 24 hours [74, 75]. Finally, Ma *et al* [76] demonstrated that in wild-type mice, PEPT1 protein levels in the small intestine increase with fasting periods of over 16 hours. This protein up regulation resulted in an increase of Gly-Sar absorption after oral administration to wild-type mice. No effect was seen in PEPT1 knockout mice, demonstrating that the increase in Gly-Sar exposure was due solely to increase in PEPT1 expression, and not in other transporters[76].

Experiments in Caco-2 cells have proven that an increased concentration of peptides in the growth medium increases the V_{max} of the PEPT1-mediated transport by increasing the number of transporters present in the apical membrane of the cells [77]. This increase in protein levels was caused by an enhanced gene

transcription [77, 78]. Other experiments in rats showed that high protein diets and therefore high concentration of peptides in the intestinal lumen increase the amount of PEPT1 in the apical membrane by increasing the gene expression [79].

Several reports reveal the effect of disease state on PEPT1 levels. For example, there is some *in vivo* and *in vitro* evidence that intestinal PEPT1 is up regulated in patients that have damaged intestinal mucosa due to infections with *cryptosporidium parvum*, a common cause of diarrhea. It is hypothesized that the damage to the mucosa causes a decrease in the absorption of peptides, which in turn causes an increase in the amount of PEPT1 mRNA being transcribed [80].

Also, PEPT1 has been reported to be aberrantly present in the colon of patients with Crohn's disease and ulcerative colitis, the two forms of the inflammatory bowel disease (IBD). Although no conclusions have yet been reached about the role of PEPT1 in the mechanism of the disease, some *in vitro* experiments have suggested that this transporter is in charge of the movement of the peptide neutrophil chemotactic factors such as fML (N-formyl-Met-Leu-Phe) and muramyl dipeptide [81-83]. New evidence suggest that in IBD patients the colonic PEPT1 acts as a gate into the enterocyte for bacterial di- and tri-peptides, which trigger an immunologic response by producing of cytokines and chemokines that induce neutrophil migration into the inflammation site [81-85].

Hormonal regulation of PEPT1 is another well-described phenomenon in this field. Experiments in Caco-2 cells and jejunal brush border vesicles show that when Insulin and EGF bind to their extracellular receptors, the Vmax of the PEPT1 mediated transport increases transiently but the mRNA levels do not, indicating that

the increase in transport is caused by an increased stability of the RNA and not an increase on the transcription of it [86] [87]. When physiological concentrations of EGF were added to the basolateral compartment of Caco-2 cells cultures for different periods of time, the transport of dipeptides was first increased, without an increase in the RNA levels [88], and then after several days of exposure the transport was inhibited due an inhibition of PEPT1 transcription [89].

On the other hand, research with leptin has revealed receptors for this hormone in the small intestine of rats, especially in the jejunum. An increase in peptide transport is noted when leptin is added in perfusion experiments [90]. Experiments with Caco-2 cells have also revealed that the transport of some betalactam antibiotics can be enhanced when this hormone is added to the medium on the apical side of the chamber, but not on the basolateral side [90]. Although more research needs to be done, it is believed that the increased transport is due to translocation of the peptide transporter from the cytoplasm to the apical membrane, and not to enhanced transcription [90, 91].

Other hormones like triiodothyronine (T3), recombinant human growth hormone (rhGH), and progesterone have been investigated to a lesser extent. When T3 is added to Caco-2 cell cultures it decreases the amount of membrane PEPT1, and therefore the uptake of dipeptides [92]. The mechanism by which the increase in transcription and/or stability of the transporter is induced is not yet known. However, *in vivo* experiments have shown that rats with hypothyroidism have a decrease in PEPT1 expression and activity in the small intestine [93]. When rhGH was added over four days to Caco-2 cell cultures the uptake of cephalexin, a

betalactam antibiotic, was enhanced due to the increase of PEPT1 mRNA in the cells [94]. Other experiments in Caco-2 cells have shown that when progesterone and norethisterone were added to the medium, the uptake and transport of cephalexin decreased with both hormones because of a decrease in the expression of PEPT1 [95, 96].

It has been shown *in vitro* and *in vivo* that some drugs affect the expression of PEPT1 by either increasing or decreasing the protein levels at the apical membrane or the mRNA levels of it. Drugs like 5-fluorouracil and clonidine have been reported to increase the transporter's level both *in vivo* and *in vitro*, though the exact mechanism is not yet known [97, 98]. Nifedipine, a calcium channel blocker, was shown to boost the activity of PEPT1 and increase the bioavailability of orally administered amoxicillin in humans. The mechanism of this enhancement relies on the decrease of intracellular calcium, which stimulates the sodium-proton exchanger and resulting in an increase of extracellular protons available for PEPT1[99]. The opposite effect is shown with amiloride, which is a blocker of the sodium-proton exchanger. When amiloride was given concomitantly with oral amoxicillin, the bioavailability of the latter one was reduced significantly[99]. Some immunosuppressive agents have been shown to reduce the transport rate of Gly-Sar *in vitro* [100].

Cefadroxil

The IUPAC chemical name for cefadroxil is (6R, 7R)-7-[(R)-2-amino-2-(p-hydroxyphenyl)acetamido]-3-methy-8-oxo-5-thia-1-azabicyclo[4.2.0]oct-2-ene-2-carboxylic acid (See structure in Figure 2.9). Its molecular weight is 363.39 and its molecular formula is $C_{16}H_{17}N_3O_5S$. It is soluble in water (Intrinsic solubility = 17.4 mg/mL) and slightly soluble in alcohol. Its apparent pKa's are: 2.64, 7.30 and 9.69 at 35 °C and its isoelectric point is 4.9 [101] .

Cefadroxil is a semi-synthetic betalactam antibiotic that belongs to the first generation of cephalosporins. It is used to treat different kinds of infections in the ear, skin, urinary tract, and upper and lower respiratory tract. It has been widely used to treat community-acquired pneumonia and infections in patients with known allergies to penicillins [102, 103].

Cefadroxil is effective against most Gram-positive cocci, but not against methicillin-resistant *Staphilococci* and *Enterococci*. It is also active against certain Gram-negative bacteria like *Klebsiella pneumoniae*, *Proteus mirabilis* and *Escherichia coli* [104].

Cefadroxil binds to transpeptidases, which are specific penicillin-binding proteins (PBP's) inside the bacterial cell wall. This binding causes the inhibition of cross-linking of peptydoglycan, a basic step in the synthesis of the bacterial wall. The inhibition of this step breaks the equilibrium between the degradation and formation of new bonds, allowing the bacterial autolysins to degrade the entire bacterial wall [105].

Cefadroxil adverse reactions are usually mild and can be reversed easily [103]. The antibiotic can cause nausea, vomiting, diarrhea, and hypersensitivity reactions like skin rashes and dermatitis. It is contraindicated in patients with known allergies to other cephalosporins [104].

Cefadroxil has a high oral bioavailability and food does not alter its absorption. Its half-life in humans is around 95 minutes, which is longer than that of other cephalosporins of the same generation. It is extensively distributed to several tissues, including the lung, tonsils, placenta, bone, muscle, and prostate and is approximately 20% bound to plasma proteins [103, 104]. Cefadroxil, like some other cephalosporins, is not metabolized and about 90% can be recovered unchanged in urine in the first 24 hours after oral administration [104]. Table 2.4 shows the pharmacokinetic parameters of cefadroxil in humans.

The absorption of cefadroxil from the small intestine has been attributed to transporters, due to the antibiotic's physicochemical characteristics and the saturable kinetics of this process [106]. Cefadroxil, being a hydrophilic drug with two oppositely charged groups at the physiological pH, is most likely to be transferred across membranes by different transporters than by passive diffusion. However, the contribution of each of these mechanisms to the total mass transfer process is still not known [107].

As mentioned previously, cefadroxil chemical structure resembles that of a tri-peptide (see Figure 2.10), and its proton-dependent transport is inhibited by other amino-cephalosporins and di- and tri-peptides [56, 107-110]. Several authors have shown that peptide transporters, like PEPT1, play a critical role in the

absorption of cefadroxil from the small intestine [107, 109]. Cefadroxil has been widely used as a substrate to study PEPT1 and PEPT2 because of its pharmacological activity, high affinity for peptide transporters, and its lack of degradation or metabolism by enzymes in the body.

PEPT2 has been shown to be responsible for most of the reabsorption of cefadroxil from the urine back to the blood, increasing the half-life of the drug and therefore increasing the exposure of different tissues to the antibiotic [111]. On the other hand, PEPT2 has also been shown to act as an efflux transporter of cefadroxil from the cerebrospinal fluid (CSF) in the choroid plexus, decreasing the concentration of this drug in the brain. Previous studies have shown that when PEPT2 null mice where treated with cefadroxil, the ratio of the CSF to plasma drug concentration was higher as compared to wild type mice [28, 29].

Since cefadroxil has a negative charge at the physiological pH, it can bind to organic anion transporters (OATs). These transporters are present in the basolateral membrane of the epithelial cells in the proximal renal tubules, and are thought to be responsible for the active secretion from blood to tubular fluid of several negatively charged endogenous and exogenous compounds, like cefadroxil. This family of transporters includes OAT1, OAT2 and OAT3 and it was shown recently that from these three proteins present in the human kidney, OAT3 plays a stronger role than OAT1 in the active secretion of cephalosporins [112]. Experiments using *Xenopous* oocytes expressing OATP2B1, the organic anion transporting polypeptide-2 A 1 expressed in the liver, show that cefadroxil is also a substrate for this transporter [113].

It has been shown that in mice where the multidrug resistance-associated protein 4 was removed, there is an increase in the blood concentration of ceftizoxime and cefazolin [114]. MRP4 is located in the basolateral membrane of the epithelial cells in the kidneys where it is involved in the tubular active secretion of some cephalosporins from the blood to the urine [114]. Also, de Waart *et al* [115] showed that MRP3 and MRP4 located on the basolateral membrane of the enterocytes could be involved in the transport of cefadroxil across the basolateral membrane (from the enterocyte into the blood) in mice.

The human multidrug and toxin extrusion/H(+)-organic cation antiporters (MATE1) have been shown to be capable of transporting some cephalosporin antibiotics. This transporter is expressed in the basolateral membrane of the kidneys [116-118].

Figures

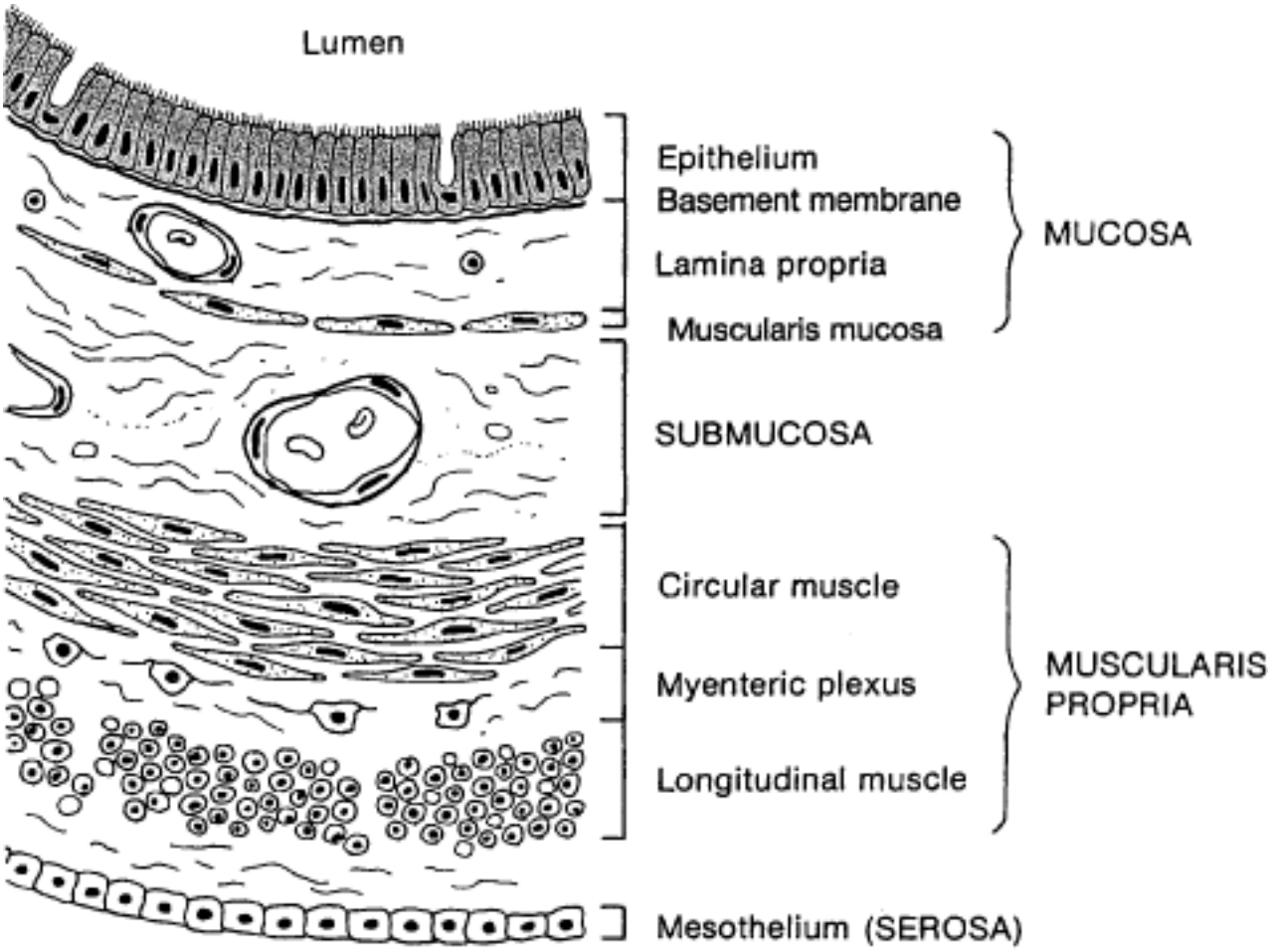

Figure 2.1. Layers of the small intestine. Extracted from Gastrointestinal Physiology, The McGraw-Hill Companies, Inc. 2008

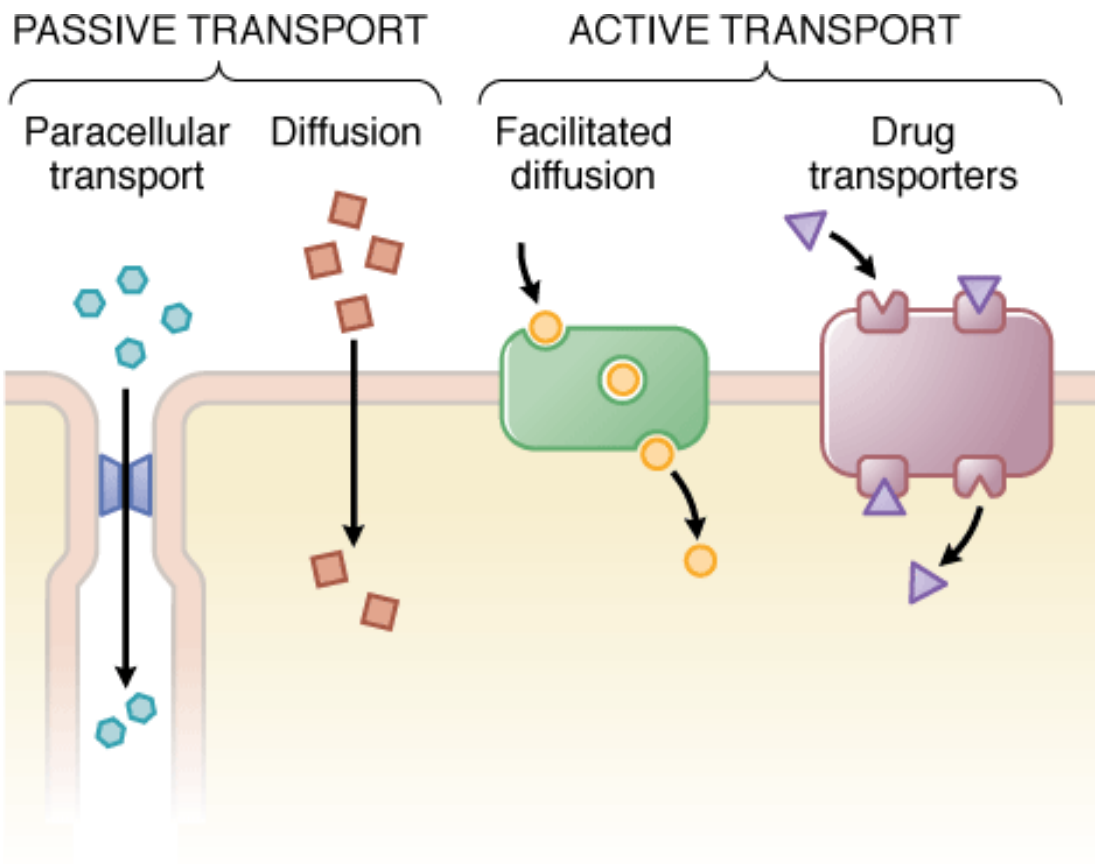

Figure 2.2. Cellular transport pathways. Paracellular transport happens between two adjacent cells, through the tight junctions. Drug transport occurs through the cell, and can happen through different mechanisms, such as A) passive diffusion and B) active transport. Source Goodman and Gilman, 12th edition, The McGraw-Hill Companies, 2010.

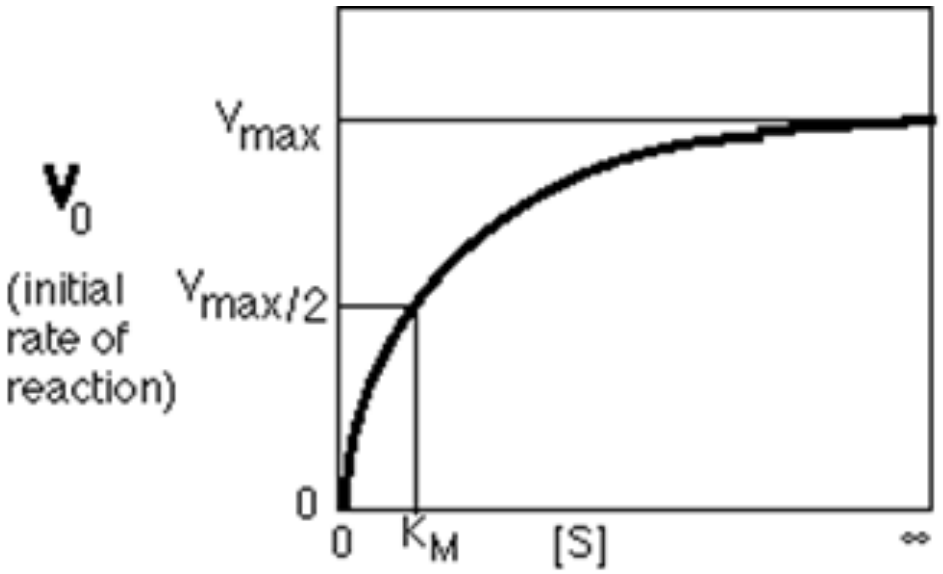

Figure 2.3. Kinetics of non-linear (saturable) transport. Image taken from http://web.campbell.edu/faculty/nemecz/323_lect/enzymes/Measuring%20KM%20and%20Vmax%202.html

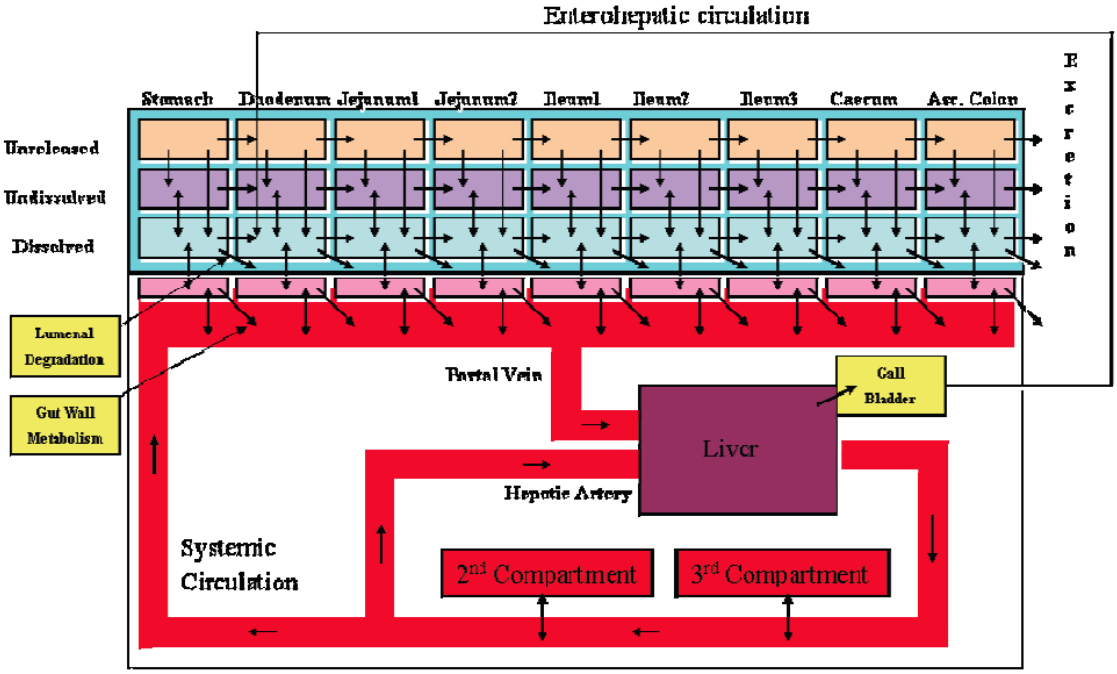

Figure 2.4. ACAT Model with Gastroplus. Extracted from Gastroplus Manual.

http://www.simulations-plus.com/Products.aspx?pID=11&lID=27

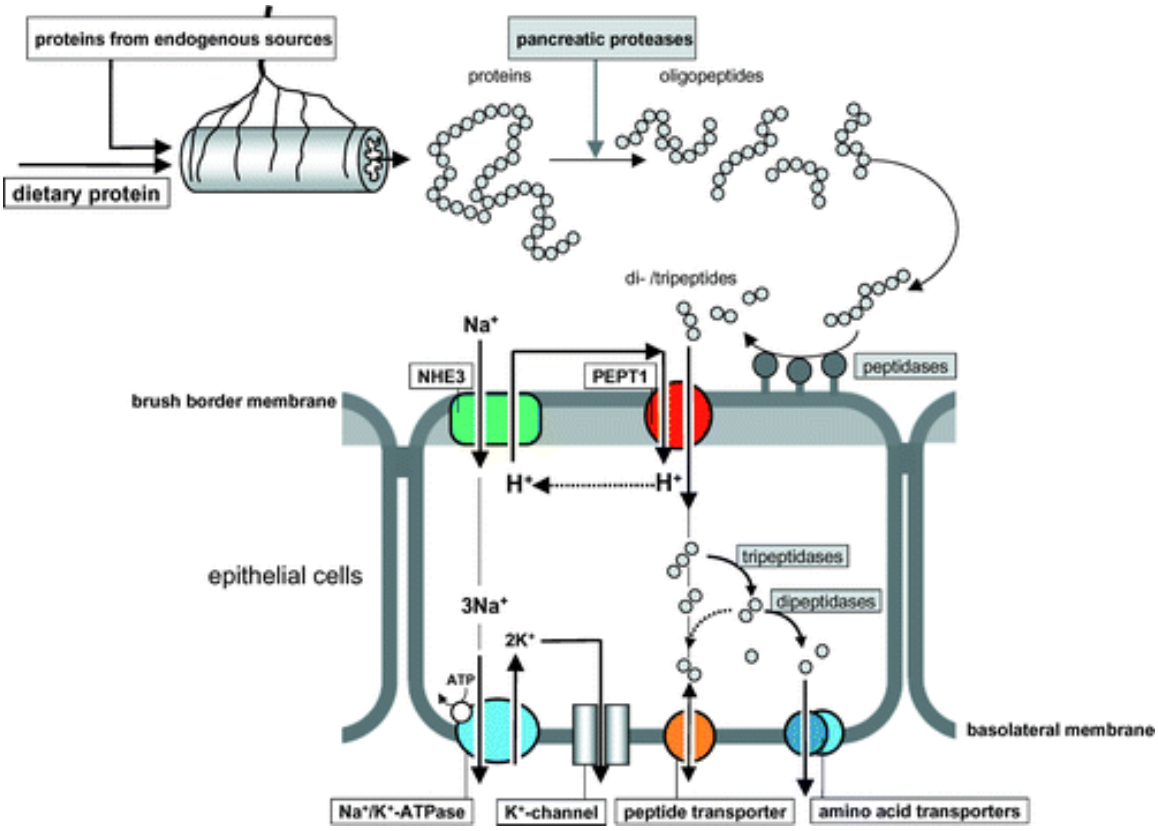

Figure 2.5. Model of peptide transport in the enterocyte. PEPT1 is located in the apical membrane of the cell and facilitates the transport of di- and tri-peptides across the brush border membrane. Once the peptides reach the cell they get degraded into amino acids and get exported out of the cell into the blood stream through the amino acid transporters present on the basolateral membrane. Extracted from: Hannelore Daniel. Molecular and integrative physiology of intestinal peptide transport. Annu. Rev. Physiol. 2004. 66:361–84.

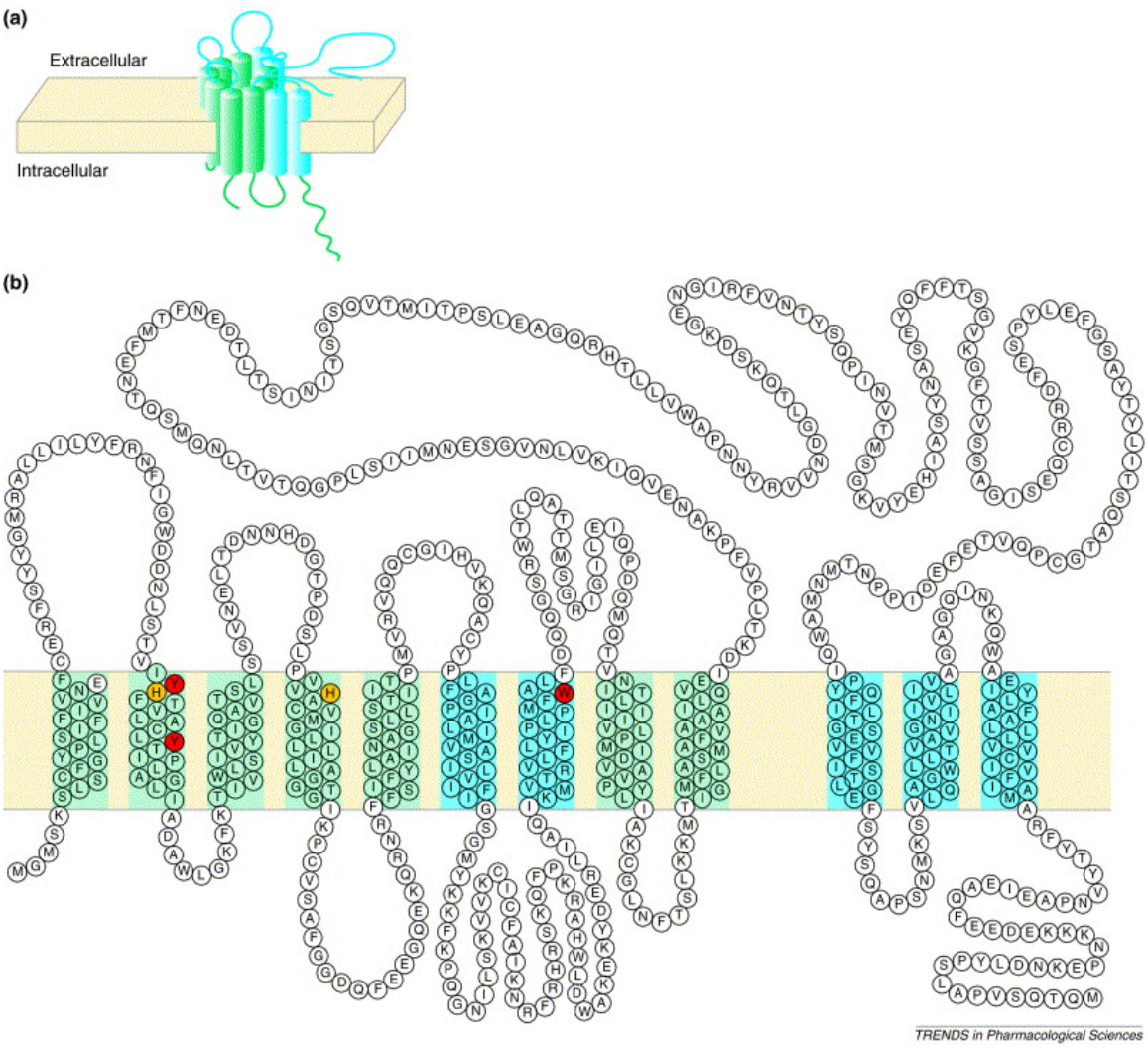

Figure 2.6. Topology of PEPT1. Analyses indicate that the transporter has 12 putative transmembrane domains. It also contains a large extracellular loop between the 9th and 10th transmembrane domain, 1 protein kinase A site, and 1 protein kinase C site. Both the amino and carboxy termini are facing the cytosol. Extracted from: Rubio I. and Daniel H. Trends in Pharmacological Sciences, Volume 23, Issue 9, 434-440, 1 September 2002.

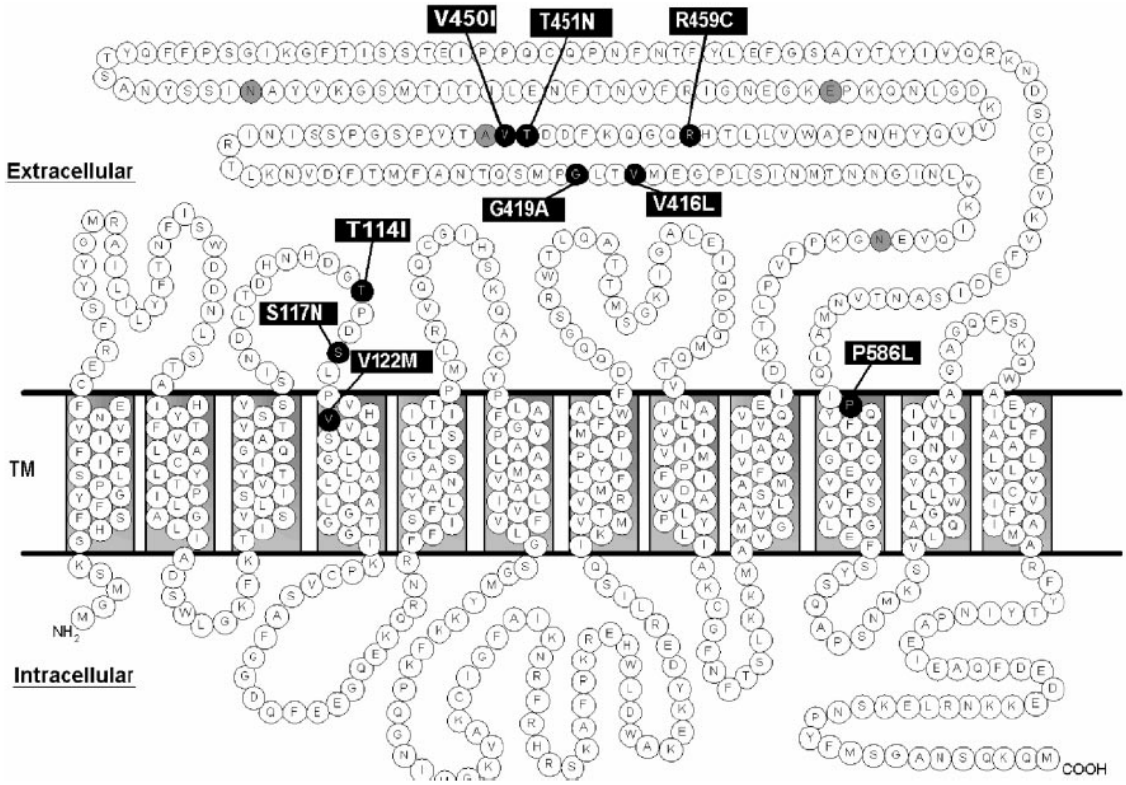

Figure 2.7. Representation of most common cSNPs of PEPT1 in humans. The 9 non-synonymous amino acid changes are in bold and numbered. Synonymous amino acid changes are depicted in grey. Figure extracted from Zhang *et al* 2004 [69].

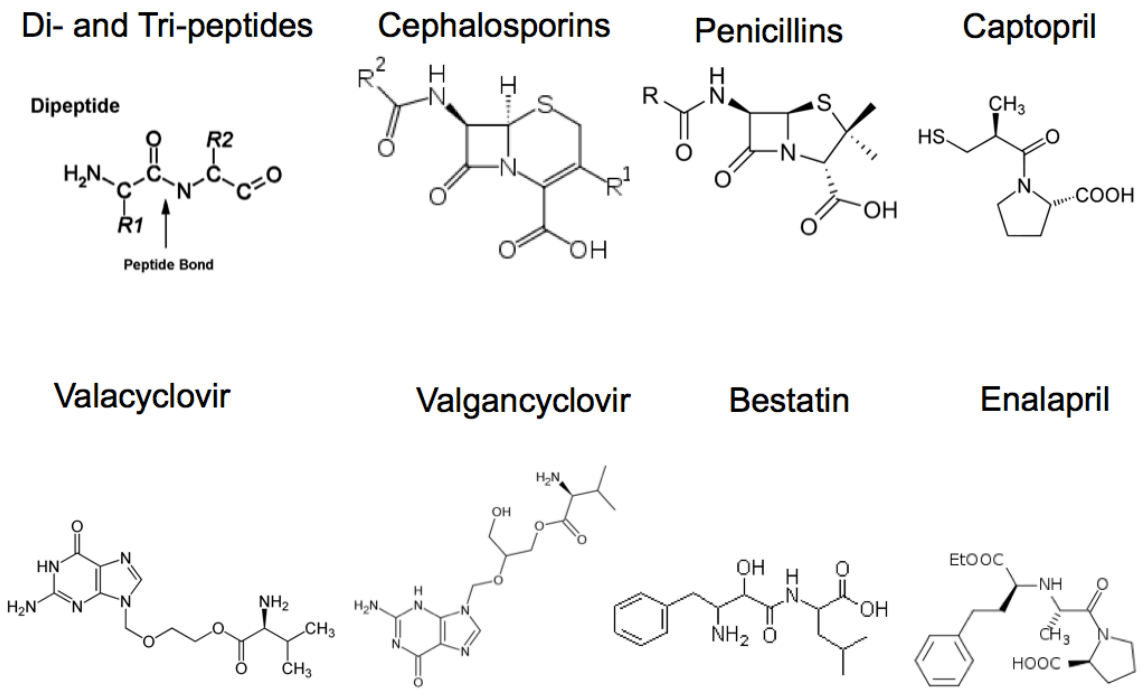

Figure 2.8. Some known substrates of the peptide transporter 1 (PEPT1).

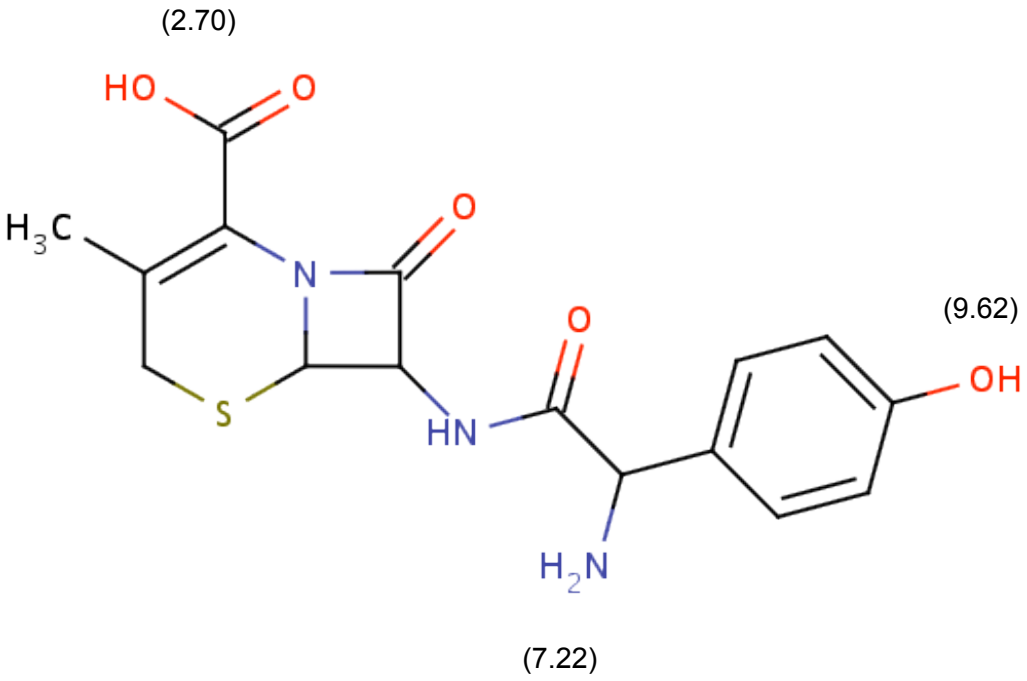

Figure 2.9. Structure of cefadroxil. This first generation amino-cephalosporin has a molecular weight of 363, a cLogP of -2.51, and pKa's of 2.70, 7.22, and 9.62 (shown in parenthesis). Its intrinsic solubility is 17.4 mg/mL (pH = 4.9), and its Log D (4.8) = -2.11.

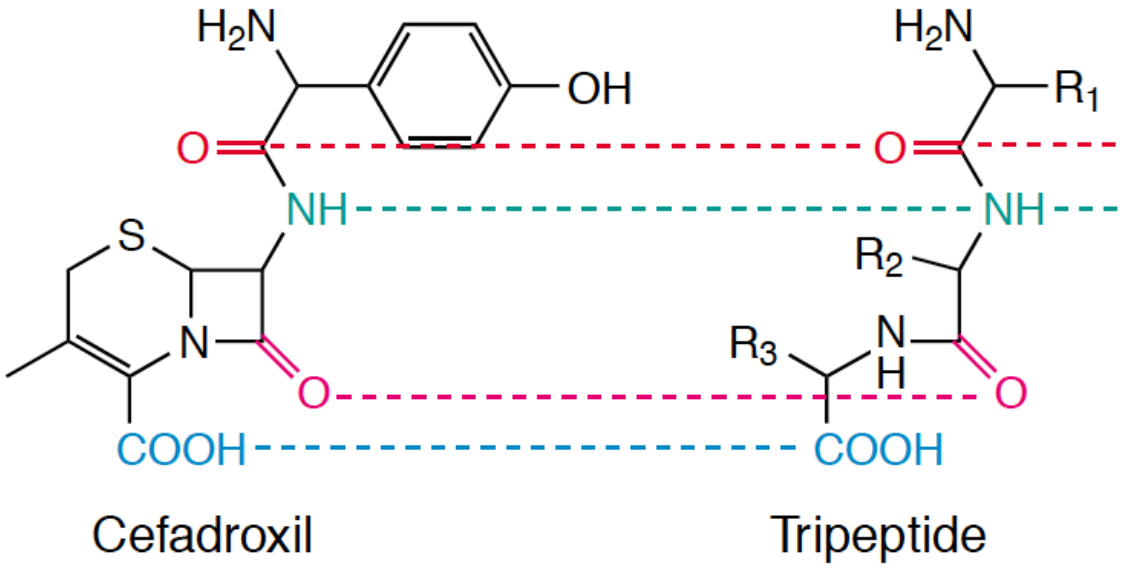

Figure 2.10. Structural similarities between a tri-peptide and cefadroxil. Both molecules have carboxylic groups and amino terminal groups separated by a carbon backbone of similar length. They also have the peptide bond in the L-conformation. Extracted from: Rubio I. and Daniel H. Trends in Pharmacological Sciences, Volume 23, Issue 9, 434-440, 1 September 2002.

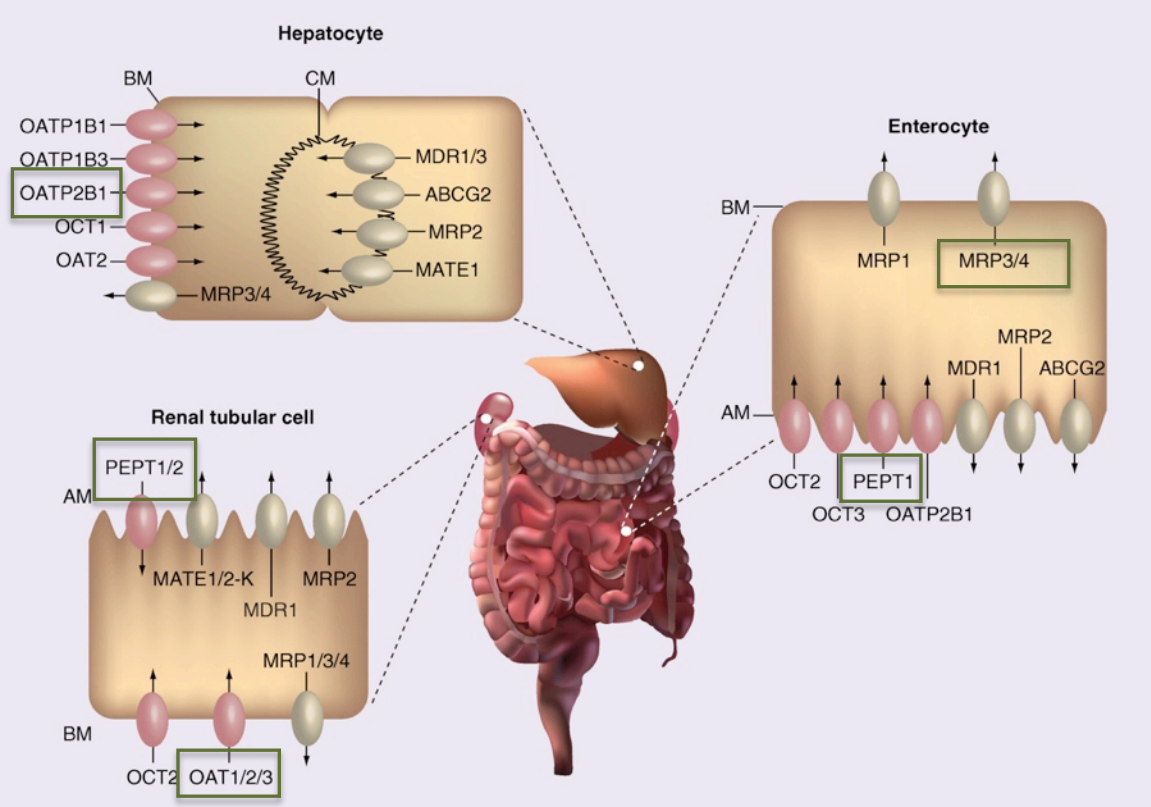

Figure 2.11. Some of the transporter proteins involved in the uptake of cefadroxil in different tissues of the body. PEPT1 is expressed mainly on the apical membrane of the enterocyte, but also at lower levels on the apical membrane of the kidney tubular cells (S1). PEPT2 is responsible for most of the reabsorption of cefadroxil in the kidney. It is expressed on the apical membrane of the renal tubular cells in the S2 and S3 segments of the proximal tubule. The organic anion transporters 1, 2, and 3 (OAT 1/2/3) have been shown to be responsible for the active secretion of cefadroxil in the kidney tubular cells. OATP2B1 expressed in the liver has been shown to uptake cefadroxil into the hepatocytes from the basolateral membrane. Extracted from: Zair *et al.* Pharmacogenomics 2008 9(5).

Tables

TRANSPOTER	SITE OF EXPRESSION	REFERENCES
PEPT1 (SLC15A1)	Small Intestine (apical membrane of enterocytes)	[78, 119, 120]
	Kidney (apical membrane of epithelial cells)	[37]
	Pancreas (lysosomes of acinar cells)	[121]
	Bile Duct (apical membrane of cholangiocytes)	[122]
	Liver (lysosomes)	[123]
	Blood (monocytes)	[124]
PEPT2 (SLC15A2)	Kidney (apical membrane epithelial cells)	[125-127]
	Brain (epithelial cells in choroid plexus, astrocytes and sub- and ependymal cells)	[28, 111]
	Lung (epithelial cells in bronchii and trachea, alveolar pneumocytes)	[26, 128, 129]
	Mammary gland (epithelial cells in glands and ducts	[130]
	Macrophages and glial cells of enteric nervous system	[23]
PHT1 (SLC15A4)	Brain	[35]
	Eye	[35]
PHT2 (SLC 15A3)	Brain	[36]
	Thymus and lymphatic system	[36]
	Lung	[36]
	Spleen	[36]

Table 2.1. Localization of peptide transporters.

PROPERTY	PEPT1	PEPT2	PHT1	PHT2
Gene	SLC15A1	SLC15A2	SLC15A4	SLC15A3
Amino Acids	707 - 710	729	572	582
Transmembrane Domains	12	12	12	12
AA identity	80 – 90 % (species)	80 – 90 % (species) 50% (PEPT1)	< 20% (PEPT1)	50% (PHT1) < 20% (PEPT1)
Amino Acids in Substrate	2-3	2-3	2-3	2-3
L-Histidine	No	No	Yes	Yes
Substrate Affinity	Low	High	High	?
K_m **range**	mM	µM	µM	?
Transport Type	Proton co-transporter	Proton co-transporter	Proton co-transporter	Proton co-transporter

Table 2.2 Molecular and functional features of the 4 identified human peptide transporters.

TRANSPORTER	LOCATION	SYSTEM USED	REFERENCE
PEPT1	Small intestine Kidney (proximal tubule)	Caco-2 cells, Oocytes Oocytes, BBMV	[45, 55, 131] [55, 132]
PEPT2	Kidney (AP) CSF	KO mice, cells, BBMV Cells, KO mice	[132] [21] [111] [55] [21, 28, 29, 55, 111]
OAT3	Kidney (BL)	S2 cells (transfected)	[133] [112, 134]
OAT1	Kidney (BL)	S2 cells (transfected)	[112, 133, 134]
OAT2 (rat)	Kidney (BL)	S2 cells (transfected)	[133, 134]
OAT4	Kidney (BL)	S2 cells (transfected)	[133, 134]
OATP2	Liver rat (BL)	Oocytes	[113]
MRP3/4	Intestine	Oocytes	[115]

Table 2.3. Transporters involved in the transport of cefadroxil.

PHARMACOKINETIC PARAMETER	VALUE	REFERENCE
Clearance (mL/min)	181.5	[135]
Vd_{ss} (L)	17.05	[135]
% Excreted after 24 hours (I.V.)	93	[135]
F (%)	90.1	[135]
$T_{1/2}$ (min)	115	[136]
C_{max} (ug/mL) (500 mg) (1000 mg)	 15.1 30.8	[136]
T_{max} (min)	50	[136]
Cl/F (mL/min)	145 - 200	[136]

Table 2.4. Pharmacokinetic parameters of cefadroxil in adult humans.

References

1. Smith, M.E. and D.G. Morton, *The digestive system*. Systems of the body2001, Edinburgh ; New York: Churchill Livingstone. 237 p.
2. Gartner, L.P. and J.L. Hiatt, *Color textbook of histology*. 3rd ed2007, Philadelphia, PA: Saunders/Elsevier. xi, 573 p.
3. Alberts, B., *Molecular biology of the cell*. 5th ed2008, New York: Garland Science.
4. Tozer, T.N. and M. Rowland, *Introduction to pharmacokinetics and pharmacodynamics : the quantitative basis of drug therapy*2006, Philadelphia: Lippincott Williams & Wilkins. x, 326 p.
5. Adibi, S.A. and D.W. Mercer, *Protein digestion in human intestine as reflected in luminal, mucosal, and plasma amino acid concentrations after meals.* J Clin Invest, 1973. **52**(7): p. 1586-94.
6. Mathews, D.M. and S.A. Adibi, *Peptide absorption.* Gastroenterology, 1976. **71**(1): p. 151-61.
7. Brandsch, M., *Transport of drugs by proton-coupled peptide transporters: pearls and pitfalls.* Expert Opin Drug Metab Toxicol, 2009.
8. Agoram, B., W.S. Woltosz, and M.B. Bolger, *Predicting the impact of physiological and biochemical processes on oral drug bioavailability.* Adv Drug Deliv Rev, 2001. **50 Suppl 1**: p. S41-67.
9. Huang, W., S.L. Lee, and L.X. Yu, *Mechanistic approaches to predicting oral drug absorption.* AAPS J, 2009. **11**(2): p. 217-24.
10. Yu, L.X., et al., *Transport approaches to the biopharmaceutical design of oral drug delivery systems: prediction of intestinal absorption.* Adv Drug Deliv Rev, 1996. **19**(3): p. 359-76.
11. Yu, L.X. and G.L. Amidon, *A compartmental absorption and transit model for estimating oral drug absorption.* Int J Pharm, 1999. **186**(2): p. 119-25.
12. Bolger, M.B., V. Lukacova, and W.S. Woltosz, *Simulations of the nonlinear dose dependence for substrates of influx and efflux transporters in the human intestine.* AAPS J, 2009. **11**(2): p. 353-63.
13. Tubic, M., et al., *In silico modeling of non-linear drug absorption for the P-gp substrate talinolol and of consequences for the resulting pharmacodynamic effect.* Pharm Res, 2006. **23**(8): p. 1712-20.
14. Abuasal, B.S., et al., *In silico modeling for the nonlinear absorption kinetics of UK-343,664: a P-gp and CYP3A4 substrate.* Mol Pharm, 2012. **9**(3): p. 492-504.
15. Paulsen, I.T. and R.A. Skurray, *The POT family of transport proteins.* Trends Biochem Sci, 1994. **19**(10): p. 404.
16. Wang, M., et al., *Comparative analysis of vertebrate PEPT1 and PEPT2 genes.* Genetica, 2010. **138**(6): p. 587-99.
17. Kamal, M.A., R.F. Keep, and D.E. Smith, *Role and relevance of PEPT2 in drug disposition, dynamics, and toxicity.* Drug Metab Pharmacokinet, 2008. **23**(4): p. 236-42.
18. Fei, Y.J., et al., *Expression cloning of a mammalian proton-coupled oligopeptide transporter.* Nature, 1994. **368**(6471): p. 563-6.

19. Boll, M., et al., *Expression cloning of a cDNA from rabbit small intestine related to proton-coupled transport of peptides, beta-lactam antibiotics and ACE-inhibitors.* Pflugers Arch, 1994. **429**(1): p. 146-9.
20. Liang, R., et al., *Human intestinal H+/peptide cotransporter. Cloning, functional expression, and chromosomal localization.* J Biol Chem, 1995. **270**(12): p. 6456-63.
21. Shen, H., et al., *Localization of PEPT1 and PEPT2 proton-coupled oligopeptide transporter mRNA and protein in rat kidney.* Am J Physiol, 1999. **276**(5 Pt 2): p. F658-65.
22. Botka, C.W., et al., *Human proton/oligopeptide transporter (POT) genes: identification of putative human genes using bioinformatics.* AAPS PharmSci, 2000. **2**(2): p. E16.
23. Ruhl, A., et al., *Functional expression of the peptide transporter PEPT2 in the mammalian enteric nervous system.* J Comp Neurol, 2005. **490**(1): p. 1-11.
24. Shu, C., et al., *Role of PEPT2 in peptide/mimetic trafficking at the blood-cerebrospinal fluid barrier: studies in rat choroid plexus epithelial cells in primary culture.* J Pharmacol Exp Ther, 2002. **301**(3): p. 820-9.
25. Biegel, A., et al., *The renal type H+/peptide symporter PEPT2: structure-affinity relationships.* Amino Acids, 2006. **31**(2): p. 137-56.
26. Groneberg, D.A., et al., *Localization of the peptide transporter PEPT2 in the lung: implications for pulmonary oligopeptide uptake.* Am J Pathol, 2001. **158**(2): p. 707-14.
27. Shen, H., et al., *Targeted disruption of the PEPT2 gene markedly reduces dipeptide uptake in choroid plexus.* J Biol Chem, 2003. **278**(7): p. 4786-91.
28. Shen, H., et al., *PEPT2 (Slc15a2)-mediated unidirectional transport of cefadroxil from cerebrospinal fluid into choroid plexus.* J Pharmacol Exp Ther, 2005. **315**(3): p. 1101-8.
29. Ocheltree, S.M., et al., *Mechanisms of cefadroxil uptake in the choroid plexus: studies in wild-type and PEPT2 knockout mice.* J Pharmacol Exp Ther, 2004. **308**(2): p. 462-7.
30. Smith, D.E., et al., *Distribution of glycylsarcosine and cefadroxil among cerebrospinal fluid, choroid plexus, and brain parenchyma after intracerebroventricular injection is markedly different between wild-type and Pept2 null mice.* J Cereb Blood Flow Metab, 2011. **31**(1): p. 250-61.
31. Rubio-Aliaga, I., M. Boll, and H. Daniel, *Cloning and characterization of the gene encoding the mouse peptide transporter PEPT2.* Biochem Biophys Res Commun, 2000. **276**(2): p. 734-41.
32. Ganapathy, V. and F.H. Leibach, *Role of pH gradient and membrane potential in dipeptide transport in intestinal and renal brush-border membrane vesicles from the rabbit. Studies with L-carnosine and glycyl-L-proline.* J Biol Chem, 1983. **258**(23): p. 14189-92.
33. Ganapathy, V. and F.H. Leibach, *Peptide transport in rabbit kidney. Studies with L-carnosine.* Biochim Biophys Acta, 1982. **691**(2): p. 362-6.
34. Daniel, H. and G. Kottra, *The proton oligopeptide cotransporter family SLC15 in physiology and pharmacology.* Pflugers Arch, 2004. **447**(5): p. 610-8.

35. Yamashita, T., et al., *Cloning and functional expression of a brain peptide/histidine transporter.* J Biol Chem, 1997. **272**(15): p. 10205-11.
36. Sakata, K., et al., *Cloning of a lymphatic peptide/histidine transporter.* Biochem J, 2001. **356**(Pt 1): p. 53-60.
37. Doring, F., et al., *Functional analysis of a chimeric mammalian peptide transporter derived from the intestinal and renal isoforms.* J Physiol, 1996. **497 (Pt 3)**: p. 773-9.
38. Terada, T., et al., *N-terminal halves of rat H+/peptide transporters are responsible for their substrate recognition.* Pharm Res, 2000. **17**(1): p. 15-20.
39. Fei, Y.J., V. Ganapathy, and F.H. Leibach, *Molecular and structural features of the proton-coupled oligopeptide transporter superfamily.* Prog Nucleic Acid Res Mol Biol, 1998. **58**: p. 239-61.
40. Chen, X.Z., A. Steel, and M.A. Hediger, *Functional roles of histidine and tyrosine residues in the H(+)-peptide transporter PEPT1.* Biochem Biophys Res Commun, 2000. **272**(3): p. 726-30.
41. Links, J.L., et al., *Cysteine scanning of transmembrane domain three of the human dipeptide transporter: implications for substrate transport.* J Drug Target, 2007. **15**(3): p. 218-25.
42. Yeung, A.K., et al., *Molecular identification of a role for tyrosine 167 in the function of the human intestinal proton- coupled dipeptide transporter (hPEPT1).* Biochem Biophys Res Commun, 1998. **250**(1): p. 103-7.
43. Amasheh, S., et al., *Transport of charged dipeptides by the intestinal H+/peptide symporter PEPT1 expressed in Xenopus laevis oocytes.* J Membr Biol, 1997. **155**(3): p. 247-56.
44. Steel, A., et al., *Stoichiometry and pH dependence of the rabbit proton-dependent oligopeptide transporter PEPT1.* J Physiol, 1997. **498 (Pt 3)**: p. 563-9.
45. Wenzel, U., et al., *Transport characteristics of differently charged cephalosporin antibiotics in oocytes expressing the cloned intestinal peptide transporter PEPT1 and in human intestinal Caco-2 cells.* J Pharmacol Exp Ther, 1996. **277**(2): p. 831-9.
46. Amasheh, S., et al., *Electrophysiological analysis of the function of the mammalian renal peptide transporter expressed in Xenopus laevis oocytes.* J Physiol, 1997. **504 (Pt 1)**: p. 169-74.
47. Knutter, I., et al., *A novel inhibitor of the mammalian peptide transporter PEPT1.* Biochemistry, 2001. **40**(14): p. 4454-8.
48. Daniel, H., *Molecular and integrative physiology of intestinal peptide transport.* Annu Rev Physiol, 2004. **66**: p. 361-84.
49. Doring, F., et al., *Minimal molecular determinants of substrates for recognition by the intestinal peptide transporter.* J Biol Chem, 1998. **273**(36): p. 23211-8.
50. Meredith, D., et al., *Modified amino acids and peptides as substrates for the intestinal peptide transporter PEPT1.* Eur J Biochem, 2000. **267**(12): p. 3723-8.
51. Theis, S., et al., *Defining minimal structural features in substrates of the H(+)/peptide cotransporter PEPT2 using novel amino acid and dipeptide derivatives.* Mol Pharmacol, 2002. **61**(1): p. 214-21.

52. Brandsch, M., et al., *Decisive structural determinants for the interaction of proline derivatives with the intestinal H+/peptide symporter.* Eur J Biochem, 1999. **266**(2): p. 502-8.
53. Theis, S., et al., *Synthesis and characterization of high affinity inhibitors of the H+/peptide transporter PEPT2.* J Biol Chem, 2002. **277**(9): p. 7287-92.
54. Okano, T., et al., *H+ coupled uphill transport of aminocephalosporins via the dipeptide transport system in rabbit intestinal brush-border membranes.* J Biol Chem, 1986. **261**(30): p. 14130-4.
55. Ganapathy, M.E., et al., *Differential recognition of beta -lactam antibiotics by intestinal and renal peptide transporters, PEPT 1 and PEPT 2.* J Biol Chem, 1995. **270**(43): p. 25672-7.
56. Tamai, I., et al., *Functional expression of transporter for beta-lactam antibiotics and dipeptides in Xenopus laevis oocytes injected with messenger RNA from human, rat and rabbit small intestines.* J Pharmacol Exp Ther, 1995. **273**(1): p. 26-31.
57. Naasani, I., et al., *Transport mechanism of ceftibuten, a dianionic cephem, in rat renal brush-border membrane.* Pharm Res, 1995. **12**(4): p. 605-8.
58. Swaan, P.W., M.C. Stehouwer, and J.J. Tukker, *Molecular mechanism for the relative binding affinity to the intestinal peptide carrier. Comparison of three ACE-inhibitors: enalapril, enalaprilat, and lisinopril.* Biochim Biophys Acta, 1995. **1236**(1): p. 31-8.
59. Saito, H. and K. Inui, *Dipeptide transporters in apical and basolateral membranes of the human intestinal cell line Caco-2.* Am J Physiol, 1993. **265**(2 Pt 1): p. G289-94.
60. Weller, S., et al., *Pharmacokinetics of the acyclovir pro-drug valaciclovir after escalating single- and multiple-dose administration to normal volunteers.* Clin Pharmacol Ther, 1993. **54**(6): p. 595-605.
61. Han, H.K. and G.L. Amidon, *Targeted prodrug design to optimize drug delivery.* AAPS PharmSci, 2000. **2**(1): p. E6.
62. Balimane, P.V., et al., *Direct evidence for peptide transporter (PEPT1)-mediated uptake of a nonpeptide prodrug, valacyclovir.* Biochem Biophys Res Commun, 1998. **250**(2): p. 246-51.
63. Hu, M., et al., *Use of the peptide carrier system to improve the intestinal absorption of L-alpha-methyldopa: carrier kinetics, intestinal permeabilities, and in vitro hydrolysis of dipeptidyl derivatives of L-alpha-methyldopa.* Pharm Res, 1989. **6**(1): p. 66-70.
64. Bai, J.P., *pGlu-L-Dopa-Pro: a tripeptide prodrug targeting the intestinal peptide transporter for absorption and tissue enzymes for conversion.* Pharm Res, 1995. **12**(7): p. 1101-4.
65. Hoffmeyer, S., et al., *Functional polymorphisms of the human multidrug-resistance gene: multiple sequence variations and correlation of one allele with P-glycoprotein expression and activity in vivo.* Proc Natl Acad Sci U S A, 2000. **97**(7): p. 3473-8.
66. Kim, R.B., et al., *Identification of functionally variant MDR1 alleles among European Americans and African Americans.* Clin Pharmacol Ther, 2001. **70**(2): p. 189-99.

67. Nishizato, Y., et al., *Polymorphisms of OATP-C (SLC21A6) and OAT3 (SLC22A8) genes: consequences for pravastatin pharmacokinetics.* Clin Pharmacol Ther, 2003. **73**(6): p. 554-65.
68. Leabman, M.K., et al., *Natural variation in human membrane transporter genes reveals evolutionary and functional constraints.* Proc Natl Acad Sci U S A, 2003. **100**(10): p. 5896-901.
69. Zhang, E.Y., et al., *Genetic polymorphisms in human proton-dependent dipeptide transporter PEPT1: implications for the functional role of Pro586.* J Pharmacol Exp Ther, 2004. **310**(2): p. 437-45.
70. Anderle, P., et al., *Genetic variants of the human dipeptide transporter PEPT1.* J Pharmacol Exp Ther, 2006. **316**(2): p. 636-46.
71. Pan, X., et al., *Diurnal rhythm of H+-peptide cotransporter in rat small intestine.* Am J Physiol Gastrointest Liver Physiol, 2002. **283**(1): p. G57-64.
72. Pan, X., et al., *Altered diurnal rhythm of intestinal peptide transporter by fasting and its effects on the pharmacokinetics of ceftibuten.* J Pharmacol Exp Ther, 2003. **307**(2): p. 626-32.
73. Pan, X., et al., *The diurnal rhythm of the intestinal transporters SGLT1 and PEPT1 is regulated by the feeding conditions in rats.* J Nutr, 2004. **134**(9): p. 2211-5.
74. Ferraris, R.P. and H.V. Carey, *Intestinal transport during fasting and malnutrition.* Annu Rev Nutr, 2000. **20**: p. 195-219.
75. Ferraris, R.P., J. Diamond, and W.W. Kwan, *Dietary regulation of intestinal transport of the dipeptide carnosine.* Am J Physiol, 1988. **255**(2 Pt 1): p. G143-50.
76. Ma, K., Y. Hu, and D.E. Smith, *Influence of fed-fasted state on intestinal PEPT1 expression and in vivo pharmacokinetics of glycylsarcosine in wild-type and PEPT1 knockout mice.* Pharm Res, 2012. **29**(2): p. 535-45.
77. Thamotharan, M., et al., *Mechanism of dipeptide stimulation of its own transport in a human intestinal cell line.* Proc Assoc Am Physicians, 1998. **110**(4): p. 361-8.
78. Walker, D., et al., *Substrate upregulation of the human small intestinal peptide transporter, hPEPT1.* J Physiol, 1998. **507 (Pt 3)**: p. 697-706.
79. Erickson, R.H., et al., *Regional expression and dietary regulation of rat small intestinal peptide and amino acid transporter mRNAs.* Biochem Biophys Res Commun, 1995. **216**(1): p. 249-57.
80. Barbot, L., et al., *Intestinal peptide transporter PEPT1 is over-expressed during acute cryptosporidiosis in suckling rats as a result of both malnutrition and experimental parasite infection.* Parasitol Res, 2003. **89**(5): p. 364-70.
81. Merlin, D., et al., *Colonic epithelial hPEPT1 expression occurs in inflammatory bowel disease: transport of bacterial peptides influences expression of MHC class 1 molecules.* Gastroenterology, 2001. **120**(7): p. 1666-79.
82. Merlin, D., et al., *hPEPT1-mediated epithelial transport of bacteria-derived chemotactic peptides enhances neutrophil-epithelial interactions.* J Clin Invest, 1998. **102**(11): p. 2011-8.

83. Vavricka, S.R., et al., *hPEPT1 transports muramyl dipeptide, activating NF-kappaB and stimulating IL-8 secretion in human colonic Caco2/bbe cells.* Gastroenterology, 2004. **127**(5): p. 1401-9.
84. Wojtal, K.A., et al., *Changes in mRNA expression levels of solute carrier transporters in inflammatory bowel disease patients.* Drug Metab Dispos, 2009. **37**(9): p. 1871-7.
85. Dalmasso, G., et al., *MicroRNA-92b regulates expression of the oligopeptide transporter PEPT1 in intestinal epithelial cells.* Am J Physiol Gastrointest Liver Physiol, 2011. **300**(1): p. G52-9.
86. Thamotharan, M., et al., *Hormonal regulation of oligopeptide transporter pept-1 in a human intestinal cell line.* Am J Physiol, 1999. **276**(4 Pt 1): p. C821-6.
87. Gangopadhyay, A., M. Thamotharan, and S.A. Adibi, *Regulation of oligopeptide transporter (Pept-1) in experimental diabetes.* Am J Physiol Gastrointest Liver Physiol, 2002. **283**(1): p. G133-8.
88. Nielsen, C.U., et al., *Epidermal growth factor and insulin short-term increase hPEPT1-mediated glycylsarcosine uptake in Caco-2 cells.* Acta Physiol Scand, 2003. **178**(2): p. 139-48.
89. Nielsen, C.U., et al., *Epidermal growth factor inhibits glycylsarcosine transport and hPEPT1 expression in a human intestinal cell line.* Am J Physiol Gastrointest Liver Physiol, 2001. **281**(1): p. G191-9.
90. Buyse, M., et al., *PEPT1-mediated epithelial transport of dipeptides and cephalexin is enhanced by luminal leptin in the small intestine.* J Clin Invest, 2001. **108**(10): p. 1483-94.
91. Adibi, S.A., *Regulation of expression of the intestinal oligopeptide transporter (Pept-1) in health and disease.* Am J Physiol Gastrointest Liver Physiol, 2003. **285**(5): p. G779-88.
92. Ashida, K., et al., *Thyroid hormone regulates the activity and expression of the peptide transporter PEPT1 in Caco-2 cells.* Am J Physiol Gastrointest Liver Physiol, 2002. **282**(4): p. G617-23.
93. Ashida, K., et al., *Decreased activity and expression of intestinal oligopeptide transporter PEPT1 in rats with hyperthyroidism in vivo.* Pharm Res, 2004. **21**(6): p. 969-75.
94. Sun, B.W., et al., *Hormonal regulation of dipeptide transporter (PEPT1) in Caco-2 cells with normal and anoxia/reoxygenation management.* World J Gastroenterol, 2003. **9**(4): p. 808-12.
95. Watanabe, K., T. Jinriki, and J. Sato, *Effects of progesterone and norethisterone on cephalexin uptake in the human intestinal cell line Caco-2.* Biol Pharm Bull, 2004. **27**(4): p. 559-63.
96. Watanabe, K., T. Jinriki, and J. Sato, *Effects of progesterone and norethisterone on cephalexin transport and peptide transporter PEPT1 expression in human intestinal cell line Caco-2.* Biol Pharm Bull, 2006. **29**(1): p. 90-5.
97. Berlioz, F., et al., *Neural modulation of cephalexin intestinal absorption through the di- and tripeptide brush border transporter of rat jejunum in vivo.* J Pharmacol Exp Ther, 1999. **288**(3): p. 1037-44.

98. Tanaka, H., et al., *Regulation of the PEPT1 peptide transporter in the rat small intestine in response to 5-fluorouracil-induced injury.* Gastroenterology, 1998. **114**(4): p. 714-23.
99. Westphal, J.F., et al., *Amoxicillin intestinal absorption reduction by amiloride: possible role of the Na(+) -H+ exchanger.* Clin Pharmacol Ther, 1995. **57**(3): p. 257-64.
100. Motohashi, H., et al., *Effects of tacrolimus and cyclosporin A on peptide transporter PEPT1 in Caco-2 cells.* Pharm Res, 2001. **18**(5): p. 713-7.
101. Connors, K.A., G.L. Amidon, and V.J. Stella, *Chemical stability of pharmaceuticals : a handbook for pharmacists*. 2nd ed1986, New York: Wiley. xii, 847 p.
102. Finch, R.G. and L.P. Garrod, *Antibiotic and chemotherapy : anti-infective agents and their use in therapy*. 8th ed2003, Edinburgh ; New York: Churchill Livingstone. xii, 964 p.
103. Queener, S.F., J.A. Webber, and S.W. Queener, *Beta-lactam antibiotics for clinical use*. Clinical pharmacology v. 41986, New York: M. Dekker. xv, 673 p.
104. Tanrisever, B. and P.J. Santella, *Cefadroxil. A review of its antibacterial, pharmacokinetic and therapeutic properties in comparison with cephalexin and cephradine.* Drugs, 1986. **32 Suppl 3**: p. 1-16.
105. Goodman, L.S., et al., *Goodman & Gilman's the pharmacological basis of therapeutics*. 11th ed2006, New York: McGraw-Hill. xxiii, 2021 p.
106. Kimura, T., et al., *Characterization of aminocephalosporin transport across rat small intestine.* J Pharmacobiodyn, 1983. **6**(4): p. 246-53.
107. Inui, K., et al., *H+ coupled transport of p.o. cephalosporins via dipeptide carriers in rabbit intestinal brush-border membranes: difference of transport characteristics between cefixime and cephradine.* J Pharmacol Exp Ther, 1988. **247**(1): p. 235-41.
108. Kimura, T., et al., *Transport of cefadroxil, an aminocephalosporin antibiotic, across the small intestinal brush border membrane.* Biochem Pharmacol, 1985. **34**(1): p. 81-4.
109. Takano, M., et al., *Transport of cephalosporin antibiotics in rat renal basolateral membranes.* J Pharm Pharmacol, 1989. **41**(11): p. 795-6.
110. Tamai, I., et al., *Functional expression of intestinal dipeptide/beta-lactam antibiotic transporter in Xenopus laevis oocytes.* Biochem Pharmacol, 1994. **48**(5): p. 881-8.
111. Shen, H., et al., *Impact of genetic knockout of PEPT2 on cefadroxil pharmacokinetics, renal tubular reabsorption, and brain penetration in mice.* Drug Metab Dispos, 2007. **35**(7): p. 1209-16.
112. Ueo, H., et al., *Human organic anion transporter hOAT3 is a potent transporter of cephalosporin antibiotics, in comparison with hOAT1.* Biochem Pharmacol, 2005. **70**(7): p. 1104-13.
113. Nakakariya, M., et al., *Predominant contribution of rat organic anion transporting polypeptide-2 (Oatp2) to hepatic uptake of beta-lactam antibiotics.* Pharm Res, 2008. **25**(3): p. 578-85.
114. Ci, L., et al., *Involvement of MRP4 (ABCC4) in the luminal efflux of ceftizoxime and cefazolin in the kidney.* Mol Pharmacol, 2007. **71**(6): p. 1591-7.

115. de Waart, D.R., et al., *Oral availability of cefadroxil depends on ABCC3 and ABCC4.* Drug Metab Dispos, 2012. **40**(3): p. 515-21.
116. Terada, T. and K. Inui, *Physiological and pharmacokinetic roles of H+/organic cation antiporters (MATE/SLC47A).* Biochem Pharmacol, 2008. **75**(9): p. 1689-96.
117. Terada, T., et al., *Molecular cloning, functional characterization and tissue distribution of rat H+/organic cation antiporter MATE1.* Pharm Res, 2006. **23**(8): p. 1696-701.
118. Masuda, S., et al., *Identification and functional characterization of a new human kidney-specific H+/organic cation antiporter, kidney-specific multidrug and toxin extrusion 2.* J Am Soc Nephrol, 2006. **17**(8): p. 2127-35.
119. Groneberg, D.A., et al., *Intestinal peptide transport: ex vivo uptake studies and localization of peptide carrier PEPT1.* Am J Physiol Gastrointest Liver Physiol, 2001. **281**(3): p. G697-704.
120. Ogihara, H., et al., *Immuno-localization of H+/peptide cotransporter in rat digestive tract.* Biochem Biophys Res Commun, 1996. **220**(3): p. 848-52.
121. Bockman, D.E., et al., *Localization of peptide transporter in nuclei and lysosomes of the pancreas.* Int J Pancreatol, 1997. **22**(3): p. 221-5.
122. Knutter, I., et al., *H+-peptide cotransport in the human bile duct epithelium cell line SK-ChA-1.* Am J Physiol Gastrointest Liver Physiol, 2002. **283**(1): p. G222-9.
123. Thamotharan, M., et al., *An active mechanism for completion of the final stage of protein degradation in the liver, lysosomal transport of dipeptides.* J Biol Chem, 1997. **272**(18): p. 11786-90.
124. Charrier, L., et al., *hPEPT1 mediates bacterial tripeptide fMLP uptake in human monocytes.* Lab Invest, 2006. **86**(5): p. 490-503.
125. Boll, M., et al., *Expression cloning and functional characterization of the kidney cortex high-affinity proton-coupled peptide transporter.* Proc Natl Acad Sci U S A, 1996. **93**(1): p. 284-9.
126. Rubio-Aliaga, I., et al., *Targeted disruption of the peptide transporter Pept2 gene in mice defines its physiological role in the kidney.* Mol Cell Biol, 2003. **23**(9): p. 3247-52.
127. Ocheltree, S.M., et al., *Role and relevance of peptide transporter 2 (PEPT2) in the kidney and choroid plexus: in vivo studies with glycylsarcosine in wild-type and PEPT2 knockout mice.* J Pharmacol Exp Ther, 2005. **315**(1): p. 240-7.
128. Groneberg, D.A., et al., *Distribution and function of the peptide transporter PEPT2 in normal and cystic fibrosis human lung.* Thorax, 2002. **57**(1): p. 55-60.
129. Groneberg, D.A., et al., *Molecular mechanisms of pulmonary peptidomimetic drug and peptide transport.* Am J Respir Cell Mol Biol, 2004. **30**(3): p. 251-60.
130. Groneberg, D.A., et al., *Peptide transport in the mammary gland: expression and distribution of PEPT2 mRNA and protein.* Am J Physiol Endocrinol Metab, 2002. **282**(5): p. E1172-9.
131. Naruhashi, K., et al., *PEPT1 mRNA expression is induced by starvation and its level correlates with absorptive transport of cefadroxil longitudinally in the rat intestine.* Pharm Res, 2002. **19**(10): p. 1417-23.

132. Ries, M., U. Wenzel, and H. Daniel, *Transport of cefadroxil in rat kidney brush-border membranes is mediated by two electrogenic H+-coupled systems.* J Pharmacol Exp Ther, 1994. **271**(3): p. 1327-33.
133. Takeda, M., et al., *Interaction of human organic anion transporters with various cephalosporin antibiotics.* Eur J Pharmacol, 2002. **438**(3): p. 137-42.
134. Khamdang, S., et al., *Interaction of human and rat organic anion transporter 2 with various cephalosporin antibiotics.* Eur J Pharmacol, 2003. **465**(1-2): p. 1-7.
135. Marino, E.L., A. Dominguez-Gil, and C. Muriel, *Influence of dosage form and administration route on the pharmacokinetic parameters of cefadroxil.* Int J Clin Pharmacol Ther Toxicol, 1982. **20**(2): p. 73-7.
136. Barbhaiya, R.H., *A pharmacokinetic comparison of cefadroxil and cephalexin after administration of 250, 500 and 1000 mg solution doses.* Biopharm Drug Dispos, 1996. **17**(4): p. 319-30.

CHAPTER 3

INTESTINAL PERMEABILITY OF CEFADROXIL IN WILD-TYPE AND PEPT1 KNOCKOUT MICE

Abstract

The purpose of this study was to determine the contribution of PEPT1 on cefadroxil intestinal permeability and the influence of concentration, segment, potential inhibitors, and pH on drug uptake. The effective permeability (P_{eff}) of cefadroxil was measured using single pass perfusion in the duodenum, jejunum, ileum and colon of wild-type and PEPT1 knockout mice. The P_{eff} values (cm/s) of cefadroxil in wild-type mice were: $4.94*10^{-5}$ in duodenum, $8.01*10^{-5}$ in jejunum, $8.81*10^{-5}$ in ileum and $6.36\ 10^{-6}$ in colon, and in knockout mice were: $2.87*10^{-7}$, $8.97*10^{-6}$, $4.19*10^{-6}$ and $3.15*10^{-6}$ cm/s, respectively. The P_{eff} values for the small intestine were significantly different between both genotypes ($p<0.05$), but there was no difference in colon. The uptake of cefadroxil was a saturable process, with a $K'_m$of 3.8 mM and a V'_{max} of 4.75 nmol/cm^2/s. The bulk pH had no significant effect on the drug uptake. There was a significant reduction in the P_{eff} when PEPT1

substrates, such as Gly-Pro and Gly-Sar, were co-perfused, but high concentrations of amino acids, as well as an organic acid and base did not affect the permeability. The findings show that PEPT1 is the major transporter involved in the uptake of cefadroxil in the small intestine, accounting for about 90% of the P_{eff} of this antibiotic.

Key Words

Cefadroxil, PEPT1, Single Pass Intestinal Perfusion, Effective permeability, Knockout Mice, Intestinal Permeability.

Introduction

Proton oligopeptide transporters (POT's) are a family of membrane transport proteins present in a broad range of species, from bacteria to mammals, that transport proteins transport di- and tripeptides—themselves products of protein degradation—and other peptide-like molecules. This uptake process occurs with the co-transport of protons into the cytosol, against a peptide concentration gradient and down an inwardly directed proton gradient and a negative membrane potential [1] [2-4].

Four types of peptide transporters have been cloned and identified: PEPT1, PEPT2, PHT1 and PHT2 [4-6]. PEPT1 is a high-capacity and low-affinity transporter that moves di- and tripeptides with different sequences and charges, but not single amino acids or peptides longer than 3 amino acid residues. [4, 7, 8] [9]. It is expressed predominantly in the small intestine, and to a lesser extent in the kidney, pancreas, and liver [10-12]. Previous studies from our group showed that PEPT1 is expressed at the apical membrane of enterocytes in the duodenum, jejunum and ileum of mice, but not in colon[8, 13]. These studies also demonstrated that in PEPT1 knockout mice, a mouse model also developed by our group, the effective permeability of Gly-Sar was significantly reduced in the small intestine (<10-fold) compared to wild-type mice [13]. Furthermore, it was also shown that the concomitant administration of cefadroxil at high concentrations reduced significantly the effective permeability of Gly-Sar in the small intestine [8].

Understanding the importance of PEPT1 contribution to the absorption and disposition of drugs has been a goal of several research groups for the past couple of

decades. This transporter has been shown to be involved in the pharmacokinetics of many drugs that resemble di- and tripeptides, such as betalactam antibiotics, ACE inhibitors, and some anticancer drugs like bestatin, but little is known about the actual contribution and relevance of PEPT1 to the absorption of cefadroxil [14-20].

Cefadroxil is a first generation cephalosporin, use to treat a diverse range of bacterial infections, such as urinary tract infections cause by E. coli and P. mirabilis, and pneumonia caused by *S. pyogenes* [21]. This broad-spectrum amino-cephalosporin has a high bioavailability, despite its charge and poor lipophilicity at intestinal pH. Cefadroxil is very stable, doesn't hydrolyze in the acidic environment of the stomach or degraded by intra- or extracellular enzymes and is eliminated almost completely intact in urine (>90%) in 24 hours. The absorption of cefadroxil isn't affected by food, and this drug's half-life is around 95 minutes, which is longer than that of other cephalosporins of the same generation. It is extensively distributed to several tissues, including the lung, tonsils, placenta, bone, muscle, and prostate and is approximately 20% bound to plasma proteins [21, 22].

The absorption of cefadroxil from the small intestine it's a process that has been shown to have Michaelis-Menten kinetics. [23-25] [26, 27]. It has also been demonstrated that due to its chemical structure resemblance to physiological occurring peptides, such as an alpha amino group, a carboxylic end, and a peptide bond, cefadroxil is a substrate of PEPT1 [14, 28]. However, other transporters also have been implicated in the transport of cefadroxil. For example, PEPT2 has been shown to be responsible for most of the reabsorption of cefadroxil from the urine back to the blood, increasing the half-life of the drug and therefore increasing the

exposure of different tissues to the antibiotic [29]. On the other hand, PEPT2 has also been shown to act as an efflux transporter of cefadroxil from the cerebro-spinal fluid (CSF) in the choroid plexus, decreasing the concentration of this drug in the brain [30, 31].

Since Cefadroxil has a negative charge at the physiological pH, it can bind to organic anion transporters (OAT). These transporters are present in the basolateral membrane of the epithelial cells in the proximal renal tubules, and are thought to be responsible for the active secretion into the blood of several negatively charged endogenous and exogenous compounds, such as cefadroxil. Although, OAT1 and OAT3 are present in human kidney, OAT3 plays a stronger role than OAT1 in the active secretion of cephalosporins [32-34]. Also, experiments using Xenopous oocytes expressing OATP2, the organic anion transporting polypeptide-2, show that cefadroxil is also a substrate for this transporter [35].

Though we know that cefadroxil is a substrate for several transporting proteins, it is still unknown the importance of the contribution of these and passive diffusion to the total mass transfer process in the small intestine. Therefore the aim of this study is to evaluate the role of PEPT1 in the absorption process of cefadroxil in the different segments of the intestine, and also to evaluate the factors that affect it.

Materials and Methods

Chemicals

All chemicals were purchased from Sigma-Aldrich (St. Louis, MO).

Animals

All studies were done in 8-10 week old gender-matched wild-type (PEPT1+/+) and PEPT1 knockout (PEPT1-/-) mice. The animals were kept in a controlled temperature room with 12-hour light, 12-hour dark cycle, and had standard diet and water ad libitum. All of the procedures were approved by the University of Michigan Committee on Use and Care of Animals (UCUCA), and were carried out in accordance with the Guide for Use of Laboratory Animals as adopted and promulgated by the US National Institutes of Health (NIH publication No. 85-23, revised in 1985).

In Situ Single-Pass Intestinal Perfusion

Gender-matched wild-type (PEPT1+/+) and PEPT1 knockout (PEPT1-/-) mice were fasted overnight. Following anesthesia using sodium pentobarbital (40 mg/kg ip) the mice were placed on a heated pad to maintain body temperature and isopropyl alcohol was used to sterilize the abdomen. The abdomen was opened through a midline incision to expose the abdominal cavity and the small intestine. An 8 cm segment of the jejunum (proximal jejunum) was isolated by partially cutting the intestinal segment at the proximal and distal ends (2 cm distal from the Treitz ligament). Then, the intestinal segment was rinsed and cleaned with isotonic

saline solution, and two glass cannulas (1.9 mm in diameter) were inserted and fixed firmly at place with silk suture at both ends of it.

Subsequently, animals were transferred to a temperature-controlled chamber (31°C) to control body temperature, where the inlet cannula was connected to a 10 mL syringe containing 0.01 0M cefadroxil in perfusion buffer at pH 6.5. The perfusion buffer contains 10 mM 2-(N-morpholino)-ethanesulfonic acid (MES), 135 mM sodium chloride (NaCl), and 5 mM of potassium chloride (KCl). The intestinal segment was perfused at a rate of 0.1 mL/min for 90 minutes using a syringe pump (Harvard Apparatus, South Natick, MA). Water flux was measured using a gravimetric method. Animals were sacrificed at the end of the experiments before recovering from anesthesia.

Regional Permeability Experiments

The effective permeability of cefadroxil was measured in all the three segments of the small intestine and in the colon. For duodenal permeability an intestinal segment of approximately 2 cm in length were isolated, starting at the end of the stomach and ending at the ligament of Treitz. For jejunal permeability experiments, an 8 cm segment was isolated starting at 2 cm distal to the ligament of Treitz. For ileum permeability a 6 cm segment was isolated 1 cm proximal of the ceacum. For the colon, a segment of 4 cm was isolated starting at 1 cm distal to the ceacum. All experiments were performed at pH 6.5, and with 0.01 mM cefadroxil.

Analytical Method

The samples from the in-situ perfusion experiments were assayed by High Performance Liquid Chromatography (HPLC) using a Waters 616 pump, a Waters 717 auto-sampler, and a photodiodode array UV detector (Waters 2487 dual λ absorbance). The column used was a Waters ODS-3 column (2.50*4.6mm), the injection volume was 20 µL, the flow rate 1 mL/min, and the detection wavelength 265 nm. The isocratic mobile phase was a mixture of 90:10 % v/v of aqueous/organic phase. The aqueous phase consisted of 0.01% trifluoroacetic acid (TFA) in water, and the organic phase of 0.01% of TFA in acetonitrile. The perfusion samples were centrifuged at 11000x g for 10 minutes and the supernatant was used for the HPLC measurements. The calibration graphs for the cefadroxil standards were linear over the concentration ranges of 0.001 to 25 mM, and the retention time for cefadroxil was 11 minutes.

Data Analysis

The effective permeability (P_{eff}) of cefadroxil was calculated according to the complete radial mixing model (parallel tube) described by [36] [37] as follow:

$$P_{eff} = \frac{-Q \ln\left(C_{out} / C_{in}\right)}{2\pi RL} \tag{3.1}$$

where Q is the perfusion rate, Cin and Cout are the concentrations of drug coming into the intestinal segment and coming out of it (corrected for water flux), and R and L are the radius and the length of the intestinal segment, respectively.

Then, the C_{in} and P_{eff} values used to obtain the steady-state flux through the epithelial membrane J:

$$J = C_{in} \cdot P_{eff} \tag{3.2}$$

The apparent Michaelis-Menten parameters V'_{max} and K'_m were calculated, using the following formula:

$$J = \frac{V'_{\max} \cdot C_{in}}{K'_m + C_{in}} \tag{3.3}$$

The problem of using this method is that it overestimates value of the K'_m, because it doesn't take into account the permeability of cefadroxil through the unstirred water layer present in the small intestine. Though, it became necessary to separate the permeability of cefadroxil through the aqueous layer (P_{aq}), from the permeability of it through the intestinal wall (P_w) using the method described by [23, 24, 38]. The following formula is used to calculate P_w:

$$P_w = \frac{P_{eff}}{1 - P_{eff}/P_{aq}} \tag{3.4}$$

Then, the boundary layer approach was used to calculate the aqueous permeability (P_{aq}), and therefore the wall permeability, according to:

$$P_{aq} = (A\frac{R}{D}G_z^{1/3})^{-1} \tag{3.5}$$

where A is a unitless constant (A = 2.50 Gz + 1.125), R is the radius, D is the diffusion coefficient of cefadroxil in water, and Gz is the Graetz number, which is the

ratio of the mean residence time of a fluid in the intestine ($t_{res} = \pi R^2 L/Q$) to the mean radial diffusion time of a solute ($t_{diff} = 2R^2/D$) and is calculated according to:

$$G_z = \frac{\pi DL}{2Q} \tag{3.6}$$

Once the aqueous and the wall and aqueous permeability were calculated, the concentration of drug at the surface of the epithelial membrane (C_w) was calculated as:

$$C_w = C_{in}\left(\frac{1 - P_{eff}}{P_{aq}}\right) \tag{3.7}$$

Then the intrinsic parameters K_m and V_{max} were be subsequently found with the following equation:

$$J = \frac{V_{\max} \cdot C_w}{K_m + C_w} \tag{3.8}$$

In addition the data was also fitted to a more complex model that included both a saturable and a non-saturable (passive diffusion) component with the three following parameters K_m, V_{max} and P_m. Since P_m had no significant difference from zero, and the fitting of the data did not improved, we decided to use the model with only saturable process, as described in equation 3.8.

Statistical Analysis

The data are presented as mean ± standard error (SE), where n=3-8. In order to determine statistically significant differences between groups, one-way analysis of variance (ANOVA) was used, followed by Tukey or Dunnett's test as post-tests,

and a $p<0.05$ was considered statistically significant. To test the quality of the fit of the linear models, the residual plots were visually inspected, and the coefficient of determination (R^2) and the standard error of the residuals were evaluated as well. All statistical analyses were performed with Prism v5.0. A *p*-value below 0.05 was considered statistically significant.

Results

Stability of Cefadroxil

Cefadroxil was not metabolized during the *in situ* intestinal permeability studies. Figure 3.1 shows chromatograms of blank perfusion buffer, cefadroxil dissolved in perfusion buffer, the mouse jejunal perfusate, and the exiting perfusate containing working solution (10 μM cefadroxil in buffer) in the jejunum of mice.

Concentration-Dependency Studies

To understand the kinetics of the transport in the jejunum, various concentrations of this antibiotic were used (0.005, 0.01, 0.1, 1, 5, 10 and 25 mM) in wild-type mice. Figure 3.2 shows that the flux of cefadroxil has a saturable component to it, and the data was fitted to the model described by equation 3, the apparent Michaelis Menten parameters V'_{max} and K'_m for cefadroxil in the jejunum were 4.75 nmol/cm^2/sec and 3.83 mM, respectively (R^2=0.89) (See Table 3.1).

Then, using the boundary layer approach, the aqueous permeability (Paq) of cefadroxil was calculated as $8.91*10^{-3}$ cm/sec. Subsequently, the concentrations of cefadroxil at the intestinal wall (C_w) and the wall permeability of cefadroxil (Pw) were also calculated, and the data was fitted again to equation 3.3. The resulting intrinsic V_{max} and K_m were 4.48 nmol/cm^2/s and 2.8 mM, respectively (R^2=0.90) (See Table 3.2). These results show that cefadroxil has low affinity for the transporter (high K_m) and high V_{max}, and are similar to the results obtained by Sinko *et al* [23, 24], and Sanchez-Pico et al [27] in rat jejunum. Similar to Sinko's results [23, 24], our results also fit the simplest model (without the passive diffusion

component) better, and it is consistent with the previously described characteristics of PEPT1 transport of amino-cephalosporins [39].

To see if one or more transporters were in charge of the transport of cefadroxil, the data was linearized using Woolf–Eadie–Augustinsson–Hofstee plot. As seen in Figure 3.4 the curve has only one slope, which indicates that only one transporter is responsible for it.

Regional Permeability Studies

To determine if the is a difference in functionality of PEPT1 along the small intestine and colon, the effective permeability of cefadroxil was measured in all 4 intestinal segments of the intestine both wild-type and PEPT1 knockout mice. As shown in Figure 3.6 the effective permeability of cefadroxil is significantly higher in the duodenum, jejunum and ileum of wild-type mice, when compared to the duodenum, jejunum, and ileum of PEPT1 knockout mice. The effective permeability of cefadroxil in knockout mice is about 2% in the duodenum, 10% in the jejunum and 5% in the ileum, of the wild-type mice. There is no significant difference in the effective permeability of cefadroxil in the colon of both genotypes. Also, the effective permeability of cefadroxil in wild-type mice is significantly higher in the duodenum, jejunum and ileum, that in the colon. There is no statistically significant difference in the effective permeability of cefadroxil for the four intestinal segments in PEPT1 knockout mice. Table 3.3 shows the mean values and standard error for the effective permeability in all 4 segments of both wild-type and PEPT1 knockout mice.

pH-Dependent Studies

The jejunal effective permeability of cefadroxil was evaluated at different relevant physiological pH values (from pH 5.5 to 7.5). This was generated by mixing different ratios of 10 mM HEPES/TRIS and 10 mM MES/TRIS, keeping the osmolarity of the buffer constant. All experiments were done with 0.01 mM of cefadroxil. As observed in Figure 3.7 the optimal uptake of cefadroxil occurs at pH 6. Though there is no statistical significant difference on the effective permeability of cefadroxil at different pH values when compared to the control with a pH of 7.5. Following these experiments, the effect of dimethyl-amiloride (DMA), an inhibitor of proton/sodium exchanger the apical membrane, was co-administered to see if the increase in the pH at the apical membrane had an effect on the permeability of cefadroxil. Results show that a direct inhibition of the proton exchanger, and therefore an increase in the pH at the apical membrane significantly decreased the effective permeability of cefadroxil.

Substrate Specificity Studies

Different molecules were used to evaluate their effect on the jejunal permeability of cefadroxil. Substrates for PEPT1 and other transporters were used, including amino acids, such as L-histidine and glycine, dipeptides such as Gly-Sar and Gly-Pro, p-aminohippuric acid (PHA) an organic anion transporter inhibitor, and n-methyl-nicotine-amide (NMN), an organic cation transporter inhibitor. Cephalexin, a first generation α-amino-cephalosporin, and cephalothin, a first generation cephalosporin that lacks the α-amino group, were also used. All compounds were used at a concentration of 25 mM and the experiments were

performed at a pH of 6.5. Figure 3.7 shows that the jejunal effective permeability of cefadroxil was significantly decreased with the addition of Gly-Sar and Gly-Pro, which indicates that this antibiotic is transported by a peptide transporter in the jejunum, such as PEPT1, capable of transporting dipeptides. On the other hand, no significant effect was seen when L-Histidine and glycine were added to the perfusate solution. This indicates that cefadroxil is not taken up by the peptide/histidine transporters (PHT1/PHT2), or by those L-histidine and glycine transporters that could be present in the mouse jejunum such as the B0+ transporters, GLYT1, LAT1 and ASCT2 [40]. The addition of a high concentration of cephalexin, another first generation amino-cephalosporin, caused a significant decrease in the effective permeability of cefadroxil. Which indicates that both of these amino cephalosporins are transported by the same system in the mouse jejunum. The concomitant administration of high concentration of cephalothin, a cephalosporin that doesn't contain the alpha amino group and therefore is not a substrate for PEPT1, did not affect the effective permeability of cefadroxil. The administration of p-aminohippuric acid didn't cause a significant reduction in the effective permeability of cefadroxil, nor did the addition of 1-methyl nicotinamide. These results indicate that neither the organic anion transporters, nor the organic cation ones, are significantly involved in the uptake of cefadroxil from the mouse jejunum.

Discussion

The work disclosed in this paper demonstrates and quantifies for the first time the importance of PEPT1 in the absorption of cefadroxil in the small intestine and in the colon. The results of the performed perfusion experiments and the preliminary *in vivo* ones gave important and novel information about the uptake of cefadroxil in mice. We found that: 1) Cefadroxil permeability in the small intestine is a carrier mediated process that is concentration dependent and is driven mainly by one transporter, PEPT1. 2) The effective permeability (P_{eff}) values for cefadroxil in wild-type mice are at least 10 fold higher in the small in the small intestine and there is no significant difference in colon for both species. 3) A K_m of 3.83 mM in the jejunum indicates that the transporter has low affinity for cefadroxil. 4) That the change of bulk in the pH doesn't significantly affect the effective permeability of cefadroxil in mice jejunum, but the actual blockage of the proton-sodium exchanger actually does affect the P_{eff} of cefadroxil.

Using PEPT1 knockout mice that were previously developed by Hu *et al* [13] we demonstrated that PEPT1 is the most important transporter in the uptake of cefadroxil from the small intestine in mice. Permeability data obtained in mice is of great importance and could be very relevant in clinical research, since it could be used to predict in someway the behavior of PEPT1 substrates when administered to humans. Although it has been shown before that permeability data obtained using perfusion experiments in rats correlates with the fraction absorbed in humans for drugs that passively diffuse through the membranes, for drugs that use transporters it might not be the case. Mice have been shown to have a very similar gene

expression pattern to humans for PEPT1 and other transporters in the small intestine, while in rats the expression of PEPT1 has been shown to be significantly higher [41]. But not only the expression pattern between mice and human is very similar, there is also a high homology (83% amino acid identity) between the structures of the human PEPT1 and the mouse PEPT1 as shown by Fei *et al* [42]. The use of mice also allows the testing of different conditions that could be difficult or sometimes impossible to perform in humans, such as testing the permeability of drugs in distal segments of the small intestine and colon, or the use of really high concentrations of potentially toxic drugs. We chose this *in situ* single pass intestinal perfusion technique over other *in vitro* and *in situ* methods, because it resembles more accurately *in vivo* conditions, such as intact blood supply.

Cefadroxil was chosen as the model drug, given its good stability [23, 29] and well-known properties, in the mist of understanding the importance of PEPT1 in the absorption of therapeutically relevant compounds. Since cefadroxil has a chemical structure that highly resembles that of a peptide, it is a substrate for peptide transporters (PEPT1 and PEPT2). A plethora of studies have demonstrated how cefadroxil can inhibit the uptake of Gly-Sar in different systems, such as Caco-2 cells [15], cells expressing PEPT1 [28, 43], Oocytes expressing PEPT1 [14, 26], mice [8]. [26]. Very few studies have actually described the kinetics and other characteristics of its transport in the small intestine [23, 24, 44]. And definitely none have yet calculated the importance of this PEPT1 in the absorption of cefadroxil. PEPT1 has been described in the literature as a low affinity transporter, which means that it has low affinity for its substrates of its substrates with K_m values in the lower

millimolar range (0.2-10 mM)[2]. In our studies we measured both the apparent (K'_m =3.8 mM) and the intrinsic K_m for cefadroxil (K_m =2.8 mM), and we found that they are in the range of PEPT1 and are also consistent to the K_m values for cefadroxil previously reported by Sinko and Amidon in rat jejunum (K_m= 5.9 mM) [24], 6.6 by Sanchez-Picó [27], and by Wenzel *et al,* in oocytes transfected with rabbit intestinal PEPT1 (K_m= 1.1mM) [14, 26].

To measure the actual relevance of PEPT1 in the uptake of cefadroxil, we compared wild-type *vs* knockout mice. These experiments showed that PEPT1 is extremely important for the absorption of cefadroxil from the small intestine, since the effective permeability of cefadroxil in is significantly lower (10% or less) in the duodenum, jejunum and ileum of PEPT1 knockout mice. Cefadroxil transport is minimal in colon, where there is no expression of PEPT1, and as expected both wild-type and PEPT1 knockout mice have very similar values.

The concentration of cefadroxil used in our perfusion experiments ranged from 0.005 mM to 25 mM. This range of concentrations allows good estimation of the K_m and V_{max} for PEPT1, since full saturation is achieved. When cefadroxil is administered to patients it is given in doses of 250, 500 or 1000 mg, once or twice daily. Since the volume of the small intestine in fasted patients has been established to be between 50 and 1100 mL, and on average 500 mL, the concentrations of cefadroxil approximately translate to values between 0.5 and 50 mM. Our experiments therefore are carried out at a range of concentrations that fall below and above the ones present in the jejunum in humans after the administration of

cefadroxil, thus allowing us to understand more accurately the behavior of cefadroxil [45].

As seen before with Gly-Sar in previously reported *in situ* experiments [8], the change in bulk pH has no significant effect on the effective permeability of cefadroxil in the small intestine. The effect of pH in the uptake of cefadroxil has been previously described *in vitro* systems, such as Caco-2 cells and Oocytes transfected with rabbit PEPT1 [26], but not in animal models. In Oocytes, Wenzel *et al* showed that the uptake of cefadroxil in Caco-2 cells is optimum between pH 6 and 6.5, and when was plotted against the apical pH it displayed a bell-shape curve. They also showed that in Oocytes expressing PEPT1, the cefadroxil-mediated inward current is at its maximum at pH 6.5 (-60mV) and it decreases to half at it at pH 5.5 [26]. The lack of significant difference observed *in situ* and *in vivo* can be explained by the presence of an acidic microclimate layer in the apical membrane of the intestinal epithelial cells. This layer, formed by mucus and proton secretion (by transporters) at the brush border membrane, creates an environment that is highly resistant to pH changes in the bulk of the intestine [46, 47]. In order to actually affect the pH at the apical membrane we used DMA, an inhibitor of the sodium-proton exchanger at the apical membrane of the enterocytes.

To fully confirm that PEPT1 was the main transporter responsible for the absorption cefadroxil different compounds, high doses of known substrates and non-substrates of PEPT1 were perfused concomitantly with cefadroxil. When known substrates of PEPT1 were used at high concentrations, such as Gly-Sar, Gly-Pro, and cephalexin, the effective permeability of cefadroxil was significantly

reduced, which confirms that cefadroxil is a PEPT1 substrate. On the other hand the lack of effect on the effective seen on the effective permeability of cefadroxil when non-PEPT1 substrates, such as the amino acids glycine and l-histidine, the organic base TEA, the organic acid PAH and the non-amino-cephalosporin cephalothin, were given at high concentrations, indicates that cefadroxil is transported mainly by PEPT1 and not by other transporters in the small intestine.

In conclusion we have extensively characterized the PEPT1-mediated uptake of cefadroxil and the factors that affect it. We shown that it is a saturable process and demonstrated that in the duodenum, jejunum and ileum it represents at least the 90% of the uptake of cefadroxil *in situ*. We have also shown that even though the change in the bulk pH has no effect on the uptake of cefadroxil, the increase in the pH by the actual depletion of protons at the apical membrane (caused by DMA) does in fact decrease the uptake of cefadroxil.

References

1. Paulsen, I.T. and R.A. Skurray, The POT family of transport proteins. Trends Biochem Sci, 1994. 19(10): p. 404.
2. Rubio-Aliaga, I. and H. Daniel, Mammalian peptide transporters as targets for drug delivery. Trends Pharmacol Sci, 2002. 23(9): p. 434-40.
3. Biegel, A., et al., The renal type H+/peptide symporter PEPT2: structure-affinity relationships. Amino Acids, 2006. 31(2): p. 137-56.
4. Daniel, H. and G. Kottra, The proton oligopeptide cotransporter family SLC15 in physiology and pharmacology. Pflugers Arch, 2004. 447(5): p. 610-8.
5. Herrera-Ruiz, D., et al., Spatial expression patterns of peptide transporters in the human and rat gastrointestinal tracts, Caco-2 in vitro cell culture model, and multiple human tissues. AAPS PharmSci, 2001. 3(1): p. E9.
6. Kamal, M.A., R.F. Keep, and D.E. Smith, Role and relevance of PEPT2 in drug disposition, dynamics, and toxicity. Drug Metab Pharmacokinet, 2008. 23(4): p. 236-42.
7. Yamashita, T., et al., Cloning and functional expression of a brain peptide/histidine transporter. J Biol Chem, 1997. 272(15): p. 10205-11.
8. Jappar, D., et al., Significance and regional dependency of peptide transporter (PEPT) 1 in the intestinal permeability of glycylsarcosine: in situ single-pass perfusion studies in wild-type and PEPT1 knockout mice. Drug Metab Dispos. 38(10): p. 1740-6.
9. Sakata, K., et al., Cloning of a lymphatic peptide/histidine transporter. Biochem J, 2001. 356(Pt 1): p. 53-60.
10. Daniel, H., Molecular and integrative physiology of intestinal peptide transport. Annu Rev Physiol, 2004. 66: p. 361-84.
11. Fei, Y.J., et al., Expression cloning of a mammalian proton-coupled oligopeptide transporter. Nature, 1994. 368(6471): p. 563-6.
12. Knutter, I., et al., H+-peptide cotransport in the human bile duct epithelium cell line SK-ChA-1. Am J Physiol Gastrointest Liver Physiol, 2002. 283(1): p. G222-9.
13. Hu, Y., et al., Targeted Disruption of Peptide Transporter PEPT1 Gene in Mice Significantly Reduces Dipeptide Absorption in Intestine. Mol Pharm, 2008.
14. Boll, M., et al., Expression cloning of a cDNA from rabbit small intestine related to proton-coupled transport of peptides, beta-lactam antibiotics and ACE-inhibitors. Pflugers Arch, 1994. 429(1): p. 146-9.
15. Bretschneider, B., M. Brandsch, and R. Neubert, Intestinal transport of beta-lactam antibiotics: analysis of the affinity at the H+/peptide symporter (PEPT1), the uptake into Caco-2 cell monolayers and the transepithelial flux. Pharm Res, 1999. 16(1): p. 55-61.
16. Brandsch, M., I. Knutter, and E. Bosse-Doenecke, Pharmaceutical and pharmacological importance of peptide transporters. J Pharm Pharmacol, 2008. 60(5): p. 543-85.
17. Balimane, P.V., et al., Direct evidence for peptide transporter (PEPT1)-mediated uptake of a nonpeptide prodrug, valacyclovir. Biochem Biophys Res Commun, 1998. 250(2): p. 246-51.

18. Okano, T., et al., H+ coupled uphill transport of aminocephalosporins via the dipeptide transport system in rabbit intestinal brush-border membranes. J Biol Chem, 1986. 261(30): p. 14130-4.
19. Saito, H. and K. Inui, Dipeptide transporters in apical and basolateral membranes of the human intestinal cell line Caco-2. Am J Physiol, 1993. 265(2 Pt 1): p. G289-94.
20. Inui, K., et al., H+ coupled active transport of bestatin via the dipeptide transport system in rabbit intestinal brush-border membranes. J Pharmacol Exp Ther, 1992. 260(2): p. 482-6.
21. Tanrisever, B. and P.J. Santella, Cefadroxil. A review of its antibacterial, pharmacokinetic and therapeutic properties in comparison with cephalexin and cephradine. Drugs, 1986. 32 Suppl 3: p. 1-16.
22. Santella, P.J. and D. Henness, A review of the bioavailability of cefadroxil. J Antimicrob Chemother, 1982. 10 Suppl B: p. 17-25.
23. Sinko, P.J. and G.L. Amidon, Characterization of the oral absorption of beta-lactam antibiotics. I. Cephalosporins: determination of intrinsic membrane absorption parameters in the rat intestine in situ. Pharm Res, 1988. 5(10): p. 645-50.
24. Sinko, P.J. and G.L. Amidon, Characterization of the oral absorption of beta-lactam antibiotics. II. Competitive absorption and peptide carrier specificity. J Pharm Sci, 1989. 78(9): p. 723-7.
25. Kimura, T., et al., Transport of cefadroxil, an aminocephalosporin antibiotic, across the small intestinal brush border membrane. Biochem Pharmacol, 1985. 34(1): p. 81-4.
26. Wenzel, U., et al., Transport characteristics of differently charged cephalosporin antibiotics in oocytes expressing the cloned intestinal peptide transporter PEPT1 and in human intestinal Caco-2 cells. J Pharmacol Exp Ther, 1996. 277(2): p. 831-9.
27. Sanchez-Pico, A., et al., Non-linear intestinal absorption kinetics of cefadroxil in the rat. J Pharm Pharmacol, 1989. 41(3): p. 179-85.
28. Ganapathy, M.E., et al., Differential recognition of beta -lactam antibiotics by intestinal and renal peptide transporters, PEPT 1 and PEPT 2. J Biol Chem, 1995. 270(43): p. 25672-7.
29. Shen, H., et al., Impact of genetic knockout of PEPT2 on cefadroxil pharmacokinetics, renal tubular reabsorption, and brain penetration in mice. Drug Metab Dispos, 2007. 35(7): p. 1209-16.
30. Ocheltree, S.M., et al., Mechanisms of cefadroxil uptake in the choroid plexus: studies in wild-type and PEPT2 knockout mice. J Pharmacol Exp Ther, 2004. 308(2): p. 462-7.
31. Shen, H., et al., PEPT2 (Slc15a2)-mediated unidirectional transport of cefadroxil from cerebrospinal fluid into choroid plexus. J Pharmacol Exp Ther, 2005. 315(3): p. 1101-8.
32. Takeda, M., et al., Interaction of human organic anion transporters with various cephalosporin antibiotics. Eur J Pharmacol, 2002. 438(3): p. 137-42.
33. Ueo, H., et al., Human organic anion transporter hOAT3 is a potent transporter of cephalosporin antibiotics, in comparison with hOAT1. Biochem Pharmacol, 2005. 70(7): p. 1104-13.

34. Khamdang, S., et al., Interaction of human and rat organic anion transporter 2 with various cephalosporin antibiotics. Eur J Pharmacol, 2003. 465(1-2): p. 1-7.
35. Nakakariya, M., et al., Predominant contribution of rat organic anion transporting polypeptide-2 (Oatp2) to hepatic uptake of beta-lactam antibiotics. Pharm Res, 2008. 25(3): p. 578-85.
36. Komiya, I., et al., Quantitative mechanistic studies in simultaneous fluid flow and intestinal absorption using steroids as model solutes, in International Journal of …1980.
37. Kou, J.H., D. Fleisher, and G.L. Amidon, Calculation of the aqueous diffusion layer resistance for absorption in a tube: application to intestinal membrane permeability determination. Pharm Res, 1991. 8(3): p. 298-305.
38. Johnson, D.A. and G.L. Amidon, Determination of intrinsic membrane transport parameters from perfused intestine experiments: a boundary layer approach to estimating the aqueous and unbiased membrane permeabilities. J Theor Biol, 1988. 131(1): p. 93-106.
39. Friedman, D.I. and G.L. Amidon, Characterization of the Intestinal Transport Parameters for Small Peptide Drugs. Journal of Controlled Release, 1990. 13(2-3): p. 141-146.
40. Tunnicliff, G., Membrane glycine transport proteins. J Biomed Sci, 2003. 10(1): p. 30-6.
41. Kim, H.R., et al., Comparative gene expression profiles of intestinal transporters in mice, rats and humans. Pharmacol Res, 2007. 56(3): p. 224-36.
42. Fei, Y.J., et al., cDNA structure, genomic organization, and promoter analysis of the mouse intestinal peptide transporter PEPT1. Biochim Biophys Acta, 2000. 1492(1): p. 145-54.
43. Tomita, Y., et al., Transport of oral cephalosporins by the H+/dipeptide co-transporter and distribution of the transport activity in isolated rabbit intestinal epithelial cells. J Pharmacol Exp Ther, 1995. 272(1): p. 63-9.
44. Naruhashi, K., et al., PEPT1 mRNA expression is induced by starvation and its level correlates with absorptive transport of cefadroxil longitudinally in the rat intestine. Pharm Res, 2002. 19(10): p. 1417-23.
45. Lobenberg, R. and G.L. Amidon, Modern bioavailability, bioequivalence and biopharmaceutics classification system. New scientific approaches to international regulatory standards. Eur J Pharm Biopharm, 2000. 50(1): p. 3-12.
46. Hogerle, M.L. and D. Winne, Drug absorption by the rat jejunum perfused in situ. Dissociation from the pH-partition theory and role of microclimate-pH and unstirred layer. Naunyn Schmiedebergs Arch Pharmacol, 1983. 322(4): p. 249-55.
47. Lucas, M., Determination of acid surface pH in vivo in rat proximal jejunum. Gut, 1983. 24(8): p. 734-9.

Tables

PARAMETER	VALUE
V'_{max} (nmol/cm^2/s)	4.8
K'_m(mM)	3.8
R^2	0.894
Std Error V_{max}' (nmol/cm^2/sec)	0.4
Std Error K'_m (mM)	1.2

Table 3.1. Apparent Michaelis-Menten parameters of cefadroxil in the jejunum of wild-type mice.

PARAMETER	VALUE
P_{aq} (cm/s)	$8.9*10^{-3}$
V_{max} (nmol/cm²/s)	4.5
K_m (mM)	2.1
R^2	0.898
Std Error V_{max} (nmol/cm²/sec)	0.3
Std Error K_m (mM)	0.6

Table 3.2. Intrinsic Michaelis-Menten parameters, and aqueous permeability (P_{aq}) of cefadroxil in the jejunum of wild-type mice.

SEGMENT	Cefadroxil P_{eff} ($cm/s \cdot 10^{-4}$)	
	Wild Type	**PEPT1 Knockout**
Duodenum	0.493 ± 0.153	0.003 ± 0.017
Jejunum	0.809 ± 0.075	0.009 ± 0.053
Ileum	0.881 ± 0.177	0.042 ± 0.023
Colon	0.063 ± 0.089	0.031 ± 0.052

Table 3.3. Effective permeability values of cefadroxil for the different segments of the intestine in wild-type and PEPT1 knockout mice. Data are expressed as mean ± S.E. (n=4-8).

Figures

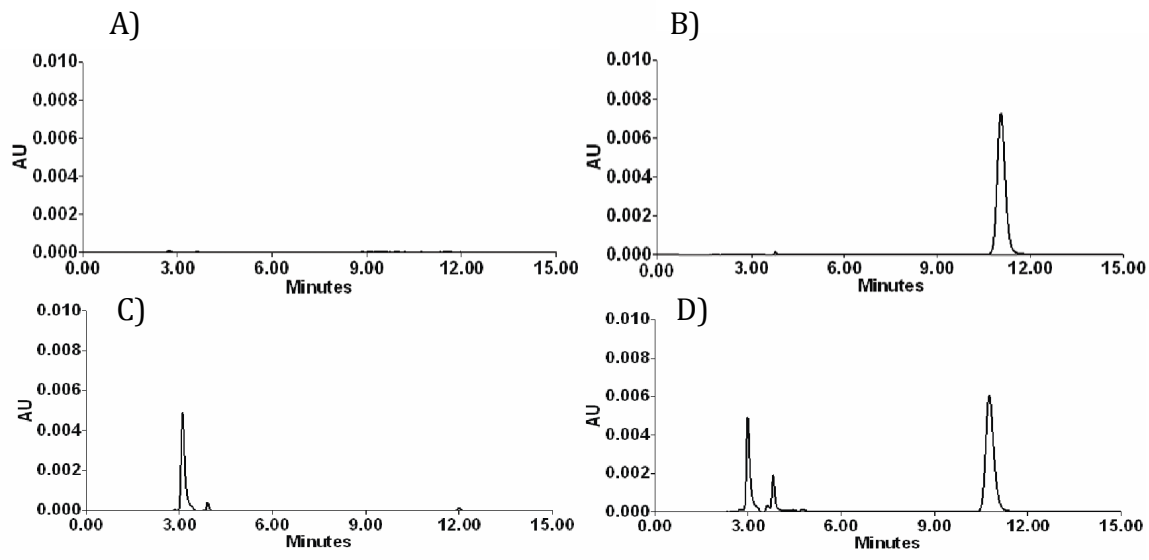

Figure 3.1. Chromatographs of A) Blank buffer, B) 10uM cefadroxil in buffer, C) Mouse jejunal perfusate and D) jejunal perfusate with 10 μM cefadroxil.

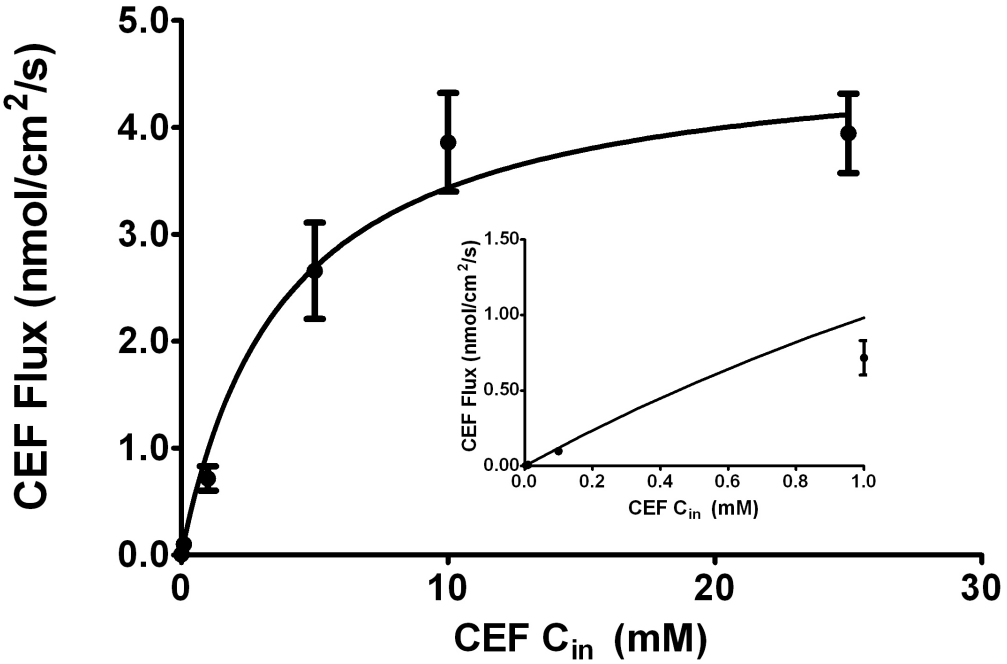

Figure 3.2. Concentration-dependent flux of cefadroxil (0.01-25 mM) in the jejunum of wild type mice. C_{in} is the concentration of cefadroxil in the perfusion buffer. All studies were done at pH 6.5. Values are expressed as mean ± S.E. (n=4-8).

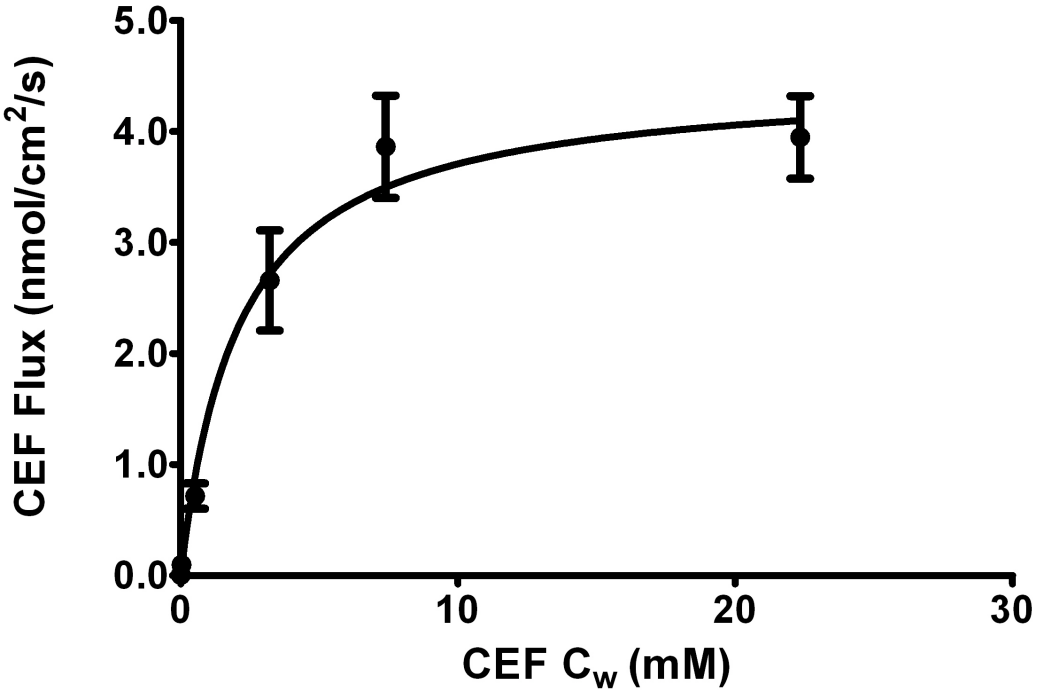

Figure 3.3 Concentration-dependent flux of cefadroxil (0.01-25 mM) in the jejunum of wild type mice. C_w is the calculated concentration of cefadroxil at the intestinal wall. All studies were done at pH 6.5. Values are expressed as mean ± S.E. (n=4-8).

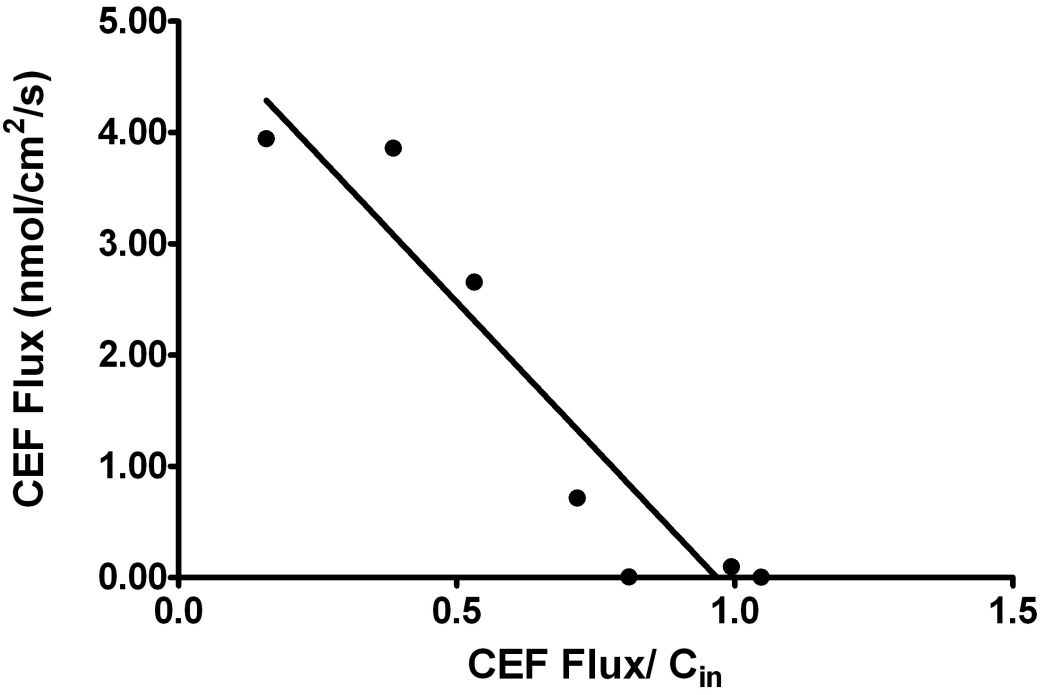

Figure 3.4. Woolf–Eadie–Augustinsson–Hofstee plot.

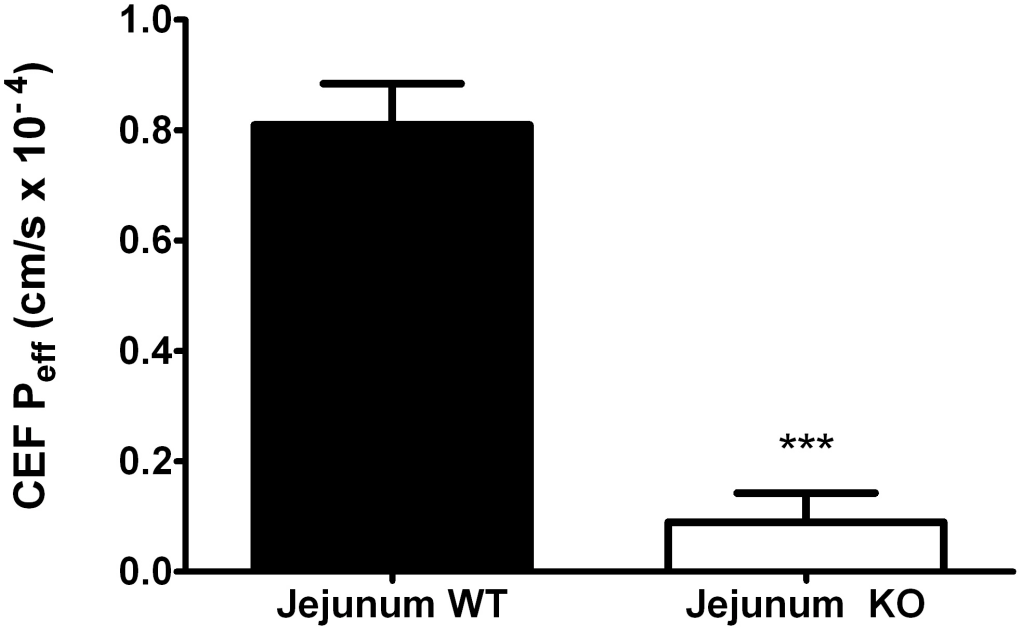

Figure 3.5. Effective permeability (P_{eff}) of 10 μM cefadroxil in the jejunum of wild type (WT) and PEPT1 knockout (KO) mice. *** $p<0.005$ Values are expressed as mean ± S.E. (n=4-8).

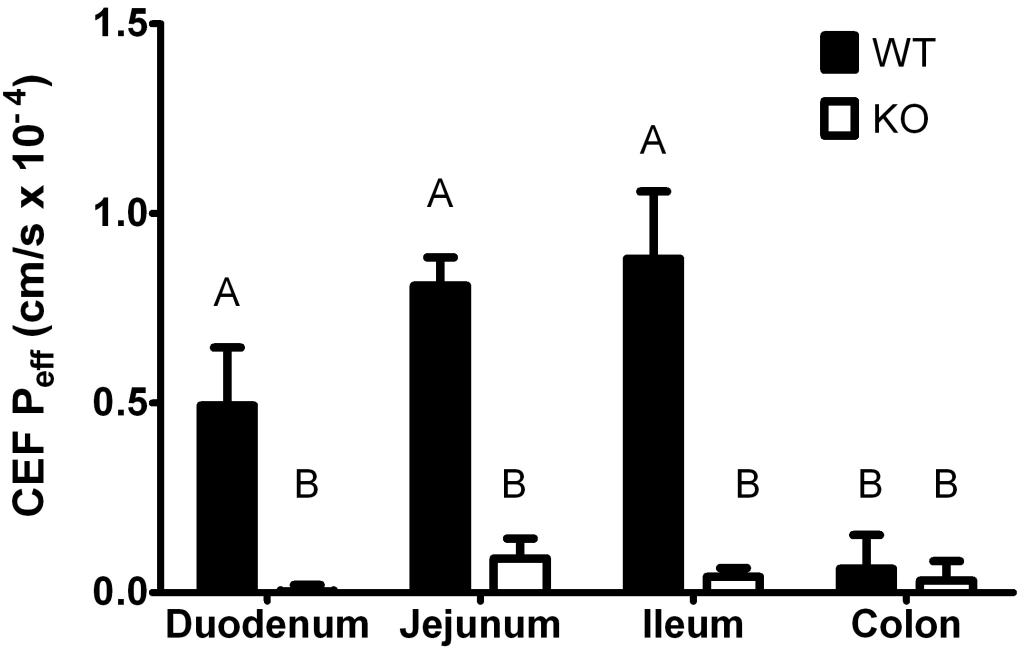

Figure 3.6. Effective permeability (P_{eff}) of 10 μM cefadroxil in the different intestinal segments of wild type (WT) and PEPT1 knockout (KO) mice. Studies were done at pH 6.5. Data are expressed as mean ± S.E. (n=4-8). Same letters represent no statistically significant difference, while different letters mean that there is a significant difference.

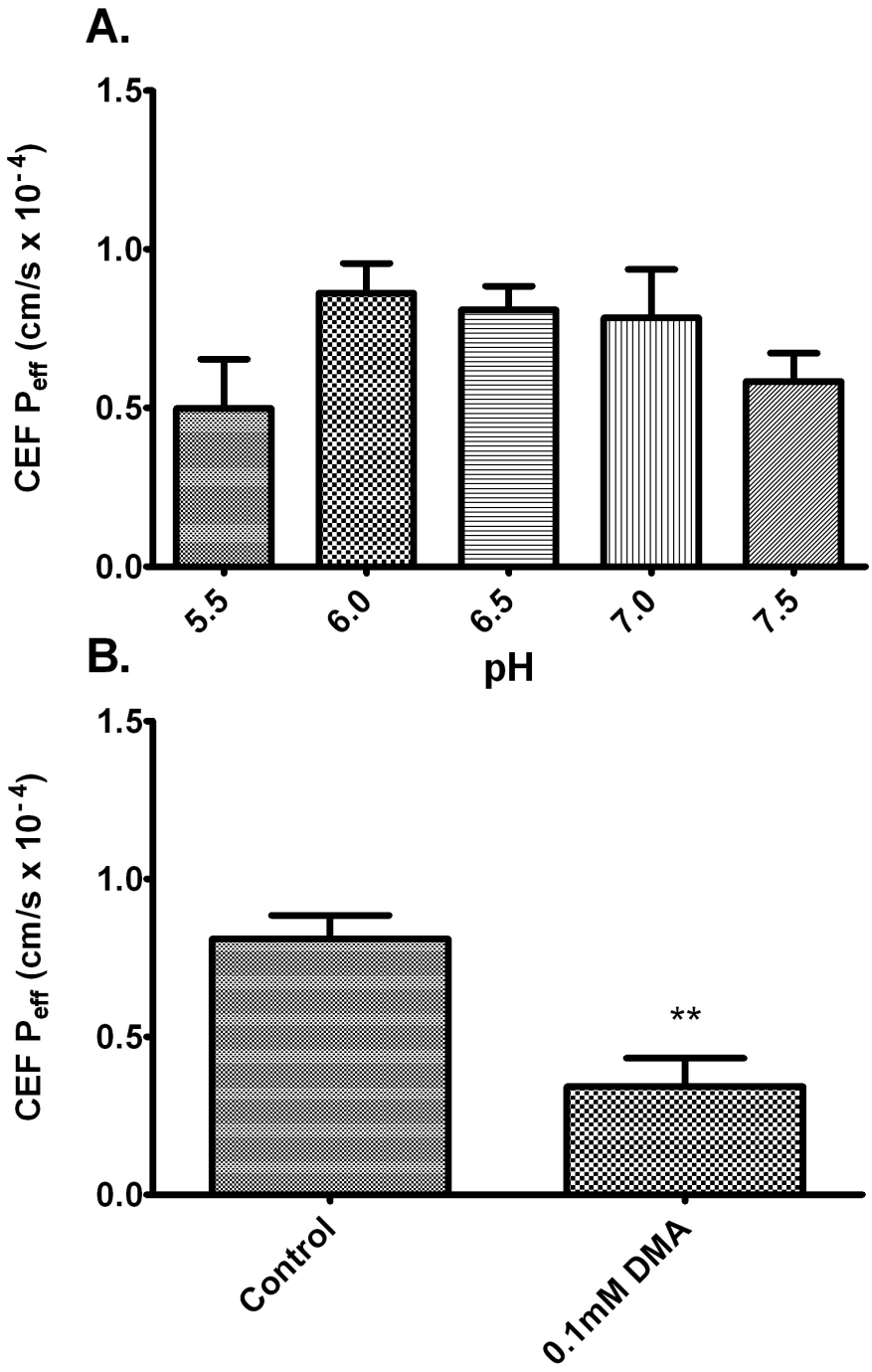

Figure 3.7. A) Effect of bulk pH on the effective permeability (P_{eff}) of cefadroxil (10 μM) in the jejunum of wild type mice. Data are expressed as Mean ± S.E. (n=4-8). B) Effect of dimethyl-amiloride (DMA) on the effective permeability of cefadroxil in the jejunum of wild-type mice at pH= 6.5. Data are expressed as mean ± S.E. (n=4-8). ** p< 0.01.

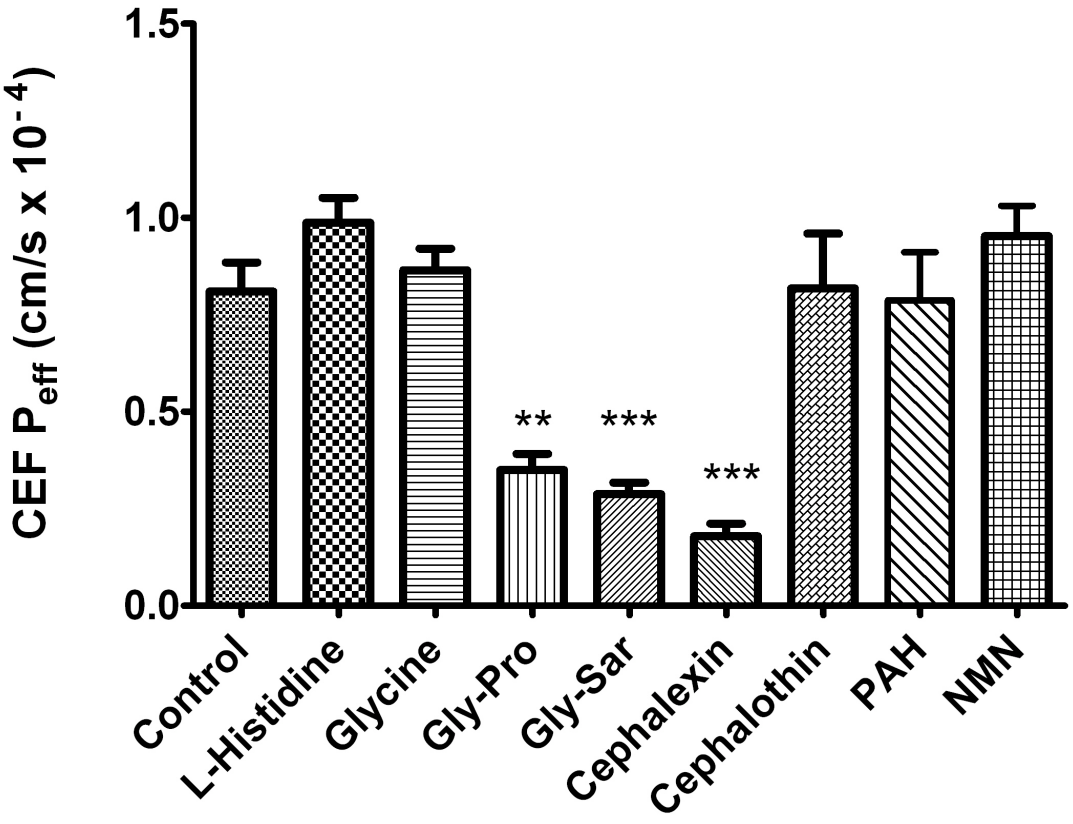

Figure 3.8. Effect of potential inhibitors on the effective permeability (P_{eff}) of cefadroxil in the jejunum of wild type mice. Data are presented as mean ± S.E. (n=4-8). ** p< 0.01 and *** p< 0.005. Concentration of cefadroxil is 10 μM and concentration of inhibitors is 25 mM.

CHAPTER 4

ORAL ABSORPTION, TISSUE DISTRIBUTION, AND DISPOSITION OF CEFADROXIL IN WILD-TYPE AND PEPT1 KNOCKOUT MICE

Abstract

Although cefadroxil is known to be a PEPT1 substrate, the relative importance of this transporter in the intestinal absorption of cefadroxil, an amino-cephalosporin antibiotic, is unknown. Therefore, the aim of this study was to determine the contribution of PEPT1 in the absorption, tissue distribution, and disposition of cefadroxil under *in vivo* conditions. The pharmacokinetics of ^{3}H-cefadroxil was studied in wild-type and *PEPT1* knockout mice after both oral (44.5, 89.1, 178 and 356 nmol/g) and intravenous (44.5 nmol/g) bolus administrations. Oral doses were scaled according to surface area using the four most prescribed human doses, and were given by oral gavage. After harvesting serial blood samples over 120 min, plasma concentrations of radioactive cefadroxil were measured using a dual-channel liquid scintillation counter. Pharmacokinetic parameters were determined using a non-compartmental analysis of the plasma concentration-time

profiles. The C_{max} and $AUC_{0\text{-}120}$ values of cefadroxil across all 4 oral doses were statistically and substantially lower for the *PEPT1* knockout mice, as compared to wild-type animals. However, dose-corrected C_{max} and $AUC_{0\text{-}120}$ estimates were not different between treatments for each genotype. Likewise, analysis of the intravenous data showed there was no significant difference in cefadroxil disposition between wild-type and PEPT1 knockout mice. These findings demonstrate that PEPT1 ablation has a substantial effect on cefadroxil absorption, reducing its systemic exposure by 8- to 10-fold. Moreover, cefadroxil exhibits an "apparent" linearity over the 44.5 - 356 nmol/g dose range. The tissue distribution experiments showed that PEPT1 was only important for the uptake of cefadroxil into the enterocytes of the small intestine, but not for the uptake of cefadroxil into other tissues of the body. Finally, the disposition of cefadroxil by non-PEPT1 processes is not different between genotypes given its virtually superimposable plasma profiles after intravenous dosing.

Key Words

Oral absorption, Tissue Distribution, Disposition, PEPT1, Cefadroxil, Preclinical Pharmacokinetics, Absorption Analysis.

Introduction

PEPT1 is a peptide transporter member of the SLC15 family. This family is constituted by 4 members: PEPT1, PEPT2, PHT1 and PHT2. All these proteins transport di- and tri-peptides, across different membranes in the body, using an electrochemical proton gradient [1, 2]. While PEPT1 and PEPT2 can only move di- and tri-peptides, PHT1 and PHT2 can move also the amino acid histidine [3]. Besides di- and tri-peptides, peptide transporters can also carry peptide-like molecules with important pharmacological activity such as the antiviral drug (valacyclovir), angiotensin converting enzyme inhibitors (captopril), the anticancer agent bestatin and amino-cephalosporins such as cefadroxil.

Cefadroxil is a broad-spectrum first generation amino-cephalosporin used to treat skin, upper respiratory, and urinary tract infections, caused by both gram-positive and gram-negative bacteria [4, 5]. Cefadroxil has a very high bioavailability in rats and humans (68 and 89 % respectively), no significant metabolism, and is excreted almost completely in the urine [4, 6].

Several transporters are involved in the transport of cefadroxil across membranes of different tissues in the body. This amino-cephalosporin has been shown to be a substrate of PEPT1 in different system such as Caco-2 cells, oocytes, rats, and mice [7-10]. In previous studies, our group showed that PEPT1 is the principal transporter involved in the permeation of cefadroxil from the small intestine into the blood stream. This transporter is expressed in the small intestine, but not in the in stomach or colon. Using single pass intestinal perfusion, a widely used *in situ* technique, in wild type and PEPT1 knockout mice, we showed that 90 %

of the effective permeability of cefadroxil in the jejunum is due to PEPT1. PEPT2, another peptide transporter expressed mainly in the kidney and choroid plexus, has also been proven to play a major role in the transport of cefadroxil [7, 11-14]. In the kidney, even though both PEPT1 and PEPT2 are present at the brush border membrane of the epithelial cells in the proximal tubule, PEPT2 is responsible for most of the re-absorption of cefadroxil back into the blood [11] [15]. In the choroid plexus epithelium, PEPT2 is in charged of the efflux of cefadroxil from the CSF (cerebrospinal fluid) into the cells, limiting the exposure of cefadroxil in the CSF [13]. At pH 7.4 (pH of the blood) almost 50% of cefadroxil molecules are negatively charged, while the other 50% are present as a zwitterions. This condition makes cefadroxil a good substrate for the organic anion transporters present in the body. In the kidney, cefadroxil is proven to be actively secreted into the urine by the organic anion transporters 1 (hOAT1), 2 (hOAT2), and 3 (hOAT3) in humans, and in rats by the rOAT2 [16-18]. Since so many different transporters can play a role in the absorption of cefadroxil *in vivo*, we decided to use the previously designed PEPT1 knockout mice[19] and compare it to the wild-type mice, to quantify the actual contribution of PEPT1 into the absorption, tissue distribution, and disposition of cefadroxil *in vivo*.

Cefadroxil, as well as other first generation amino-cephalosporins, is usually prescribed as an initial empiric medication to treat a wide variety of community acquired infections, such as skin, respiratory and urinary tract infections, because of its broad spectrum and low toxicity. Understanding the pharmacokinetics of cefadroxil and other antibiotics is important, since it plays an important role in the

efficacy of the treatment. Our main goals with this project are 1) to quantify the role of PEPT1 in the absorption and disposition of cefadroxil, and 2) to determine the role of PEPT1 in the tissue distribution of cefadroxil.

Methods

Materials

^{3}H-Cefadroxil (0.8 Ci/mmol) and ^{14}C-dextran-carboxyl 70.000 (1.1 mCi/g) were obtained from Moravek Biochemicals and Radiochemicals (Brea, CA). Hyamine hydroxide was purchased at ICN radiochemicals (Irvine, CA). All other chemicals were purchased from Sigma. (St. Louis, MO).

Animals

All studies were done in 6-8 week old gender-matched wild type (*PEPT1*$^{+/+}$) and *PEPT1* knockout (*PEPT1*$^{-/-}$) mice. The animals were kept in a temperature-controlled room with 12-hour light, 12-hour dark cycle, and had standard diet and water *ad libitum*. All of the procedures were approved by the University of Michigan Committee on Use and Care of Animals (UCUCA), and were carried out in accordance with the Guide for Use of Laboratory Animals as adopted and promulgated by the US National Institutes of Health (NIH publication No. 85-23, revised in 1985).

Oral Administration of Cefadroxil

Gender-matched wild type (*PEPT1*$^{+/+}$) and *PEPT1* knockout (*PEPT1*$^{-/-}$) mice were fasted 14 hours before the beginning of the experiment. Cefadroxil was dissolved in 200-250 µL of water and administered to the mice using a 20G oral gavage needle at the following doses. Doses were scaled down from human relevant doses using a surface area adjustment. For all doses 0.5 µCi/ gram of body weight of radiolabeled cefadroxil (^{3}H-cefadroxil) were administered. Plasma was harvested

from blood samples (15 - 20 µL) that were collected by tail nicks at the following times: 5, 10, 15, 20, 30, 45, 60, 90, and 120 minutes after oral dosing. The blood was collected using a PCR tube containing 1 µl of 7.5% EDTA and centrifuged at 3300 rfc for 3 minutes. Then, 5 µL of plasma were collected and placed in a scintillation vial with 6 mL of CytoScint scintillation fluid (MP Biomedicals, Solon, OH). The radioactivity in the sample was measured using dual channel Scintillation Counter (Beckman LS 6000 SC; Beckman Coulter Inc., Fullerton, CA). Mice had free access to water during the whole experiment.

Systemic Administration of Cefadroxil

Gender-matched wild type (*PEPT1*$^{+/+}$) and *PEPT1* knockout (*PEPT1*$^{-/-}$) mice were injected with cefadroxil dissolved in saline solution via the tail vein using a 27G needle. The dose used was 44.5 nmol/g and it was scaled down from the lowest human relevant dose. 0.5 µCi/ gram of body weight of radiolabeled cefadroxil (^{3}H-cefadroxil) were administered. Plasma was harvested from blood samples (15-20 µL) that were collected by tail nicks at the following times: 0.5, 2, 5, 15, 30, 45, 60, 90, and 120 minutes after I.V. dosing. The blood was collected using a PCR tube containing 1 µl of 7.5% EDTA and centrifuged at 3300 rfc for 3 minutes. Then, 5 µL of plasma were collected and placed in a scintillation vial with 6 mL of CytoScint scintillation fluid (MP Biomedicals, Solon, OH). The radioactivity in the sample was measured using dual channel Scintillation Counter (Beckman LS 6000 SC; Beckman Coulter Inc., Fullerton, CA). Mice had free access to water during the total duration of the experiment.

Tissue Distribution after Oral Administration of Cefadroxil

Gender-matched wild type (*PEPT1*$^{+/+}$) and *PEPT1* knockout (*PEPT1*$^{-/-}$) mice were fasted 14 hours before the beginning of the experiment. Cefadroxil was dissolved in water and administered to the mice using a 20G oral gavage needle at 178.2 nmol/g. After 15 minutes, 100 µL of ^{14}C-Dextran 70.000 were injected via the tail vein, and 5 minutes later the animal was euthanized. Whole blood and tissues were collected and incubated overnight with 330 µL of Hyamine Hydroxide at 37°C. Then, 40 µL of Hydrogen Peroxide 30% were added, followed by of 6 mL of CytoScint scintillation fluid (MP Biomedicals, Solon, OH). The radioactivity in the sample was measured using dual channel Scintillation Counter (Beckman LS 6000 SC; Beckman Coulter Inc., Fullerton, CA).

Data Analysis

The plasma concentration-time profiles of cefadroxil in both genotypes were analyzed using non-compartment analysis with Phoenix (Pharsight, Mountain View, CA), and parameters

Tissue concentrations of cefadroxil was calculated as:

$$C_{tiss,\ corr} = C_{tiss} - DS * C_b$$

where $C_{tiss,\ corr}$ is the corrected concentration of Cefadroxil in each tissue (in nmol/g of wet tissue, DS is the vascular volume in the tissue (in mL/g) calculated using ^{14}C-dextran, and C_b is the concentration of cefadroxil in the blood.

Statistical Analysis

All the data are reported as mean ± SE. To test for statistically significant differences between wild-type and PEPT1 knockout mice a t-test was performed. An ANOVA was used to test for statistical differences between multiple treatments followed either by a Dunnett's test for pairwise comparisons with the control group, or a Tukey test for multiple comparisons. To test the quality of the fit of the linear models, the residual plots were visually inspected, and the coefficient of determination (R^2) and the standard error of the residuals were evaluated as well. All statistical analyses were performed with Prism v5.0. A *p*-value below 0.05 was considered statistically significant.

Results

Oral Administration of Cefadroxil

As seen in figure 4.1 (A-D), the average plasma concentration-time profiles of cefadroxil in wild-type mice are significantly different than the knockout ones. For wild-type mice the concentration of cefadroxil raises really fast after oral administration, has a Tmax at around 20 minutes, and then it decreases rapidly with time. Instead for the knockout mice, the concentration tends to increase slower and plateau out at around 60 minutes (Figure 4.1). Since the concentration of cefadroxil in the knockout mice doesn't decrease (stays at the same level until the end of the experiments) it was impossible to determine the half-life and Tmax of cefadroxil. The AUC and C_{max} for each genotype at each dose are shown in Table 4.1, as well as the ratios between them. The C_{max} of cefadroxil in wild-type mice is at least 16-fold higher than the C_{max} in *PEPT1* knockout animals. Likewise, the AUC is significantly reduced in the *PEPT1* knockout mice compared to the wild-type mice (8- to 10-fold lower). One can see that the ratios of AUCwt/AUCko are between 9 and 11, which means that most of the cefadroxil (~90%) is being absorbed through PEPT1. These results are comparable to the previously obtained results from *in situ* experiments.

To test for saturation of the cefadroxil transport, the C_{max} and AUC for the 4 doses were compared using linear regression analysis and ANOVA of the dose corrected pharmacokinetic parameter. As seen in both figures 4.3 and 4.4, both the C_{max} and the AUC are linear with the dose and the dose corrected parameters are not different for the 4 doses. This means that cefadroxil pharmacokinetics exhibit an apparent linearity after oral administration over the 44.5 - 356 nmol/g range.

To better understand the differences between the absorption process and absorption rates of cefadroxil in wild type and PEPT1 knockout mice we performed a partial AUC analysis. In this analysis, the partial cumulative AUC's were plotted versus time after 4 oral doses from 0 to 120. Then the initial slopes, from 10-30 minutes, were compared between wild type and PEPT1 knockout mice. Both genotypes show a single slope from 10 to 30 minutes. The linear regression analysis showed that the knockout mice slopes were significant slower than the wild type ones. A two-way ANOVA of the initial dose-corrected slopes of the partial AUC's between 10-30 minutes, shows that there is a significant difference between wild-type and PEPT1 knockout mice, but not difference for the doses in each of the genotypes. As shown in table 4.2 the initial slope (10-30 minutes) was around 25 times slower than the PEPT1 knockout mice.

Systemic Administration of Cefadroxil

After intravenous injection of cefadroxil, both genotypes have very similar disposition profiles, almost superimposable (Fig 4.6). This phenomenon indicates that this antibiotic is cleared from the body through the same mechanisms in both genotypes, and PEPT1 is not significantly involved in its clearance. Since we know that cefadroxil is not metabolized in the body and is mainly eliminated by the kidney, we can assume that other processes or transporters, different than PEPT1, are in charge of its disposition. These results are in accordance with the previously reported data, which showed that PEPT2 is in charge of 95% of the reabsorption of cefadroxil in the kidney, while PEPT1 is in charge of only 5% of its reabsorption [11]. As seen in table 4.3, there is no significant difference in pharmacokinetic parameters

such as clearance, AUC, and half-life between genotypes after systemic administration of this amino-cephalosporin.

Tissue Distribution of Cefadroxil

The tissue distribution of cefadroxil was performed 20 minutes after oral dosing. This particular time was chosen given its proximity to the T_{max} observed when cefadroxil was administered orally to wild-type mice. Evidently, there are significant differences in concentration values in different tissue for the two genotypes as seen in figure 4.7. But is important to note that the concentration of cefadroxil in blood is also significantly higher (12-fold) in the wild-type mice compared to the PEPT1 knockout mice as seen in figure 4.7. In order to capture the actual difference between the tissues, and not the difference because of drug absorption, we normalized the concentration of cefadroxil in the tissue by the concentration of cefadroxil in the blood. Once the data was normalized by the concentration of cefadroxil in blood (Figure 4.8), the difference in the cefadroxil concentration in the other tissues for both genotypes disappears. This shows that the initially observed difference in tissue concentration was due to differences in drug absorption, and not because of PEPT1 functionality in the other tissues.

In figure 4.9, one can see the difference in the cefadroxil concentrations in different segments of the gastrointestinal tract after 20 minutes of drug administration. The highest concentration in wild-type mice is present in the duodenum, and is significantly higher than the concentration of cefadroxil in the duodenum of the PEPT1 knockout mice. It is also significantly higher than the concentration of cefadroxil in the stomach, jejunum, ileum and colon of the wild-

type mice. There was no difference between the stomach, the jejunum, the ileum and the colon for both genotypes.

Discussion

This work presents new findings on the *in vivo* oral absorption, tissue distribution and disposition of cefadroxil in mice. We reported for the first time that 1) the deletion of PEPT1 reduces by 90% the systemic exposure of cefadroxil after its oral administration. Likewise, 2) the C_{max} of cefadroxil is significantly lower in the PEPT1 knockout mice. Also, we showed that 3) there is an apparent linearity in the C_{max} and AUC for the 4 clinically relevant doses administered. Moreover, we found out that 5) the systemic exposure of cefadroxil is not affected by PEPT1 erasure after intravenous administration, and finally, 6) that the distribution into tissues depends majorly on the actual concentration of cefadroxil in blood, and not on expression of PEPT1 in them.

The reduction of the exposure of cefadroxil *in vivo* by approximately 90%, for the 4 doses used, in the *PEPT1* knockout mice correlates extremely well with our previous results from the *in situ* studies in mice. In the previously performed single pass intestinal perfusion experiments we demonstrated that the ablation of PEPT1 reduces the effective permeability (P_{eff}) of cefadroxil also by 90%. Unsurprisingly, these results are consistent because the amount of drug absorbed *in vivo* after oral administration depends directly on its membrane permeability, and other factors such as the drug concentration in the intestinal lumen, the pH, and the transit time [20, 21]. Our results show that the absorption of cefadroxil in wild-type mice is quite fast, displaying a Tmax at approximately 20 minutes. Therefore we can suggest that the absorption of cefadroxil is happening mostly in the upper portion of the GI tract. Since we know that cefadroxil isn't absorbed in the stomach, because there is no

PEPT1 present in this organ, we can suggests that the absorption happens mostly in the upper segment of the small intestine, probably in the duodenum and upper jejunum. This hypothesis in then confirmed with the results of the tissue distribution experiments, which showed that the highest concentration of cefadroxil along the gastrointestinal tract after 20 minutes occurred in the duodenum of wild-type mice. We can hypothesize then, that the absorption of cefadroxil in the small intestine is driven mostly by the concentration of drug in the lumen, because it would be the concentration of drug in the lumen the only factor that significantly changes in the small intestine of these mice. McConnell *et al* showed that the pH along the gastrointestinal tract of fasted mice remains very similar, between 4 and 5, so we can conclude that this would not have a direct impact in the differences of cefadroxil observed in the small intestine of wild-type mice. Similarly, we have shown in our previous experiments that there was no significant difference in the effective permeability of cefadroxil in the 3 segments of the small intestine (duodenum, jejunum, and ileum), so it can be assumed that this is not the cause of the different concentrations along the gastrointestinal tract.

On the other hand, for the PEPT1 knockout mice one can see a significantly lower C_{max} and $AUC_{0\text{-}120}$, and also a very slow absorption of cefadroxil. In the wild-type mice the plasma concentration of cefadroxil increases very fast, and probably the luminal concentration of cefadroxil also decreases very fast as the drug gets absorbed along the small intestine. In the knockout mice something different happens, the plasma concentration of cefadroxil increases very slowly and reaches a plateau at a later time. This is probably because the drug isn't being absorbed in the

upper segments of the small intestine so high concentrations of it reach the lumen of the lower segments causing an increase in the driving force for passive diffusion.

In preliminary studies of the pharmacokinetics of cefadroxil in wild-type mice, Buck *et al* showed that the C_{max} of cefadroxil occurs around 30 minutes after oral administration and that it is linear with the dose, between 25 mg/kg and 200 mg/kg (68.9 and 550 nmol/g)[4]. Our results are very similar to these ones. Though their Tmax is at 30 minutes and not 20 like ours, we believe that ours is more accurate because they report only 1 data point before the Tmax, while we sampled 3 times (at 5, 10, and 15 minutes) before it [4] .

Though we observed a dose-proportional increase of the $AUC_{0\text{-}120}$ and C_{max}, and no change in the clearance of cefadroxil, we know that its intestinal absorption, and renal secretion and reabsorption are handled by transporters, and with a high enough dose, these transporters will eventually be saturated and the dose-proportionality in the C_{max} and AUC will be lost. So, we can say that what we observed is an "apparent" linearity of the pharmacokinetics of cefadroxil. The doses used for these experiments were scaled down from the four most prescribed human doses (125, 250, 500 and 1000 mg) using a surface area approach. Our doses of (44.5, 89.1, 179 and 356 nmol/g) would then result in stomach concentrations of 1.5, 3, 6, and 12 mM. According to these calculations, the two highest doses would surpass the high K_m of cefadroxil in the small intestine (3.8 in the bulk of the intestine, 2.1 at the intestinal wall). So one would expect that at least the highest dose used would cause a saturation of the peptide transporter in the small intestine, causing a decrease in the fraction absorbed. On the other hand, an increase in the

dose, and subsequently in the plasma concentration, could cause a saturation of the active reabsorption of cefadroxil by PEPT2, and therefore causing an increase in the clearance and a lower than proportional increase in the AUC and C_{max}. One can also run into the situation where the active secretion transporters, OAT's are saturated and then the clearance could be higher, causing an increase in the dose corrected AUC and C_{max} of cefadroxil.

In the literature there is mixed information about the linearity of the pharmacokinetics of cefadroxil. While a some authors report that cefadroxil exhibits non-linear kinetics after oral administration of cefadroxil in rats and humans [22, 23], others show that cefadroxil displays a dose-proportional increase of AUC and C_{max} and a dose independent clearance within therapeutic doses in mice and humans [4, 24]. Although all studies were performed under similar circumstances and with similar doses, we think that the mixed results rely on the already mentioned complexity of the processes involved in the absorption and elimination in the kidney of cefadroxil.

For both genotypes, the tissue distribution of cefadroxil is not different after the concentration of cefadroxil in tissue is normalized for the blood one. This means that after cefadroxil is absorbed into, PEPT1 ablation has no effect in distribution of cefadroxil. Also, one can observe a high variability in the tissue concentration values for each genotype. This phenomenon can be attributed to the time of tissue collection and/or the lack of equilibrium between drug present in the tissue and in the blood.

Our results show that after intravenous administration of cefadroxil the exposure and disposition of this antibiotic is the same for both genotypes, concluding that the ablation of PEPT1 doesn't affect the elimination of cefadroxil. This is in agreement with previous studies from our group that showed that PEPT1 accounted only for 5% of the reabsorption of cefadroxil in the kidney, while PEPT2 accounted for 95% of it in wild-type mice [11]. Also our group showed that cefadroxil is not significantly metabolized in the mice, and almost 90% of it can be recovered intact in the urine after 24 hours [11]. Therefore, we can conclude that the clear differences observed in both genotypes after oral administration can be attributed to differences in the absorption process, and not to the tissue distribution, metabolism, or elimination of cefadroxil in mice.

Figures

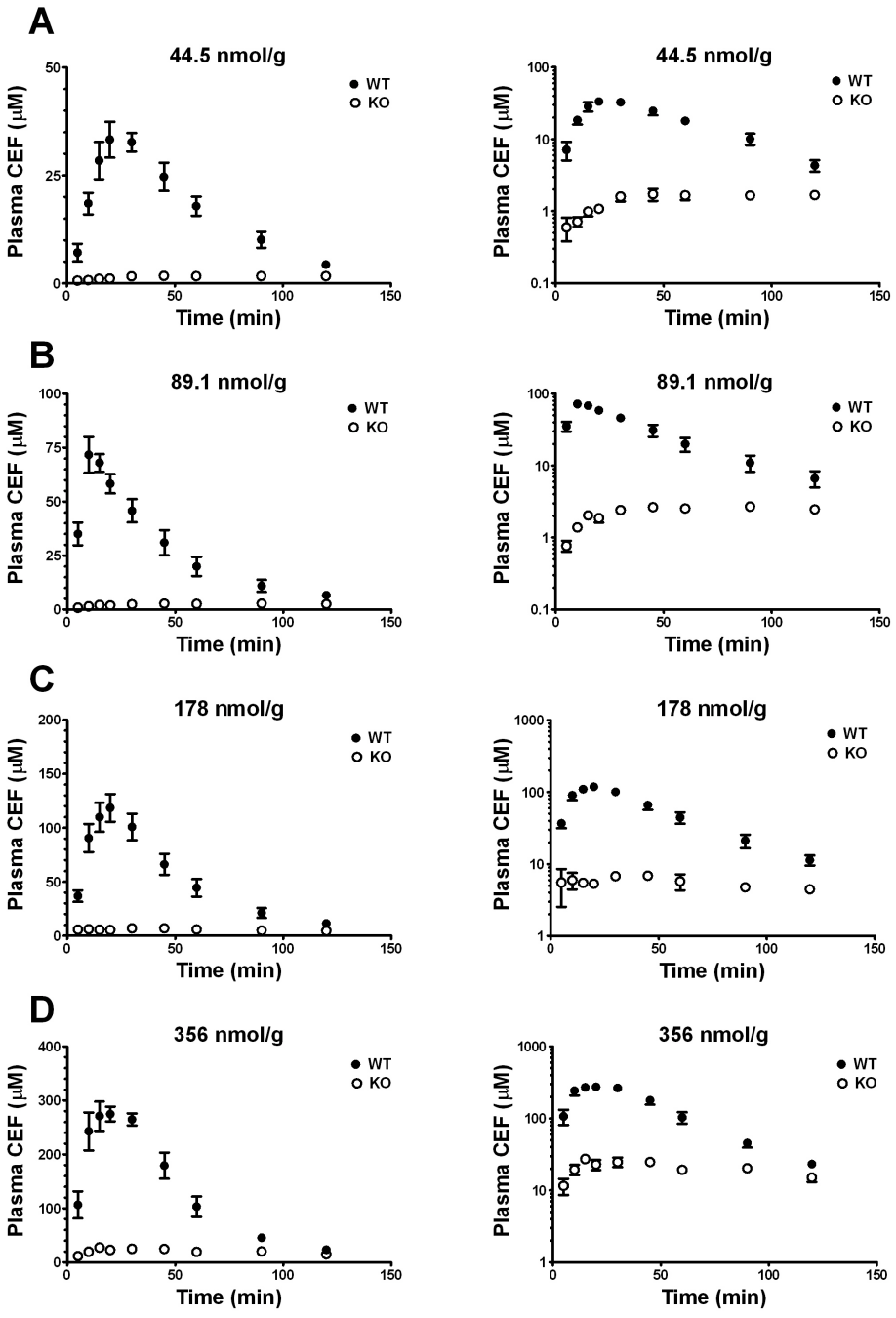

Figure 4.1. Plasma concentration-time profiles of cefadroxil in wild-type (WT) and PEPT1 knockout (KO) mice after oral dosing of A) 44.5 nmol/g, and B) 89.1 nmol/g, C) 178 nmol/g, and D) 356 nmol/g. Data are presented as mean ± S.E. (n=6).

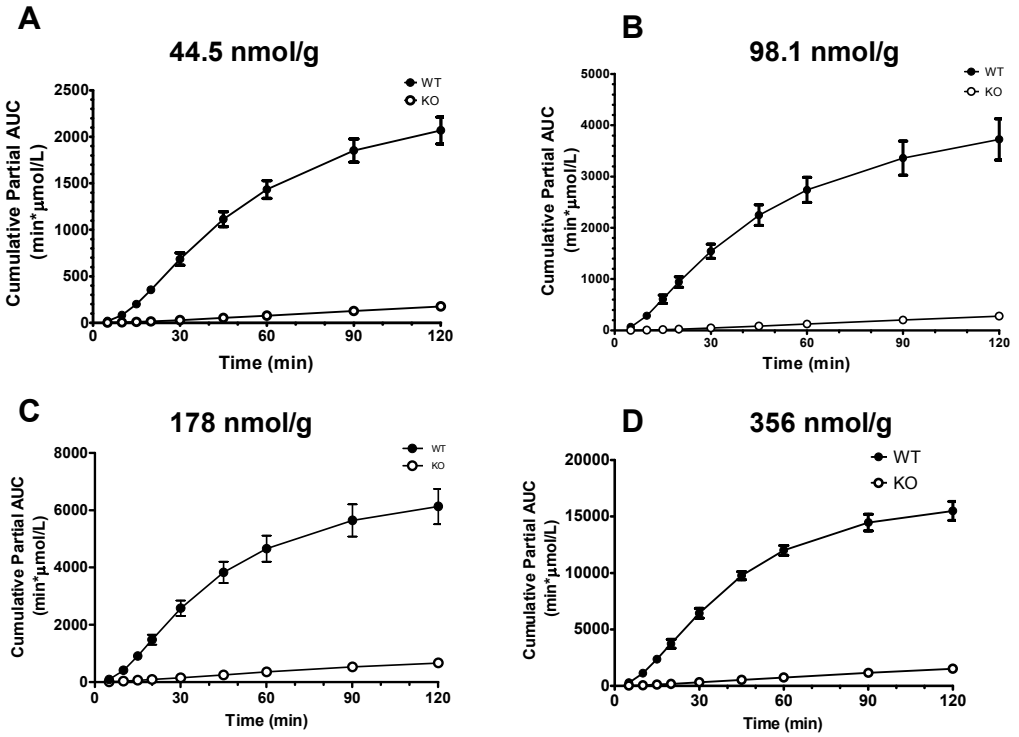

Figure 4.2. Cumulative partial area under the plasma concentration-time (AUC) vs time of cefadroxil after oral dosing of A) 44.5nmol/g, B) 89.1nmol/g, C) 178 nmol/g and D) 356 nmol/g. Data are presented as mean ± S.E. (n=6-8).

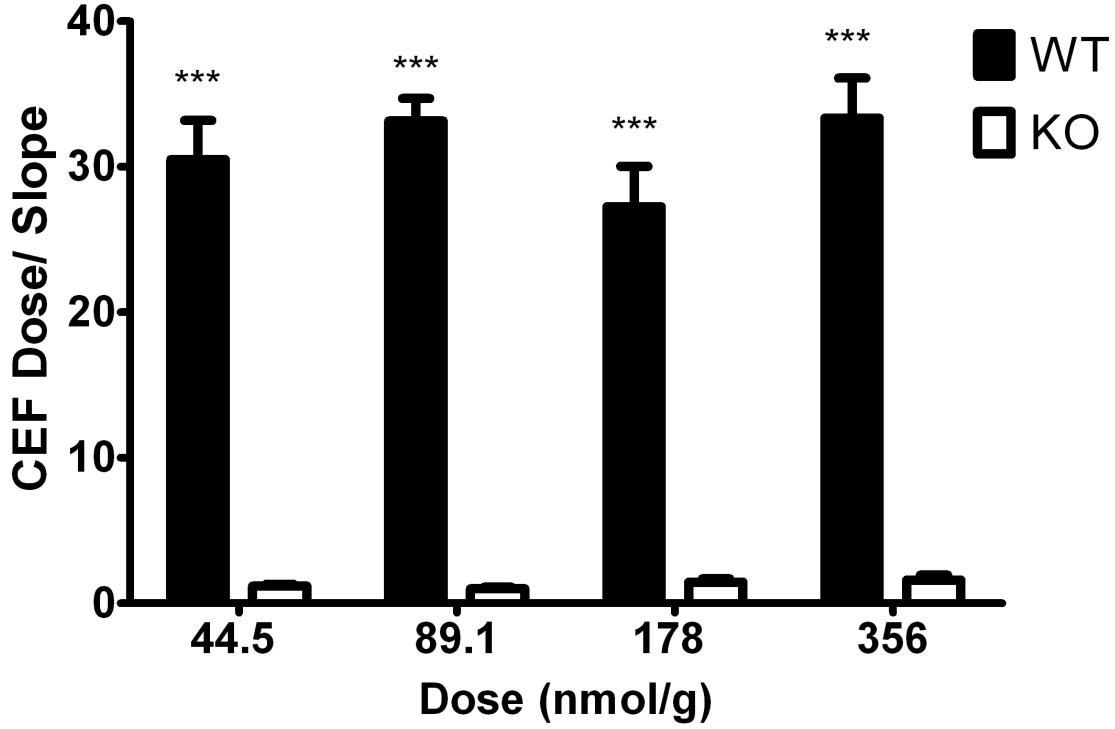

Figure 4.3. Dose-corrected initial slope of the cumulative partial AUC of ^{3}H-cefadroxil from 0-30 minutes in wild-type and PEPT1 knockout mice. Data are presented as mean ± S.E. (n=6-8). *** $p<0.005$.

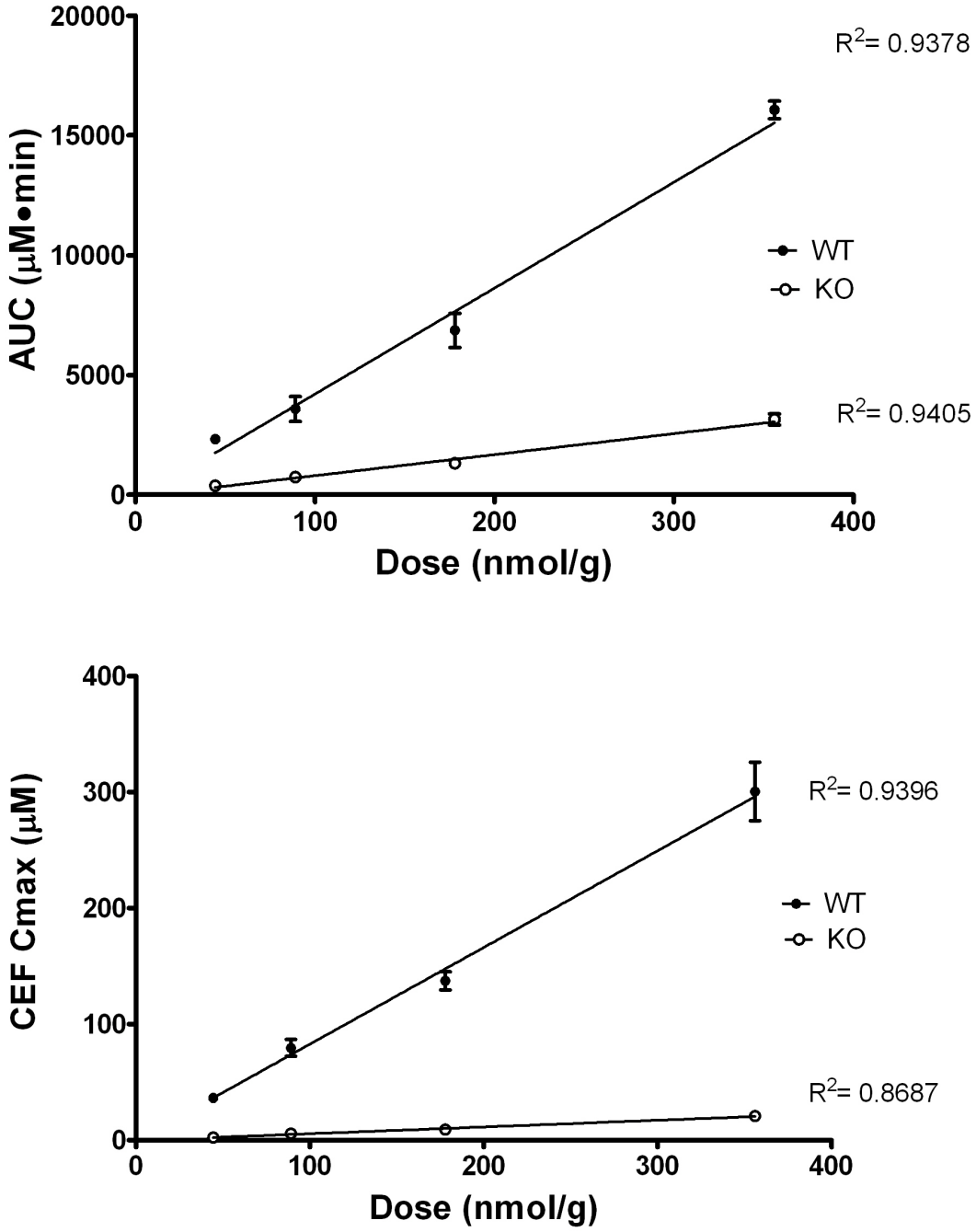

Figure 4.4. A) $AUC_{0\text{-}120}$ *vs* dose after 4 oral doses of ^{3}H-cefadroxil in wild-type and PEPT1 knockout mice. B) C_{max} vs dose for 4 oral doses of ^{3}H-cefadroxil in wild-type mice and PEPT1 knockout mice. Data are expressed as mean ± S.E. (n=6-8).

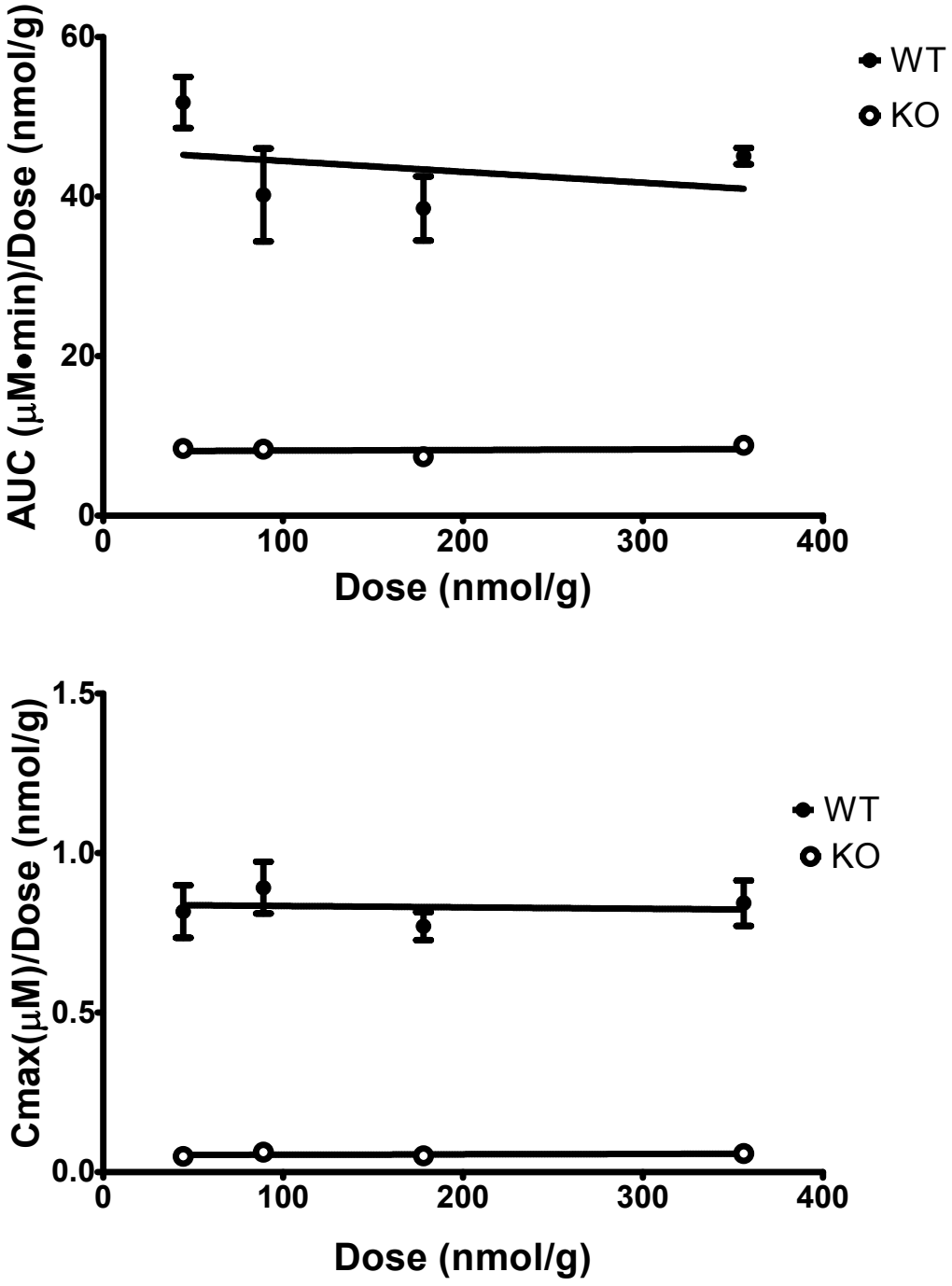

Figure 4.5. A) Dose corrected $AUC_{0\text{-}120}$ for 4 oral doses of ^{3}H-cefadroxil and B) Dose corrected C_{max} after 4 oral doses of ^{3}H-cefadroxil in wild-type and PEPT1 knockout mice. Data are presented as mean ± SE (n=6-8).

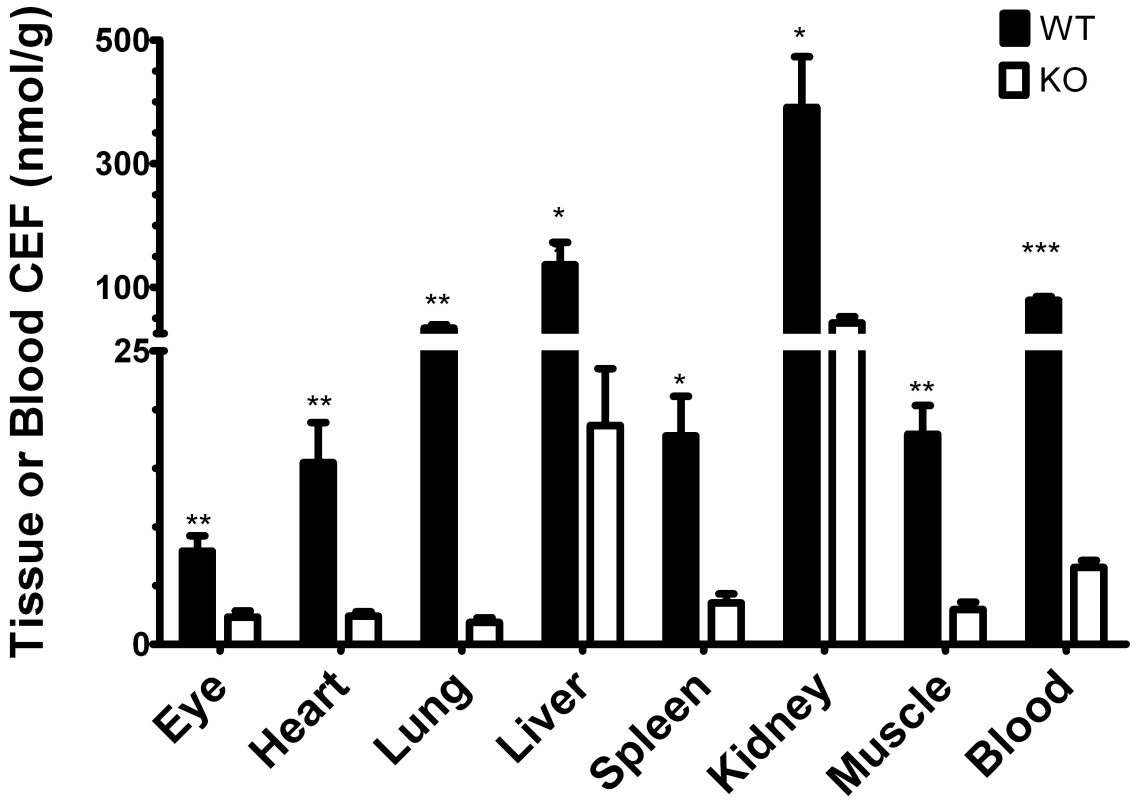

Figure 4.6. Tissue distribution of cefadroxil in wild-type (WT) and PEPT1 (KO) knockout mice 20 minutes after oral dosing of 178 nmol/g ^{3}H-cefadroxil. Data are presented as mean ± S.E. (n=6), * $p < 0.05$, ** $p < 0.01$, *** $p < 0.005$.

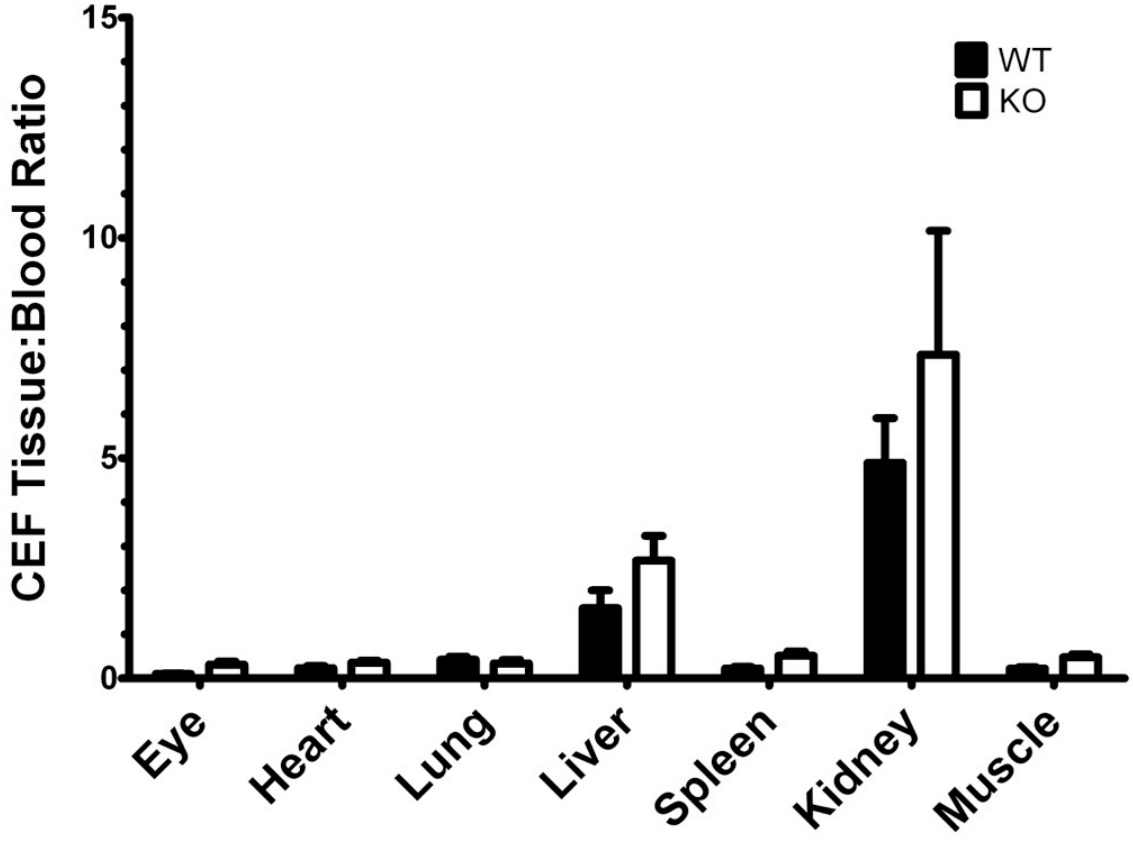

Figure 4.7. Blood corrected tissue distribution of cefadroxil in wild-type (WT) and PEPT1 knockout (KO) mice 20 minutes after oral dosing of 178 nmol/g of ^{3}H-cefadroxil. Data are presented as mean ± SE (n=6).

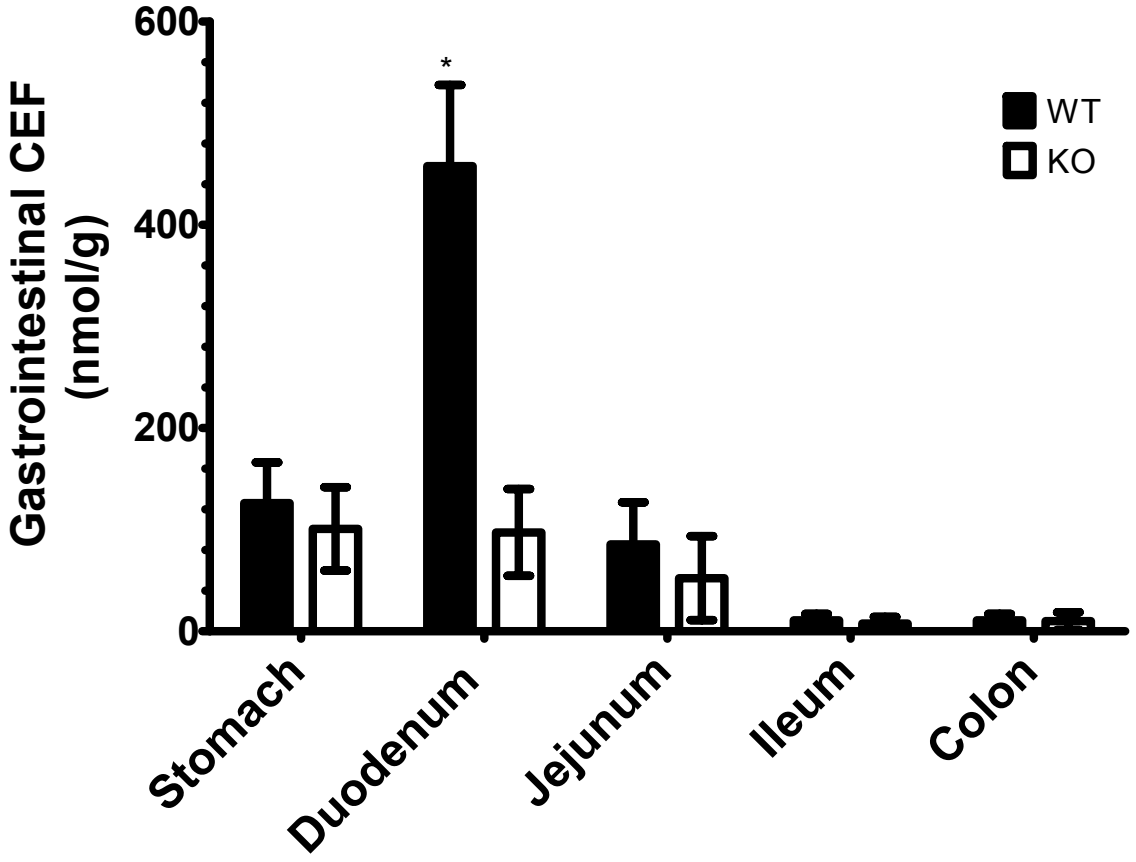

Figure 4.8. Tissue distribution of cefadroxil in the gastrointestinal tract of wild-type (WT) and PEPT1 knockout (KO) mice 20 minutes after oral dosing of 178 nmol/g of ^{3}H-cefadroxil. Data are presented as mean ± SE (n=6). *$p < 0.05$.

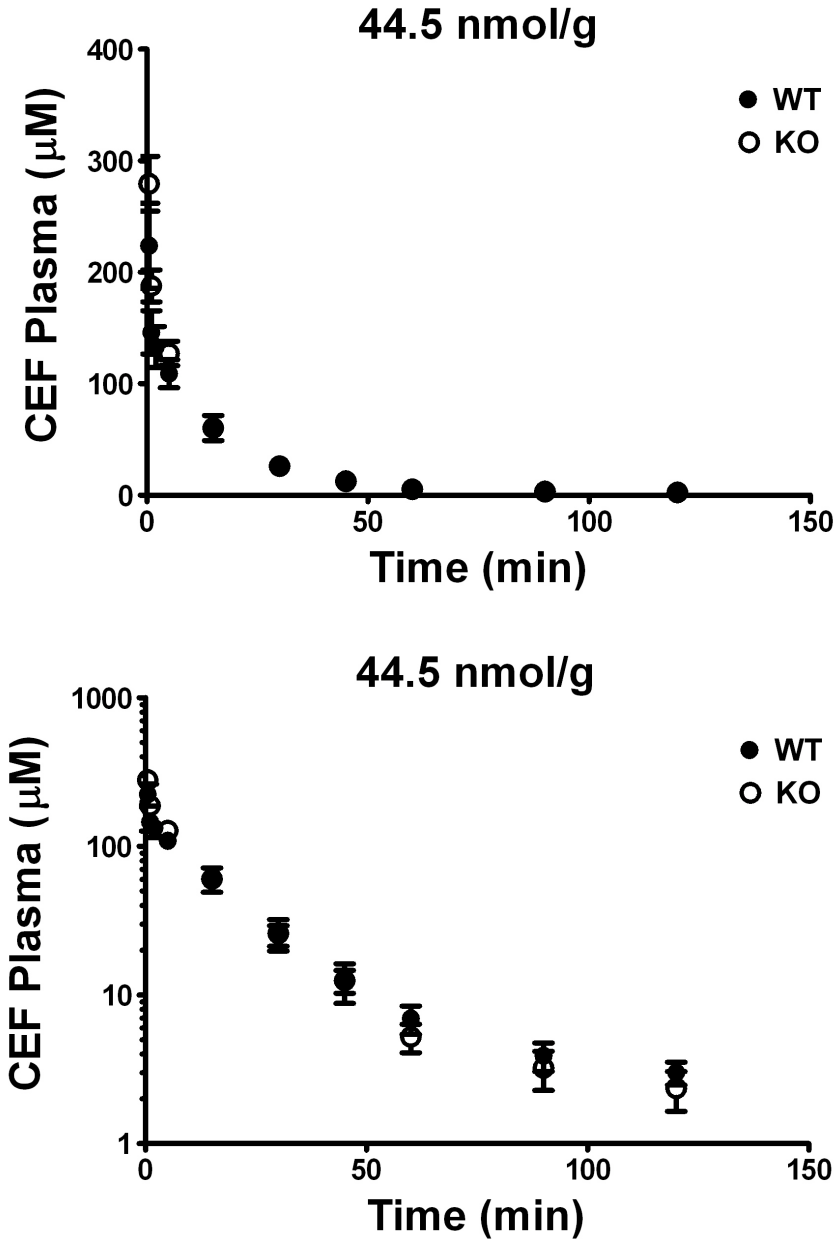

Figure 4.9. Plasma concentration-time profiles in wild-type (WT) and PEPT1 knockout (KO) mice after intravenous dosing of 44.5nmol/g of ^{3}H-cefadroxil. Data are presented as mean ± S.E. (n=6-8).

Tables

Dose (nmol/g)	Wild-type	PEPT1 KO	WT/KO
AUC 0-120 (min * μM)			
44.5	2041 ± 145	176 ± 22	11.6
89.1	3166 ± 340	279 ± 19	11.3
178	6032 ± 608	634 ± 42	9.5
356	15063 ± 733	1634 ± 281	9.2
C_{max} (μM)			
44.5	36.6 ± 3.6	2.0 ± 0.3	18.3
89.1	77.4 ± 6.4	2.9 ± 0.2	26.7
178	125 ± 14	8.9 ± 0.9	14.0
356	300 ± 16	19.6 ± 3.6	15.3

Table 4.1. Pharmacokinetic parameters of cefadroxil in wild-type and knockout mice after oral administration of ^{3}H-cefadroxil. Data are presented as mean ± S.E. (n=6-8).

Dose (nmol/g)	Wild-type	PEPT1 KO	WT/KO
	Initial Slope		
44.5	30.5 ± 2.7	1.18 ± 0.1	25.9
89.1	62.9 ± 6.1	2.00 ± 0.2	31.5
178	109 ± 11	5.79 ± 0.9	18.8
356	267 ± 22	12.8 ± 2.8	20.9

Table 4.2. Initial slopes (10-30 min) of dose-corrected partial AUC versus time plots of of ^{3}H-cefadroxil in wild-type and PEPT1 knockout mice. Data are presented as mean ± S.E. (n=6-8).

Parameter	Wild-type	PEPT1 Knockout
AUC 0-120 (min * µM)	3224 ± 312	3363 ± 488
Cl (mL/min)	0.29 ± 0.03	0.29 ± 0.03
MRT 0-inf (min)	27.0 ± 1.9	27.2 ± 1.6
Half-life (min)	32.6 ± 1.9	27.2 ± 2.5
Vdss (mL)	10.8 ± 1.2	10.0 ± 2.0

Table 4.3. Pharmacokinetic parameters of ^{3}H-cefadroxil after intravenous administration of 44.5nmol/g of cefadroxil to wild-type and PEPT1 knockout mice. Data are presented as mean ± S.E. (n=6-8).

REFERENCES

1. Herrera-Ruiz, D., et al., *Spatial expression patterns of peptide transporters in the human and rat gastrointestinal tracts, Caco-2 in vitro cell culture model, and multiple human tissues.* AAPS PharmSci, 2001. **3**(1): p. E9.
2. Daniel, H. and G. Kottra, *The proton oligopeptide cotransporter family SLC15 in physiology and pharmacology.* Pflugers Arch, 2004. **447**(5): p. 610-8.
3. Daniel, H., et al., *From bacteria to man: archaic proton-dependent peptide transporters at work.* Physiology (Bethesda), 2006. **21**: p. 93-102.
4. Buck, R.E. and K.E. Price, *Cefadroxil, a new broad-spectrum cephalosporin.* Antimicrob Agents Chemother, 1977. **11**(2): p. 324-30.
5. Tanrisever, B. and P.J. Santella, *Cefadroxil. A review of its antibacterial, pharmacokinetic and therapeutic properties in comparison with cephalexin and cephradine.* Drugs, 1986. **32 Suppl 3**: p. 1-16.
6. Marino, E.L., A. Dominguez-Gil, and C. Muriel, *Influence of dosage form and administration route on the pharmacokinetic parameters of cefadroxil.* Int J Clin Pharmacol Ther Toxicol, 1982. **20**(2): p. 73-7.
7. Ganapathy, M.E., et al., *Differential recognition of beta -lactam antibiotics by intestinal and renal peptide transporters, PEPT 1 and PEPT 2.* J Biol Chem, 1995. **270**(43): p. 25672-7.
8. Naruhashi, K., et al., *PEPT1 mRNA expression is induced by starvation and its level correlates with absorptive transport of cefadroxil longitudinally in the rat intestine.* Pharm Res, 2002. **19**(10): p. 1417-23.
9. Ries, M., U. Wenzel, and H. Daniel, *Transport of cefadroxil in rat kidney brush-border membranes is mediated by two electrogenic H+-coupled systems.* J Pharmacol Exp Ther, 1994. **271**(3): p. 1327-33.
10. Wenzel, U., et al., *Transport characteristics of differently charged cephalosporin antibiotics in oocytes expressing the cloned intestinal peptide transporter PEPT1 and in human intestinal Caco-2 cells.* J Pharmacol Exp Ther, 1996. **277**(2): p. 831-9.
11. Shen, H., et al., *Impact of genetic knockout of PEPT2 on cefadroxil pharmacokinetics, renal tubular reabsorption, and brain penetration in mice.* Drug Metab Dispos, 2007. **35**(7): p. 1209-16.
12. Ocheltree, S.M., et al., *Mechanisms of cefadroxil uptake in the choroid plexus: studies in wild-type and PEPT2 knockout mice.* J Pharmacol Exp Ther, 2004. **308**(2): p. 462-7.
13. Shen, H., et al., *PEPT2 (Slc15a2)-mediated unidirectional transport of cefadroxil from cerebrospinal fluid into choroid plexus.* J Pharmacol Exp Ther, 2005. **315**(3): p. 1101-8.
14. Terada, T., et al., *Recognition of beta-lactam antibiotics by rat peptide transporters, PEPT1 and PEPT2, in LLC-PK1 cells.* Am J Physiol, 1997. **273**(5 Pt 2): p. F706-11.
15. Shen, H., et al., *Localization of PEPT1 and PEPT2 proton-coupled oligopeptide transporter mRNA and protein in rat kidney.* Am J Physiol, 1999. **276**(5 Pt 2): p. F658-65.

16. Takeda, M., et al., *Interaction of human organic anion transporters with various cephalosporin antibiotics.* Eur J Pharmacol, 2002. **438**(3): p. 137-42.
17. Khamdang, S., et al., *Interaction of human and rat organic anion transporter 2 with various cephalosporin antibiotics.* Eur J Pharmacol, 2003. **465**(1-2): p. 1-7.
18. Ueo, H., et al., *Human organic anion transporter hOAT3 is a potent transporter of cephalosporin antibiotics, in comparison with hOAT1.* Biochem Pharmacol, 2005. **70**(7): p. 1104-13.
19. Hu, Y., et al., *Targeted Disruption of Peptide Transporter PEPT1 Gene in Mice Significantly Reduces Dipeptide Absorption in Intestine.* Mol Pharm, 2008.
20. Kimura, T. and K. Higaki, *Gastrointestinal transit and drug absorption.* Biol Pharm Bull, 2002. **25**(2): p. 149-64.
21. Masaoka, Y., et al., *Site of drug absorption after oral administration: assessment of membrane permeability and luminal concentration of drugs in each segment of gastrointestinal tract.* Eur J Pharm Sci, 2006. **29**(3-4): p. 240-50.
22. Garcia-Carbonell, M.C., et al., *Nonlinear pharmacokinetics of cefadroxil in the rat.* Drug Metab Dispos, 1993. **21**(2): p. 215-7.
23. Garrigues, T.M., et al., *Dose-dependent absorption and elimination of cefadroxil in man.* Eur J Clin Pharmacol, 1991. **41**(2): p. 179-83.
24. Barbhaiya, R.H., *A pharmacokinetic comparison of cefadroxil and cephalexin after administration of 250, 500 and 1000 mg solution doses.* Biopharm Drug Dispos, 1996. **17**(4): p. 319-30.

CHAPTER 5

IN SILICO PREDICTIONS OF THE ABSORPTION AND PHARMACOKINETICS OF CEFADROXIL IN WILD-TYPE AND PEPT1 KNOCKOUT MICE

Abstract

The aim of this study was to retrospectively model the absorption and pharmacokinetics of cefadroxil in mice, using the advanced compartmental absorption and transit model (ACAT) built within Gastroplus®. The ACAT model was used to explain mechanistically the plasma concentration-time profiles of cefadroxil in mice after oral administration of escalating doses of the antibiotic (44.5, 89.1, 178 and 356 nmol/g.) The P_{eff} and K_m values obtained in the *in situ* perfusion experiments, along with the *in vivo* disposition parameters of cefadroxil in mice, were used as input parameters in the model. A parameter sensitivity analysis was performed in order to determine the sensitivity of the $AUC_{0\text{-}120}$ and C_{max} to changes in the experimental input parameters. In the knockout mice, a fairly good prediction of plasma concentration-time profiles was obtained. In the wild-type mice, the observed plasma concentration-time profiles for the lowest 2 doses were fairly well

reproduced, and the C_{max} and AUC_{0-120} were comparable with those obtained *in vivo*. However, the model under-predicted the C_{max} and AUC_{0-120} of the highest 2 doses, perhaps because of PEPT1 saturation in the small intestine. It is important to note that cefadroxil undergoes both active tubular secretion and reabsorption, and the clearance changes constantly at a given dose. Therefore, we hypothesize that the observed linearity in C_{max} and AUC_{0-120} could be an "apparent" linearity caused by a simultaneous decrease in the fraction absorbed (due to saturation of PEPT1) and a decrease in clearance (saturation of OATs). Although the ACAT model has been proven a good tool to predict absorption and pharmacokinetics during for the first two doses, for the latter two doses it becomes necessary to connect the ACAT model to a new PBPK model that includes several non-linear processes for the disposition of cefadroxil.

Key Words

ACAT model, Cefadroxil, Absorption, PEPT1, Knockout mice, Modeling and Simulation.

Introduction

The past few decades have seen important changes in the practice of drug development, shifting from empirical towards more mechanistic and model-based approaches. These systematic methods of drug development have benefited immensely from model building software and computational tools. The design of *in silico* predictive tools has expanded considerably in the pharmaceutical research world, where it has helped immensely in go/no-go decisions and reducing cost and time of first in human trials. Despite most of the modeling in the pharmaceutical industry occurring in the clinical phases of drug development, more of it is starting to be done in early stages of drug discovery, formulation, and preclinical research [1-3].

The accurate prediction of a drug's pharmacokinetics and absorption behavior from *in vitro* and preclinical data is crucial in reducing time and money in drug development and drug discovery settings. Moreover, the early prediction of ADME properties can aid in the selection of the best candidates for development, resulting in a faster progression into phase I clinical studies by eliminating compounds with poor pharmacokinetic properties earlier on in the development process [3].

Oral administration is the major and preferred route of drug delivery due to its convenience, safety, low cost, and patient compliance. However, predicting the absorption behavior and pharmacokinetics of orally administered drugs is not an easy task. Predicting drug absorption and pharmacokinetics is challenging due to the complexity of the physical, physiological and biochemical processes involved in

the GI tract such as drug release and dissolution, precipitation, absorption and efflux transporters, metabolism, and others [3-5].

The prediction of a drug's absorption rate and extent is benefitted immensely from understanding what factors play important roles in drug absorption. Some of the key ones are: 1) the physicochemical characteristics of the drug, 2) the anatomy and physiology of the gastrointestinal tract, and 3) the dosage form. Since the mid 1990's a few research groups have tried to integrate their knowledge about all these phenomena, which resulted in the development of different dynamic models that allow the prediction of the extent and rate of drug absorption in the GI tract [4]. Some of these prediction models include the dispersion model, the mixing tank model, the compartmental absorption and transit model (CAT), the advanced dissolution and absorption and metabolism model (ADAM), the Grass model, the gastrointestinal transit and absorption (GITA) model, and the advanced compartmental absorption and transit (ACAT) model [4].

The CAT or compartmental absorption and transit model, developed by Amidon and Yu, divides the GI tract into 7 compartments and describes the transport of drug through them by a series of differential equations. The CAT model can be used to predict passive absorption and/or saturable absorption, drug degradation in the intestine, and drug pharmacokinetics. The caveats of this model include its inability to predict absorption from the stomach and colon, and inability to predict the permeability of compounds based on their chemical structure [4, 6] [7].

The ADAM (advanced dissolution absorption and metabolism) model used by SimCyp® is based on the CAT model. It uses solubility, permeability, gastrointestinal transit times and surface area, enzyme distribution, and blood flow to predict the extent and rate of absorption of drugs. Though this model is really useful in the prediction of enzymatic related processes such as drug-drug interactions and metabolism, its limitations include the lack of prediction of absorption in the stomach and colon, and the inability to predict intestinal transporter related drug-drug interactions [8] [9].

The Grass model, developed by Grass *et al* [10, 11], is a multicomponent physiologically based model used to predict drug absorption. It is an easy to use model that incorporates solubility, permeability and surface area data to predict drug absorption. However, its biggest limitation is that it does not incorporate first-pass metabolism or active transport processes.

The GITA model, developed by Kimura *et al* [12-15], divides the intestine into 8 segments and calculates the absorption rate coefficient for each of them. The GITA model can predict a first-pass effect, but unfortunately is unable to incorporate active transport into the simulations and predictions.

The ACAT model used in Gastroplus® was developed by Simulations Plus and divides the gastrointestinal tract into 9 compartments, all of which can have absorption occurring from them. The ACAT defines one compartment for stomach, one for the duodenum, 2 compartments for the jejunum, 3 for the ileum, 1 for the ceacum, and 1 compartment for the ascending colon. The above 9 compartments are then sub-divided into the following 4 sub-compartments: unreleased drug,

undissolved drug, dissolved drug, and the enterocyte. The disintegration, dissolution, permeation and gastrointestinal transit of drug between all of these compartments and sub-compartments are described by a series of differential equations, including linear and non-linear processes. By knowing a drug's structure and its *in vitro* (or *in situ*) affinity for the transporter, one can predict the fraction absorbed and bioavailability of the compound in preclinical and clinical settings, if it interacts with food or other drugs and its tissue distribution and disposition.

Among other qualities, Gastroplus can simulate changes of pH along the gastrointestinal tract, which may affect the solubility and permeability of ionizable molecules such as cefadroxil. Gastroplus® also takes into account changes in volume of fluid in the small intestine and colon, which can affect the concentration of drug in the GI tract and, therefore its uptake velocity by transporters and/or its propensity to precipitate. Moreover, it takes into account the surface area in the small intestine and how it changes along the GI tract in order to get a better prediction of the permeability. Gastroplus has a module called ADMET™ predictor, which can predict the effective permeability of a drug molecule, based on its chemical structure. Not only can it predict drug permeability, it can also predict other properties, including ionization constants, diffusion coefficient, solubility, supersaturation ratio, logP, logD, fraction of drug unbound in plasma, and blood to plasma ratio.

Cefadroxil (Figure 5.1) is a first generation amino-cephalosporin used to treat skin, upper respiratory tract and urinary tract infections caused by both gram positive and negative bacteria. It was chosen as a model drug because of its

metabolic and chemical stability, and its commercial availability as a radiolabeled drug. Although cefadroxil absorption is primarily due to PEPT1-mediated transport, it has been shown to have apparent linear $AUC_{0\text{-}120}$ and C_{max} values with increasing doses in humans and in mice. The antibiotic has a molecular weight of 363, an intrinsic solubility of 17.4 mg/mL, and a $logD_{4.96}$ of -2.41. It has three ionization constants (pka's) at 2.70, 7.22, and 9.62. Cefadroxil has high permeability and excellent oral bioavailability (~90% in humans). It also has high solubility and a low drug dose number (Do= maximum dose strength (mg)/lowest solubility (mg/mL) /250 mL = 0.23) of ≤ 1, and its absorption is not affected by food intake. Cefadroxil chemical degradation is marginal at physiological pH, with lower degradation rate constants in more acidic environment. Also, cefadroxil is metabolically stable and almost all of it is excreted unchanged in the urine [16].

PEPT1 a member of the solute carrier (SLC) superfamily of transporters is present in the apical membrane of the enterocytes of the duodenum, jejunum, and ileum, but not in the stomach or colon. Our group previously published mRNA levels and protein expression patterns in both wild type and PEPT1 knockout mice [17, 18]. Expression levels of PEPT1 in mouse are similar along regions of the small intestine, but significantly higher than in colon [17]. Also, our previous studies in wild-type and PEPT1 knockout mice showed that the major site of cefadroxil absorption after oral administration is the small intestine (Chapter 3 and Chapter 4). Likewise, we showed that PEPT1 is the most important absorption pathway for cefadroxil, accounting for over 90 % of the uptake of this antibiotic in the small intestine during *in situ* perfusion studies. Previous studies showed that in the kidney,

cefadroxil is primarily reabsorbed from the renal tubules by PEPT2 expressed on the apical membrane of the renal epithelial cells[16], and secreted by organic anion transporters at the basolateral membrane of the renal epithelial cells (more information and references in Table 1).

In this chapter our main objectives are to integrate, using the ACAT built within Gastroplus®, the acquired knowledge about PEPT1 functionality and the physiological and physicochemical properties of cefadroxil, and to retrospectively model the extent and rate of absorption and pharmacokinetics of this antibiotic in mice.

Material And Methods

Simulations

All simulations were run on a Dell Dimension 5150 computer using GastroPlus® software (version 8.0.002, Simulations Plus, Inc, Lancaster, CA). The ACAT model was to predict the rate and extent of absorption of cefadroxil (Figure 1) from the gastrointestinal tract.

ACAT model

The advanced compartmental absorption and transit (ACAT) model numerically integrates a set of over 80 differential equations that describe different processes with linear and non-linear kinetics, occurring after drug administration. These processes include: disintegration, dissolution, precipitation, absorption, exsorption, excretion, degradation, metabolism (in gut and liver), distribution, and clearance (renal and non-renal). The ACAT model divides the gastrointestinal into a set of 9 compartments: stomach, duodenum, jejunum 1, jejunum 2, ileum 1, ileum 2, ileum 3, ceacum, and ascending colon. Each of these compartments is divided into 4 sub-compartments, based on the state of the drug: unreleased, undissolved, dissolved, and enterocyte [19].

In this project, the ACAT model was used to simulate retrospectively the rate and extend of absorption and pharmacokinetics of four oral doses of cefadroxil administered to mice. The four doses of cefadroxil (Table 5.10) were administered in solution to both wild-type and PEPT1 knockout mice as described below. A schematic representation of the tailored ACAT model used in this project is shown

in Figure 5.2. The tissue expression levels of PEPT1 used in the simulations of wild-type mice were extracted and/or adapted from the literature, based on RNA and protein levels in mice and in humans (Table 5.2). All PEPT1 expression levels are relative values based on the expression of PEPT1 transporter in the ileum.

ACAT Model Assumptions

The following assumptions were made in order to model the absorption of cefadroxil in mice using GastroPlus®: 1) there is no degradation of cefadroxil in the gastrointestinal tract; 2) all transit through the gastrointestinal tract are first-order processes; 3) there is no absorption of cefadroxil in the stomach; 4) the disposition of cefadroxil is the same in both wild-type and PEPT1 knockout mice and follows linear kinetics (i.e. no saturation is present); and 5) in wild-type mice, PEPT1 is the only transporter responsible for the absorption of cefadroxil into the enterocyte and it is only expressed in the apical membrane of the small intestine.

Cefadroxil

Cefadroxil is a polar ampholyte with medium-high solubility in water and low passive permeability. It has been shown by *in situ* perfusion that at least 90% of its transport in the small intestine of mice is dependent on PEPT1, with an apparent K_m of 3.8 mM. Cefadroxil has 3 pKa's, two acidic ones at 2.7 and 9.62, and one basic pKa at 7.22. More information about its properties can be found in Table 5.3 and Table 5.4. Cefadroxil has been found to have negligible metabolism in the small intestine and plasma. Cefadroxil has also been reported to have very low luminal

degradation in different species, especially at low pH. After intravenous administration to mice, 98% of cefadroxil is found intact in urine after 24 hours [16].

Animal Studies with Cefadroxil

All *in vivo* and *in situ* studies were done in 8-10 week old gender-matched wild-type ($PEPT1^{+/+}$) and PEPT1 knockout ($PEPT1^{-/-}$) mice. The animals were kept in a temperature-controlled room with 12-hour light and dark cycles, and given a standard diet and water *ad libitum*. All of the procedures were approved by the University of Michigan Committee on Use and Care of Animals (UCUCA), and were carried out in accordance with the Guide for Use of Laboratory Animals as adopted and promulgated by the US National Institutes of Health (NIH publication No. 85-23, revised in 1985).

The permeability of cefadroxil in the small intestine and colon (P_{eff}) was determined according to the procedures described in Chapter 3. Briefly, mice were anesthetized, and their duodenum, jejunum, ileum, and colon were isolated and perfused with ascending concentrations of cefadroxil (0.001 - 25 mM) at a rate of 0.1 mL/min, pH of 6.5. The samples were collected at steady state (after ~ 30 min) and were analyzed by high performance liquid chromatography coupled to an ultraviolet detector. The effective permeability (P_{eff}, cm/sec) of cefadroxil was calculated with the following formula:

$$Peff = \frac{-Q \ln(Co / Cin)}{2\pi RL} \tag{5.1}$$

where Q is the perfusion rate (ml/sec), C_{out} is the water flux-corrected concentration of cefadroxil coming out of the perfused segment (μg/mL), C_{in} is the input

concentration of cefadroxil (μg/mL), and R and L are the radius and length of the perfused segment (cm), respectively.

The plasma concentration-time profiles of cefadroxil in mice used in these simulations were determined in our laboratory with standard procedures as described in Chapter 4. Briefly, all studies were done in 8-10 week old gender-matched wild-type ($PEPT1^{+/+}$) and PEPT1 knockout ($PEPT1^{-/-}$) mice. Cefadroxil was dosed via oral gavage (0.323, 0.646, 1.292, 2.584 mg) or tail-vein injection (0.323 mg), and the plasma was harvested after serial blood sampling, from 0 and 120 minutes. The radioactivity in plasma was measured using a dual channel liquid scintillation counter. The pharmacokinetic values of cefadroxil after intravenous administration were fitted using WinNonlin, and the goodness of fit was evaluated by visual inspection of the predicted values and residual plots.

Absorption Models and Gastrointestinal Physiology

GastroPlus® defines absorption as the movement of drug from the intestinal lumen into the enterocyte, and calculates the absorption rate constant as a product of the effective permeability of the drug and the absorption scale factor, according to the following formula

$$ka = P_{eff}\,\alpha \tag{5.2}$$

where P_{eff} is the effective permeability and α is the absorption scale factor (ASF) for each intestinal segment. The absorption scale factor is used to scale regional permeability to the absorption rate constant and is defined as the ratio of the volume of the intestinal segment and its surface area, as seen in the formula:

$$\alpha = \frac{(cylinder\ surface)\ 2\pi RL}{(cylinder\ volume)\pi\ R^2\ L} = \frac{2}{R} \quad (5.3)$$

Therefore, the ka can be defined as:

$$ka = P_{eff}\frac{2}{R} \quad (5.4)$$

Gastroplus has different models to calculate and scale the absorption scale factor (ASF) for different segments of the intestine, according to differences in surface area and width of the tight junctions. The 8 different models were compared based on their sum of squares errors and the differences between the predicted and observed plasma-concentration time profiles and pharmacokinetic parameters.

Parameter Sensitivity Analysis

Initially, a parameter sensitivity analysis (PSA) was performed using data for the lowest dose of cefadroxil (44.5nmol/g) in knockout mice, thus providing an understanding of the sensitivity of the predicted C_{max} and $AUC_{0\text{-}120}$ of cefadroxil to several input properties including effective permeability (P_{eff}), clearance (Cl), volume of distribution in the central compartment (V_c), and the distribution micro-rate constants (K12, K21).

Subsequently, a second parameter sensitivity analysis was performed using data for lowest dose of cefadroxil (44.5 nmol/g) in the wild-type mice. In this analysis, we tested the sensitivity of the predicted C_{max} and $AUC_{0\text{-}120}$ to changes in the previously mentioned pharmacokinetic parameters, and in the PEPT1 affinity constant (K_m), and maximum transport rate constant (V_{max}).

Optimization

The optimization function in GastroPlus® was used to calibrate the model by minimizing the objective function (error function) of different model parameters specified by the user in order to get a better prediction of the $AUC_{0\text{-}120}$ and C_{max}, These optimizations were performed in the training data sets which were the lowest dose (44.5 nmol/g) in both wild-type and PEPT1 knockout mice. The parameters that were optimized were V_{max} for PEPT1 in the wild-type mice, since the value obtained in the *in situ* perfusion experiments cannot be directly scaled to the *in vivo* value in the simulations. In addition to V_{max}, some pharmacokinetics parameters obtained after intravenous administration of cefadroxil in mice were optimized such as clearance, volume of distribution in the central compartment, and the distribution rate constants.

Simulation Strategy

The following strategy was followed for the retrospective simulation of the absorption of cefadroxil in mice:

1. Development of an absorption model using the lowest dose of cefadroxil (44.5 nmol/g) in PEPT1 knockout mice (training set A).
2. Parameter sensitivity analysis and model optimization for training set A .
3. Development of an absorption model using the lowest dose (44.5 nmol/g) in wild-type mice (training set B).
4. Parameter sensitivity analysis and model optimization of training set B.
5. Simulation of absorption and pharmacokinetics of cefadroxil in wild-type and PEPT1 knockout mice for 3 higher doses (89.1, 178, and 356 nmol/g).

6. Evaluation of the quality of the simulations, as judged by: 1) an evaluation of the coefficient of determination R^2 and the sum of squares of error (SSE), 2) a visual inspection of the plasma concentration-time profiles, and finally 3) a comparison of the observed and the predicted pharmacokinetic parameters C_{max}, and $AUC_{0\text{-}120}$.

Results

Disposition of Cefadroxil

The plasma concentration-time data obtained after the intravenous administration of cefadroxil in wild-type and PEPT1 knockout mice, were fitted using a two-compartment model with a weighting factor of $1/Y^2$. This model was chosen because it had the lowest Akaike Information Criterion (AIC), the lowest Schwartz Bayesian Criterion (SBC), the lowest R^2, and produced the best estimates for the parameters and standard errors. Since there were no significant differences between wild-type and PEPT1 knockout mice, the data were pooled together and the average values of the pharmacokinetic parameters were used for the model. The clearance (Cl), volume of distribution in the central compartment (V_c), and peripheral compartment distribution micro- rate constants (K_{12} and K_{21}) obtained in the fitting with WinNonlin® are shown in Table 5.5.

Parameter Sensitivity Analyses (PSA)

The parameter sensitivity analyses performed in the in the PEPT1 knockout mice show that clearance and effective permeability are the two parameters that most affected the C_{max} of cefadroxil, followed by k12 and the volume of distribution in the central compartment. As shown in Figure 5.3 A for knockout mice, when the effective permeability (P_{eff}) of cefadroxil was increased by two orders of magnitude, the C_{max} changed from 0.23 to 1.53 μg/mL (~7-fold increase). In contrast, when the clearance was increased by two orders of magnitude, the C_{max} decreased from 2.15

to 0.07 μg /mL (30-fold difference). Similarly, when V_c and K_{12} increased by 2 orders of magnitude, the C_{max} decreased by 2 fold.

For wild-type mice, the C_{max} was found to be sensitive to changes in volume of distribution in the central compartment (V_c), V_{max}, K_m, clearance (CL) and the distribution micro-rate constant (K_{12}) as seen in Figure 5.3 B. When the volume of distribution in the central compartment was increased by 2 orders of magnitude, the C_{max} decreased from 52 to 4.2 μg /mL (~13-fold difference). When the V_{max} increased by 2 orders of magnitude, the C_{max} increased from 12 to 44 μg/mL (4-fold difference). When the K_m increased by 2 orders of magnitude, the C_{max} decreased from 41 to 11 μg /mL (4-fold difference). When the clearance increased by 2 orders of magnitude, the C_{max} decreased from 37 to 6.5 μg /mL (~5-fold difference). When the k12 increased by 2 orders of magnitude, the C_{max} decreased from 28 to 10 μg /mL (~3-fold difference).

As seen in Figure 5.4 A, the $AUC_{0\text{-}120}$ for PEPT1 knockout mice was most affected by the effective permeability (P_{eff}), the clearance (CL), and the volume of distribution in the central compartment (V_c). When the effective permeability was increased by 2 orders of magnitude, the $AUC_{0\text{-}120}$ increased from 378 to 16,636 μg /mL* hr (~44-fold). When the clearance was increased by 2 orders of magnitude, the $AUC_{0\text{-}120}$ decreased from 2236 to 34 μg/mL* hr (~65-fold). When the volume of distribution in the central compartment was increased by 2 orders of magnitude, the $AUC_{0\text{-}120}$ decreased from 1477 to 626 μg /mL* hr (~2-fold).

As seen in Figure 5.4 B, the predicted $AUC_{0\text{-}120}$ in wild-type mice was the most sensitive to changes in clearance (CL) and volume of distribution in the central

compartment (V_c). When the clearance increased by 2 orders of magnitude, the $AUC_{0\text{-}120}$ decreased from 51,000 to 17,700 μg /mL* hr (~3-fold difference). When the volume of distribution in the central compartment was increased by 2 orders of magnitude, the $AUC_{0\text{-}120}$ decreased from 17,000 to 6,400 μg /mL* hr (~2.5-fold difference).

Optimization

The first optimization step was performed with the first dose in the knockout mice data. The results are listed on Table 5.5. The optimized parameters in the knockout mice were CL, K_{12}, K_{21}, and V_c. In the wild-type mice, V_{max} was also optimized. These values are also shown on Table 5.5.

Simulation of Cefadroxil Absorption and Pharmacokinetics

Figure 5.5 shows the results for the simulation of cefadroxil plasma concentration profiles in PEPT1 knockout mice after oral administration of 44.5 nmol/g (0.323 mg), 89.1 nmol/g (0.646mg), 178 nmol/g (1.292 mg), and 356 nmol/g (2.584 mg). All 4 doses were simulated using the same optimized parameters listed in Table 5.5. All the simulated curves are within the range of individually observed data. Table 5.6 shows that the simulated C_{max} and $AUC_{0\text{-}120}$ values are very similar to the experimental ones, and that all simulations had a R^2 higher than 0.6.

Figure 5.6 shows the results for the simulation of cefadroxil plasma concentration time profiles in wild-type mice. When all doses were simulated using the same input pharmacokinetic parameters, only the plasma concentration-time

profiles for the first 2 doses looked similar to the observed profiles. The simulations of the 3rd and 4th doses significantly under predicted the profiles, which may be due to saturation of the PEPT1 transporter in the small intestine. We tested 4 different gastrointestinal tract distributions of PEPT1 based on the literature and previously obtained results in our research group. No matter which distribution was used, the simulation always predicted saturation of the 2 highest doses, with lower C_{max} and $AUC_{0\text{-}120}$ values and a shift to the right for the T_{max}.

Figure 5.7 shows the estimated percent of cefadroxil dose absorbed in each of the segments of the gastrointestinal tract in the PEPT1 knockout mice. For all four doses, the total percent absorbed was about 13 %, which is very close to the systemic exposure obtained in the *in vivo* experiments in Chapter 4. Similarly, the absorption of cefadroxil was lower and fairly consistent for each segment along the GI tract for all 4 doses. Given that PEPT1 is absent in these mice, higher amounts (and concentrations) of cefadroxil are available for absorption at each segment along the GI, from the duodenum to the lower colon. Furthermore, results of the simulation show that cefadroxil is mostly absorbed via transcellular passive diffusion in the PEPT1 knockout mice and very little drug is absorbed through paracellular diffusion (<10%).

Figure 5.8 shows the estimated percent of cefadroxil dose absorbed in different segments of the GI tract of wild-type mice for the four doses. The results show that most of this antibiotic is absorbed in the early segments of the small intestine, especially the duodenum and jejunum. At the lower doses, about 80 % of

cefadroxil gets absorbed in the first 2 hours while, at higher doses, PEPT1 gets saturated and less drug is absorbed from the GI tract (< 80%).

Discussion

This work presents a new example in which *in silico* models can be useful in the analysis and prediction of peptide/mimetic absorption in genetically modified animals. Although this model is based on previously acquired data, we believe it could be useful in understanding the role of PEPT1 in the absorption of drugs and the impact on the variability of this transporter in drug concentrations in the body. Possibly, it could also help predict the outcomes of PEPT1 substrates in other preclinical species and in humans.

In this project we predicted retrospectively the importance of PEPT1 in the rate and extent of cefadroxil absorption in mice, by integrating information acquired from our own *in situ* and *in vivo* experiments with data collected from the literature. We were able to establish a model that predicted the effect of PEPT1 on the absorption and pharmacokinetics of cefadroxil using the ACAT model built into Gastroplus®. In our model, we successfully simulated the rate and extent of absorption of 4 clinically relevant doses of cefadroxil in PEPT1 knockout mice and the 2 lower doses in wild-type mice.

From our point of view the model revealed the following important findings 1) PEPT1 has an important effect on the absorption rate and extent of cefadroxil, and it is responsible for about 90% of the drug absorbed in wild-type mice; 2) in wild-type mice, the absorption of cefadroxil occurs mostly in the proximal segments of the small intestine; 3) in PEPT1 knockout mice, most of the drug is absorbed via passive transcellular diffusion, and this process is evenly distributed along the GI tract (i.e. duodenum to colon); 4) paracellular absorption plays a minor role in the

permeability of cefadroxil in both genotypes; and 5) the model predicts saturation of PEPT1 at the 2 highest doses in wild-type mice.

Given the inter-subject variability that is usually observed in oral absorption, a parameter sensitivity analysis was performed in order to study the effect of intravenous input parameters on the predicted $AUC_{0\text{-}120}$ and C_{max} of cefadroxil in both wild-type and PEPT1 knockout mice. For the knockout mice the effective permeability and clearance had the most influence on the C_{max} and $AUC_{0\text{-}120}$ of cefadroxil. For the wild-type mice, the input parameters with the most impact on C_{max} and $AUC_{0\text{-}120}$ were the clearance and the V_{max} and K_m of PEPT1.

A parameter optimization was performed on those input variables that showed to have an important effect on the $AUC_{0\text{-}120}$ and C_{max} of cefadroxil in both genotypes, which in this case were the volume of distribution in the central compartment, clearance, and K_{12} and K_{21}. As mentioned previously, the values of the optimized parameters were similar to the fitted ones, with a maximum 2-fold difference between them. Although the sensitivity analysis revealed that the jejunal effective permeability (P_{eff}) had a big effect on the $AUC_{0\text{-}120}$ and C_{max} in knockout mice, we decided not to optimize it given the good results that were obtained in the knockout mice simulations. For wild-type mice, in addition to the already optimized intravenous pharmacokinetic parameters, we optimized the V_{max} value of PEPT1 obtained from our *in situ* experiments. In Gastroplus, this parameter is intended to be from *in vitro* experiments and not from *in situ* perfusion experiments, like it is in this particular case.

The ACAT model was very useful in predicting the plasma concentration-time profiles of cefadroxil in knockout mice. The simulated plasma concentration-time curves were very similar to the experimental ones, and the R^2 values were high enough suggesting the prediction was reliable. When analyzing the shape of the curves, the plateau of the curves and T_{max} suggest that the absorption of cefadroxil happens very slowly relative to the wild-type mice, and the absorption can be explained by flip-flop kinetics (i.e. absorption is slow compared to elimination). Results of the simulation show that the regional absorption pattern of cefadroxil in knockout mice is fairly uniform along the gastrointestinal tract. The percent of drug absorbed is similar along the different segments of the gastrointestinal tract and, given the long residence time in the intestines, absorption occurs passively in all regions including the colon.

The simulated values for percent dose absorbed of cefadroxil were very similar to the experimental values observed for knockout mice. The simulations predict that 13% of the orally administered cefadroxil dose is absorbed in the first 2 hours after dosing. Our *in vivo* results also show similar percentages, around 14%, for the relative systemic exposure of cefadroxil for this genotype. For the lower oral doses in wild-type mice, the simulated values for percent dose absorbed of cefadroxil were around 80%. This again, is very similar to the 78 % relative systemic exposure observed in the *in vivo* experiments in this genotype described in Chapter 4. The agreement between the simulated and experimental results gives us confidence in the correctness of our model.

For wild-type mice, the simulations results of the lower 2 doses (0.323 and 0.646 mg) look similar to the experimental plasma concentration-time profiles. The regional absorption results show that most of the absorption occurs in the upper regions of the gastrointestinal tract, in particular in the duodenum and jejunum. In knockout mice the lack of PEPT1 results in higher absorption of cefadroxil in the later part of the intestinal segments. This compensatory effect has been observed and described previously [20], in which passive diffusion becomes more important in lower segments of the gastrointestinal tract when PEPT1 is not present in the small intestine.

While the experimental data showed no change in the dose-corrected $AUC_{0\text{-}120}$ and C_{max} for the 4 doses, the model predicts saturation of the PEPT1-mediated absorption of cefadroxil in the small intestine. To better understand this phenomenon, we calculated what the concentrations of cefadroxil in the mouse small intestine would be for the four different doses and compared it with the K_m obtained from *in situ* experiments. As seen on Table 5.10, the calculated small intestinal concentrations of cefadroxil in the mouse for the 2 highest doses are well above the K_m of 3.8 mM (at least 2-fold higher), indicating that saturation of the PEPT1-related transport may be occurring at these doses.

Still, this lack of fit of our model in wild-type mice prompted us to start thinking about the potential of having inaccurate input parameters in our model. For example, it is possible that the Km we measured in the perfusion experiments may not be directly translatable to the *in vivo* setting. It is also possible that the

actual concentrations of drug available for PEPT1 at the apical membranes of enterocytes was lower than the calculated concentrations.

We believe our *in situ* Km value of 3.8 mM is correct and similar to what has been reported by other authors. For example, Sinko *et al* reported a K_m value of 5.8 mM for cefadroxil in rat perfusion experiments [21, 22], and Wenzel *et al* [23] reported a K_m of 1.1 mM for cefadroxil in Xenopus oocytes transfected with PEPT1. However, *in vitro* and *in situ* conditions do not necessarily reflect what happens in vivo and the Km estimate may not be extrapolated directly to *in vivo* conditions. This value of 3.8 mM was measured in the jejunum of wild-type mice using a cefadroxil perfusion rate of 0.1 ml/min. However, if one uses allometric scaling to calculate the intestinal flow rate (Q) in mice from the human value (2-3mL/min) using the following equation

$$Q_{mice} = \left(\frac{0.025kg}{70kg} \right)^{0.73} (2.5mL/\min) \tag{5.1}$$

the resulting value would be approximately 0.01 mL/min. Thus, *in vivo* perfusion rate is actually 10 times lower than the perfusion rate of 0.1 mL/min used in the *in situ* experiments, which could result in an *in situ* K_m value that is significantly different than the *in vivo* one. This is because, according to Johnson *et al* [47], a high perfusion rate decreases the resistance of the aqueous layer to the diffusion of drug from the bulk fluid towards the wall of the intestine. A lower resistance results in a lower Graetz number. This would in turn result in higher carrier permeability and a lower Km. In summary, a high perfusion rate might cause an under-prediction of the Km for the transporter, and therefore predict saturation

at higher doses. To see what would happen in to our simulations using a higher Km, we developed a model with a K_m of 35 mM, which is 10-fold higher than our *in situ* experimental value. By using this artificial K_m, no under-predictions of the AUC_{0-120} T_{max} , or C_{max} occurred, and really good correlations were observed for all 4 doses (Table 5.12).

As mentioned earlier, another reason why the model may not fit the experimental results could be that the actual concentrations of cefadroxil available for PEPT1 at the membrane surface are significantly lower than the concentrations of cefadroxil in the bulk fluid of the intestinal segment. This happens because the drug has to diffuse from the middle of the tube towards the intestinal wall, creating a gradient with higher concentrations of drug in the middle than at the wall, especially in the presence of a mucous layer barrier. In that case the concentration of cefadroxil at the apical membrane could be lower than the K_m, which would mean no saturation of this transport process.

Another possible hypothesis could be that the saturation of PEPT1 is being masked *in vivo* by other processes, and we believe that a decrease of cefadroxil clearance in the kidney is one of the responsible mechanisms. Cefadroxil, as previously described, is actively secreted in the kidney by the organic anion transporters, OAT1, OAT3, and OAT4 [24] [25, 26]. With a cefadroxil plasma concentration level above the K_m of these transporters, the active secretion of the antibiotic would become saturated and the clearance would decrease significantly with increasing doses. Therefore, the dose corrected area under the curve (AUC/D)

would not change significantly if both the fraction absorbed (F) and clearance (Cl) decrease simultaneously and proportionally, according to the following formula:

$$\frac{AUC}{D} = \frac{F}{Cl} \tag{5.2}$$

We believe that contradicting results on the pharmacokinetics of cefadroxil are the result of competing saturable processes such as active tubular secretion and reabsorption in the kidney, and PEPT1-mediated absorption in the intestine. While one paper describes the linear pharmacokinetics of cefadroxil in mice after oral administration of the antibiotic, in rats and humans there is significant controversy on the linearity of the pharmacokinetics of cefadroxil. Granero *et al* [27] showed in their renal excretion experiments with rats, that the clearance of cefadroxil first increases with an increase in infusion rate, but then decreases at even higher infusion rates. They hypothesized, that the initial increase in clearance was related to a saturation of the active reabsorption of cefadroxil, and that at even higher doses there was saturation of active secretion mechanisms. Several years later, when more sophisticated molecular techniques became available, Shen *et al* [16] demonstrated that reabsorption of cefadroxil in the kidney was primarily dependent on the peptide transporter 2 (PEPT2) [16, 28]. The authors confirmed the expression of PEPT2 on the apical membrane of renal epithelial cells, specifically in the S2 and S3 segments of the proximal tubules of kidney [28, 29]. Their experiments demonstrated that, at their highest dose, the clearance of cefadroxil in wild-type mice increased due to saturation of PEPT2. On the other hand, in their PEPT2

knockout mice experiments, the clearance of cefadroxil decreased significantly with the increasing dose, indicating saturation of active secretion [16].

Another strategy to better fit the observed results would be to couple the ACAT model to a physiologically-based pharmacokinetic model (PBPK), instead of the 2-compartment model used in this project. The PBPK model allows the addition of saturable clearance mechanisms in the kidney, such as the reabsorption and secretion by PEPT2 and OAT transporters, respectively. Several papers have already shown the benefit of coupling a PBPK model to the ACAT model in Gastroplus®. These models have been shown superior at predicting the pharmacokinetics of drugs, especially of those drugs that are subject to active transport, metabolism and convoluted pharmacokinetics[30, 31].

Additionally, a recent publication by De Waart *et al* [32] suggests that MRP3/MRP4, expressed on the basolateral membrane of the enterocytes, could be involved in the transport of cefadroxil from the enterocyte into the blood. The authors show that the *in vitro* K_m values of these transporters are 2.5 and 0.25 mM for MRP3/4, respectively [32]. Most likely, the concentration of cefadroxil in the enterocyte is higher than the K_m of these transporters at the doses of drug administered. This means that these transporters would also be saturated, and increasing concentrations of drug would not have an effect on the uptake velocity and transfer rate into the blood. These processes could be a rate-limiting step in the absorption of cefadroxil, and in conjunction with the decrease in clearance, a reason why we are unable see the non-linearity *in vivo*.

In their paper, Bolger *et al* [33] use different PEPT1 protein expression patterns in the human gastrointestinal tract, and found that the distribution by Herrera-Ruiz *et al* [34] gave them the best results. Though, the PEPT1 distributions used by the authors were based on RNA levels and not protein levels. RNA levels are not always predictive of protein levels. For example, RT-PCR shows PEPT1 RNA expression in the colon of wild-type mice, though western-blot experiments show no presence of this transporter protein in this tissue. In this project we examined different physiological distributions of PEPT1, including the 3 human distributions tested by Bolger *et al*, and mouse PEPT1 protein distribution from our lab. From all the compared distributions we got the best fits with the distribution obtained in our lab for mouse PEPT1 protein levels.

In conclusion, this study illustrated the ability of the advanced compartmental absorption and transit model, of GastroPlus®, to simulate the absorption and pharmacokinetics of cefadroxil. With the ACAT model we were able to integrate our experimental data and simulate the importance of the intestinal PEPT1 in the absorption of cefadroxil in mice. We were also able to improve our understanding of the physicochemical and biopharmaceutical factors that affect the active and passive absorption processes of PEPT1 substrates, and the resulting concentration versus time profiles. The use of Gastroplus also revealed certain pharmacokinetic aspects that were not accounted for during our previous *in vivo* and *in situ* experiments. Though we are pleased with our initial modeling attempts and results, we believe at least 3 different issues should be further considered in order to improve the prediction of plasma concentration-time profiles in wild-type

mice, and to extrapolate the results to humans. First, a physiologically-based pharmacokinetic model should be incorporated into the ACAT model to take into account the non-saturable elimination processes in the kidney. Second, one should also consider that even at higher doses the concentration of cefadroxil at the apical membrane could be smaller than the Km, due to the radial diffusion gradient of the drug across the intestinal tube. And finally, one should also take into account that a higher Km would reflect the *in vivo* situation better and could provide better predictions, given that the actual residence time of the drug in the intestine is longer *in vivo* than in the *in situ* experiments.

Figures

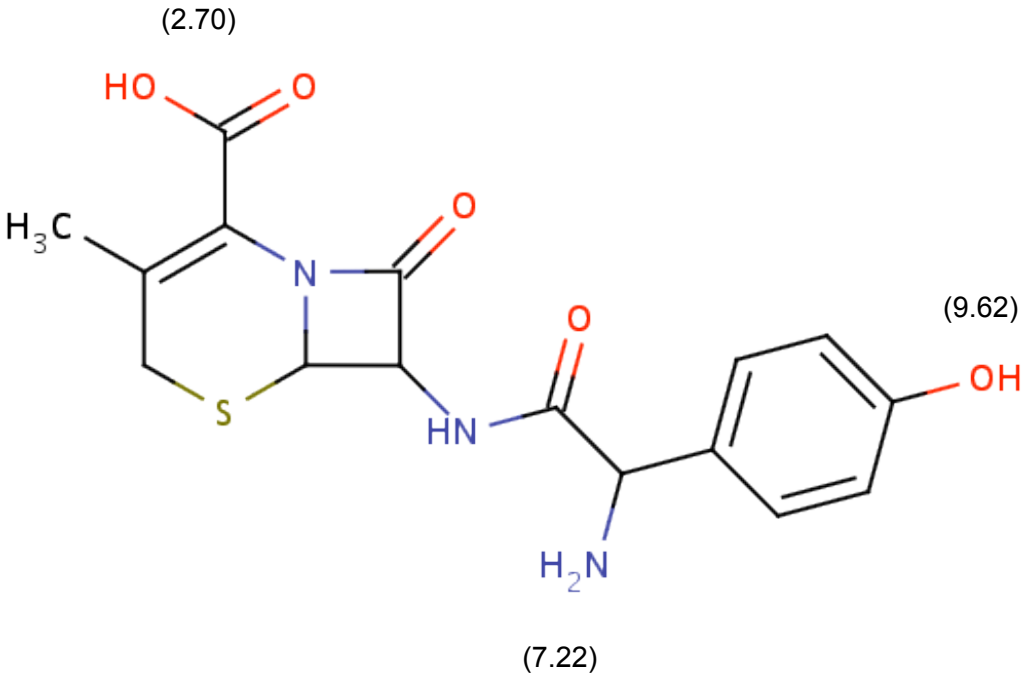

Figure 5.1. Cefadroxil monohydrate molecular structure.

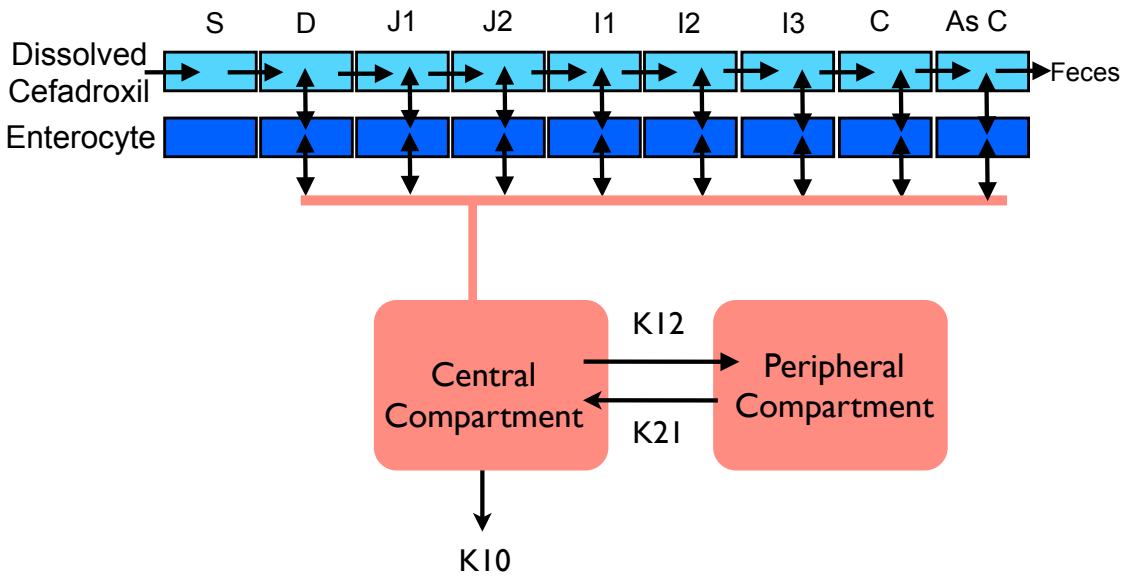

Figure 5.2. Diagram of the ACAT model used for the simulations of cefadroxil in wild-type and PEPT1 knockout mice. S= stomach, D= duodenum, J= jejunum, I= ileum, C= Ceacum, and As C = ascending colon.

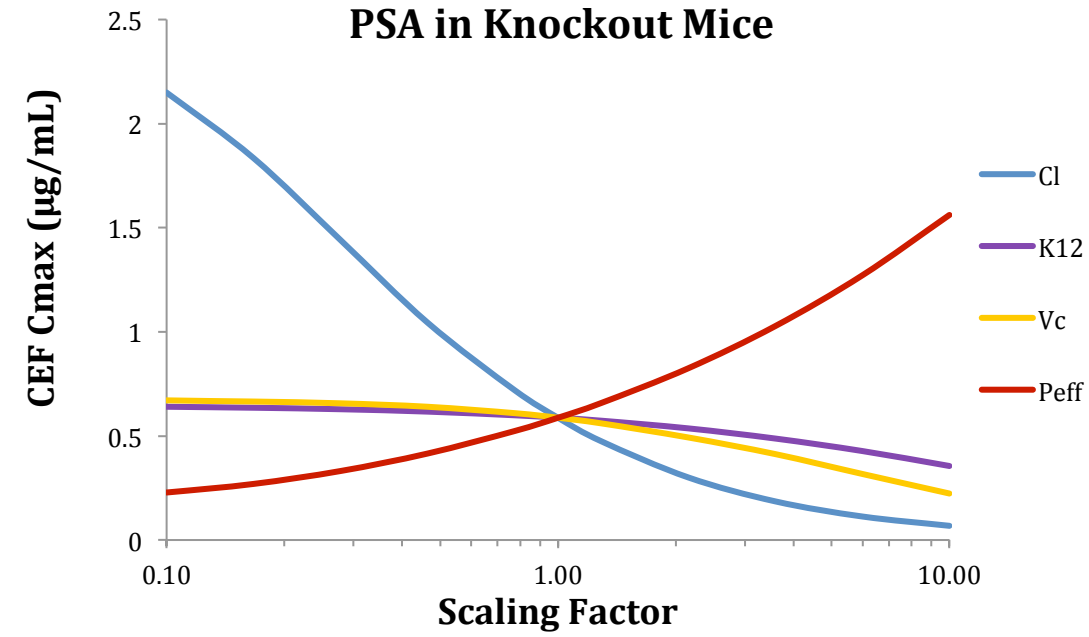

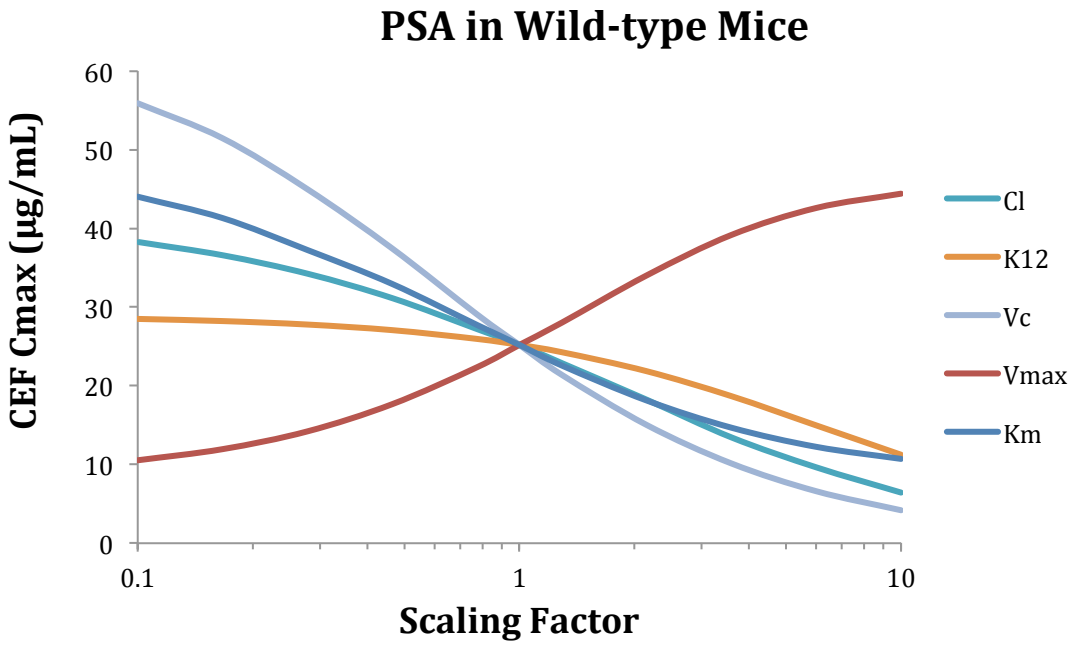

Figure 5.3. Parameter sensitivity analysis of the maximum concentration (C_{max}) of cefadroxil in PEPT1 knockout and wild-type mice.

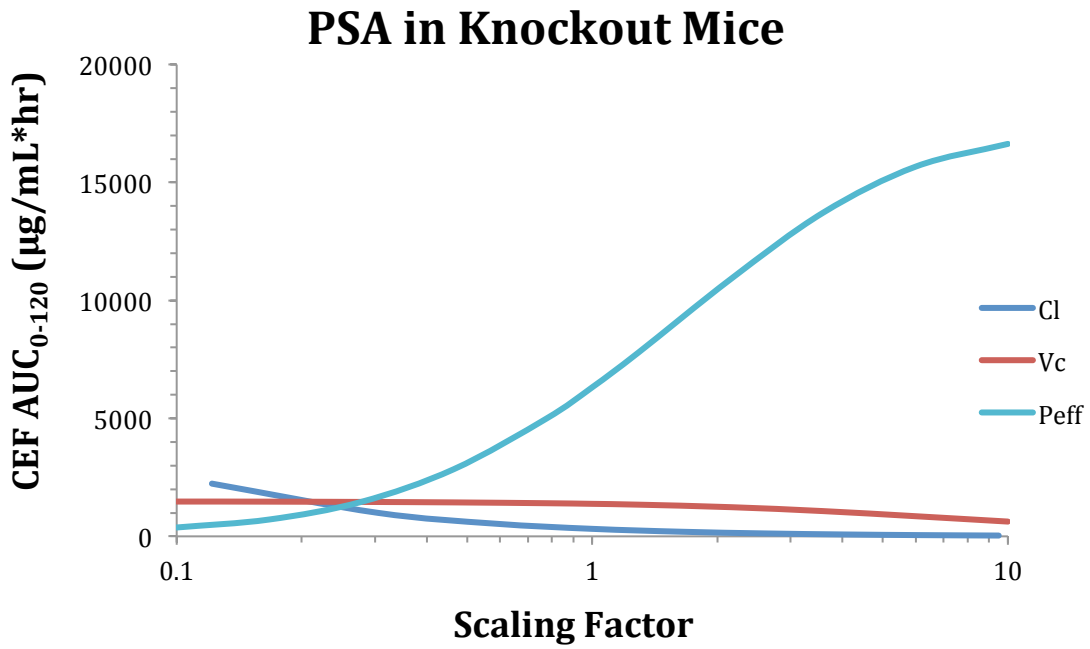

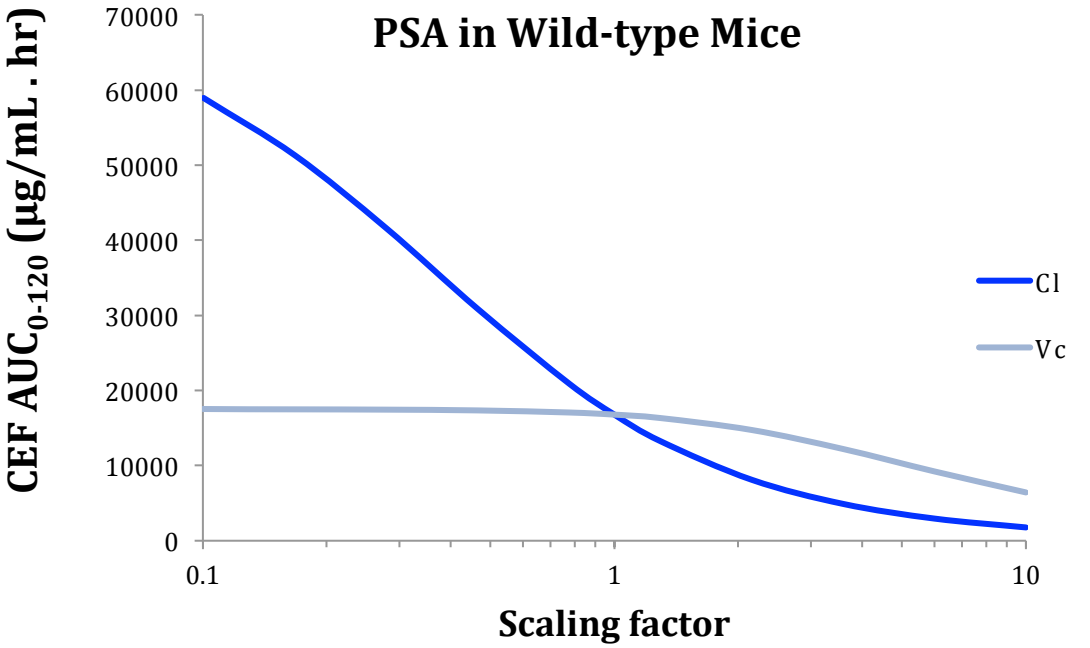

Figure 5.4. Parameter sensitivity analysis for the area under the plasma concentration-time curve ($AUC_{0\text{-}120}$) of cefadroxil in PEPT1 knockout and wild-type mice.

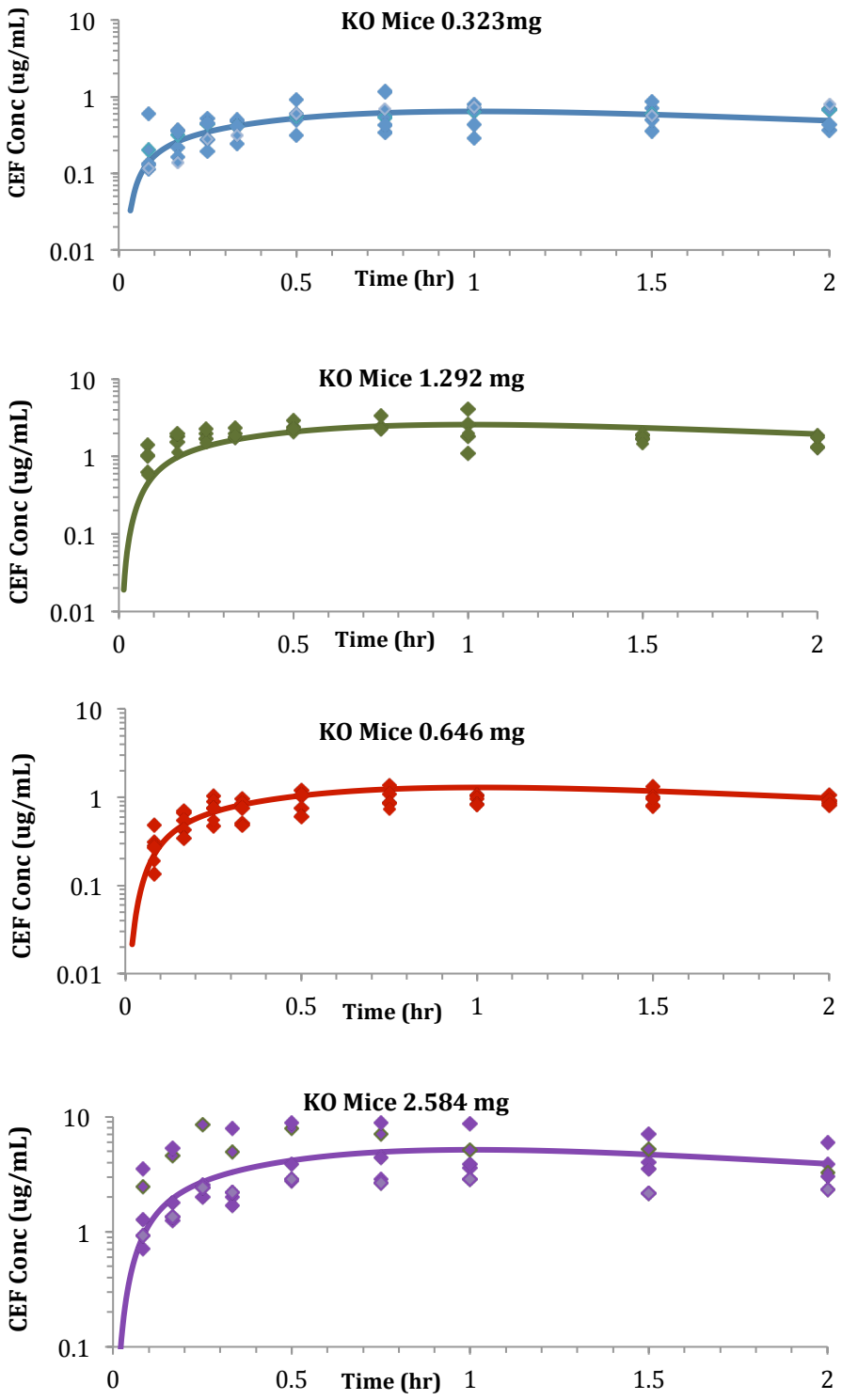

Figure 5.5. Simulation results in PEPT1 knockout mice after oral administration of 44.5, 89.1, 178 and 356 nmol/g of cefadroxil (Doses = 0.323, 0.646, 1.292, and 2.582 mg, respectively).

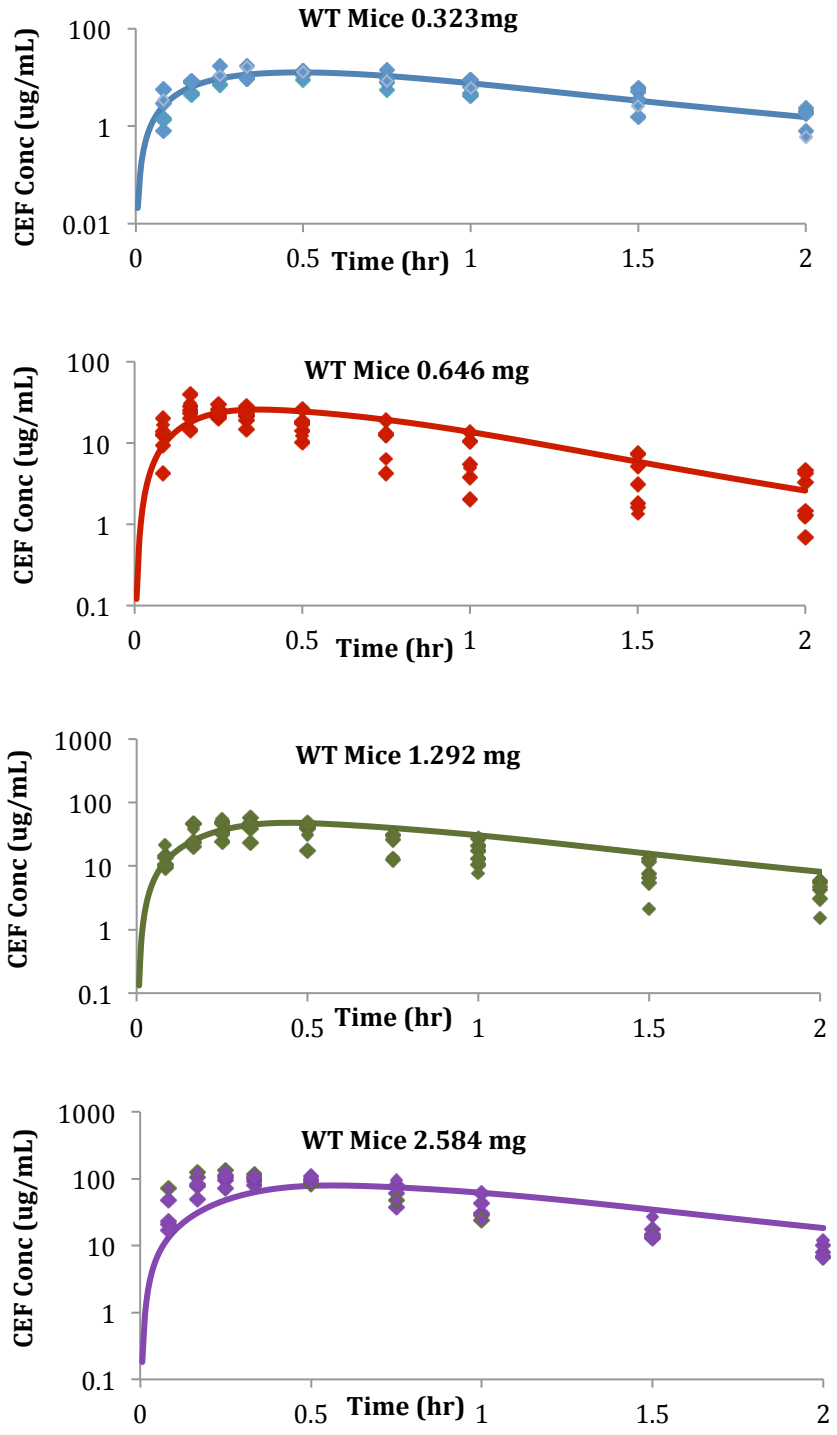

Figure 5.6. Simulation results in Wild-type mice after oral administration of 44.5, 89.1, 178 and 356 nmol/g of cefadroxil (Doses = 0.323, 0.646, 1.292, and 2.582 mg, respectively.

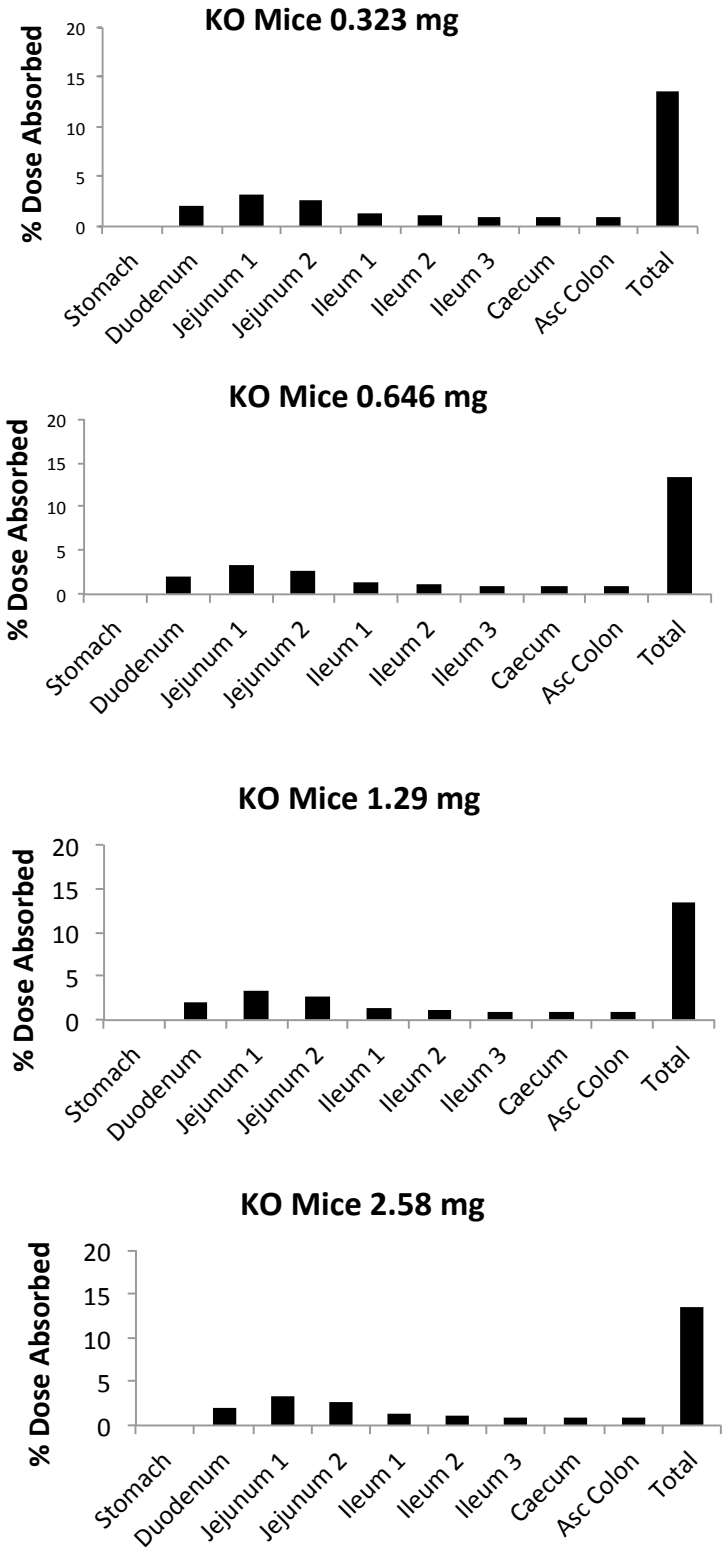

Figure 5.7. Percent of cefadroxil dose absorbed in different segments of the gastrointestinal tract in PEPT1 knockout mice.

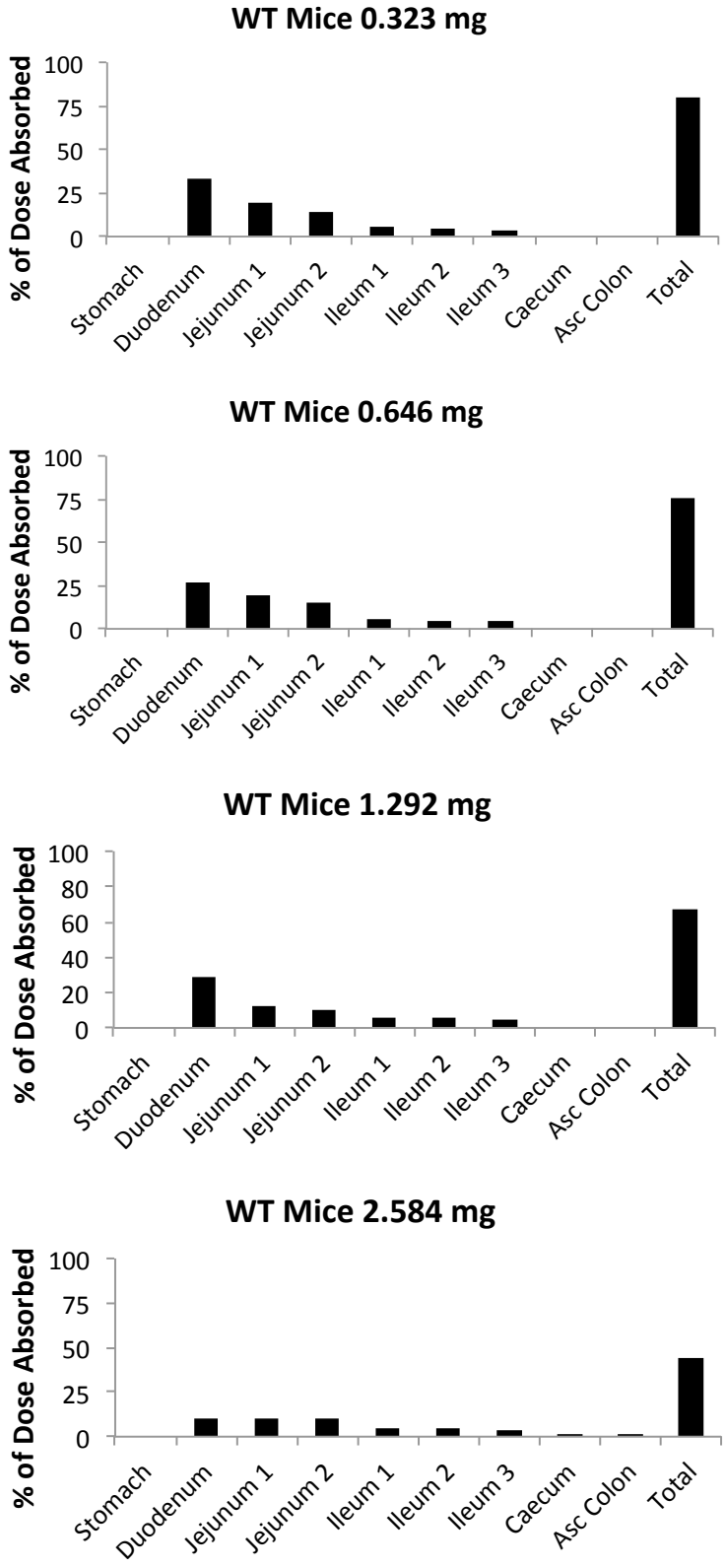

Figure 5.8. Percent of cefadroxil dose absorbed in different segments of the gastrointestinal tract in wild-type mice.

Tables

NAME	LOCATION	SYSTEM USED	REFERENCE
PEPT1	Small intestine Kidney (proximal tubule)	Caco-2 cells, Oocytes Oocytes, BBMV	[35-37] [37, 38]
PEPT2	Kidney (AP) CSF	KO mice, cells, BBMV cells, KO mice	[38] [28] [16] [37] [16, 28, 37, 39, 40]
OAT3	Kidney (BL)	S2 cells (transfected)	[24] [25, 26]
OAT1	Kidney (BL)	S2 cells (transfected)	[24-26]
OAT2 (rat)	Kidney (BL)	S2 cells (transfected)	[24, 25]
OAT4	Kidney (BL)	S2 cells (transfected)	[24, 25]
OATP2	Liver rat (BL)	Oocytes	[41]
MRP3/MRP4	Intestine (BL)	Oocytes	[32]

Table 5.1. Proteins involved in the transport of cefadroxil.

COMPARTMENT	SMITH PEPT1 (MICE PROTEIN)	HERRERA PEPT1 (HUMAN RNA) [33, 34]	ENGLUND PEPT1 (HUMAN RNA) [33, 42]
Duodenum	3.8	8.42	0.72
Jejunum 1	9.4	1.48	0.92
Jejunum 2	9.4	1.48	0.92
Ileum 1	3.58	1.00	1.00
Ileum 2	3.58	1.00	1.00
Ileum 3	3.58	1.00	1.00
Ceacum	0	0	0.02
Colon	0	0	0.02

Table 5.2. PEPT1 distributions tested in our ACAT model.

PROPERTY	VALUE	REFERENCE
Intrinsic Solubility (mg/mL)	17.4	Tsuji 1983 [43]
pKa (37 °C)	Acid = 2.70 Base = 7.22 Acid = 9.62	Tsuji 1983 [43] and 1981 [44]
Degradation (%/h; rat intestine)	2.1	Tsuji 1980 [45]
Degradation $T_{1/2}$ (h) pH=4 T=37°C	5.76	Mariño 1982 [46]
Degradation $T_{1/2}$ (h) pH=7 T=37°C	8.6	Mariño 1982[46]
Intrinsic solubility (mg/mL) pH=4.96	17.5	Tsuji 1983 [43]
LogP	-2.103	Estimated by ADMET predictor
LogD (pH=4.8)	-2.11	Estimated by ADMET predictor

Table 5.3. Physicochemical properties of cefadroxil

PROPERTY	VALUE	REFERENCE
Body Weight (Kg)	0.02	Mice
In situ K_m transporter (mg/L)	1380	Perfusion Experiments
Passive Jejunal Permeability (cm/s)	$0.09*10^{-4}$	Perfusion Experiments
Fu% (mice)	80	Shen 2007 [16]
Blood to plasma ratio	0.92	Estimated by ADMET predictor

Table 5.4. Input parameters of cefadroxil for ACAT model in mice.

PARAMETER	FITTED VALUE	OPTIMIZED VALUE	FITTED/OPTIMIZED
Clearance (L/h)	0.018	0.018	1
Vc (L)	0.2	0.09	2.2
K_{12} (h^{-1})	2.841	3.2207	0.88
K_{21}(h^{-1})	3.954	4.9757	0.79

Table 5.5. Pharmacokinetic parameters of cefadroxil in wild-type and PEPT1 knockout mice after intravenous administration.

DOSE (mg)	AUC_{0-120} (µg *h/mL)			C_{max} (µg/mL)			R^2
	Observed	Predicted	Obs/pred	Observed	Predicted	Obs/pred	
0.323	1.0611	1.0369	1.023	0.6211	0.6456	0.962	0.929
0.646	1.69	2.0739	0.815	0.979	1.2	0.816	0.788
1.292	3.8917	4.1478	0.938	2.5097	2.5824	0.972	0.609
2.584	9.0541	8.2955	1.091	5.4159	5.1648	1.049	0.750

Table 5.6. Simulation results in PEPT1 knockout mice.

DOSE (mg)	AUC_{0-120} (µg *h/mL)			C_{max} (µg/mL)			R^2
	Observed	Predicted	Obs/pred	Observed	Predicted	Obs/pred	
0.323	12.332	13.376	0.922	12.014	14.562	0.825	0.823
0.646	19.91	25.966	0.767	24.144	25.585	0.944	0.793
1.292	36.529	34.03	1.073	42.978	27.789	1.547	0.439
2.584	88.336	54.045	1.634	99.753	40.618	2.456	0.378

Table 5.7. Simulation results in wild-type mice.

DOSE	% OF TOTAL DOSE ABSORBED IN INTESTINES BY DIFFERENT PATHWAYS IN WILD-TYPE MICE		
	PASSIVE	PEPT1	PARACELLULAR
0.323	2.3	97.2	0.5
0.646	8.0	91.3	0.8
1.292	16.9	81.6	1.6
2.584	22.8	75.2	2.1

Table 5.8. Contribution of different pathways toward the absorption of cefadroxil in wild-type mice. Percent is based on total dose absorbed of cefadroxil.

DOSE	% OF TOTAL DOSE ABSORBED IN INTESTINES BY DIFFERENT PATHWAYS IN PEPT1 KNOCKOUT MICE		
	PASSIVE	PEPT1	PARACELLULAR
0.323	91.2	0.00	8.8
0.646	91.2	0.00	8.8
1.292	91.2	0.00	8.8
2.584	91.2	0.00	8.8

Table 5.9. Contribution of different pathways toward the absorption of cefadroxil in PEPT1 knockout mice. Percent is based on total dose absorbed of cefadroxil.

DOSE			SMALL INTESTINAL CONCENTRATION (mM)
#	(mg)	(nmol/g)	
1	0.323	44.5	1.62 – 2.23
2	0.646	89.1	3.24 – 4.41
3	1.292	178	6.48 – 8.91
4	2.584	356	12.96 – 17.82

Table 5.10. Estimated concentrations of cefadroxil in the small intestine of mice. (Assumed small intestinal volumes are between 0.4 and 0.6 mL and mouse body weight = 0.02 kg).

DOSE	DOSE (mg)	STOMACH CONCENTRATION (mM)
1	125	1.38
2	250	2.75
3	500	5.51
4	1000	11.02

Table 5.11. Estimated concentrations of cefadroxil in the stomach of humans (Assumed stomach volume of 250 mL).

$AUC_{0\text{-}120}$ (hr • µg/mL)				R^2
Dose (mg)	**Observed**	**Predicted**	**Observed/Predicted**	
0.323	12.33	12.32	1.00	0.779
0.646	19.91	24.35	0.82	0.904
1.292	36.53	47.65	0.77	0.857
2.584	88.34	91.5	0.97	0.913
Cmax (µg/mL)				R^2
Dose (mg)	**Observed**	**Predicted**	**Observed/Predicted**	
0.323	12.01	13.48	0.89	0.779
0.646	24.14	26.24	0.92	0.904
1.292	42.98	49.93	0.86	0.857
2.584	99.75	91.7	1.09	0.913
Tmax (hr)				R^2
Dose (mg)	**Observed**	**Predicted**	**Observed/Predicted**	
0.323	0.33	0.29	1.15	0.779
0.646	0.25	0.3	0.83	0.904
1.292	0.33	0.32	1.04	0.857
2.584	0.33	0.35	0.95	0.913

Table 5.12. Results of ACAT simulation in wild-type mice using a Km value of 35 mM.

References

1. Stone, J.A., et al., *Model-based drug development survey finds pharmacometrics impacting decision making in the pharmaceutical industry.* J Clin Pharmacol, 2010. **50**(9 Suppl): p. 20S-30S.
2. Wetherington, J.D., et al., *Model-based drug development: strengths, weaknesses, opportunities, and threats for broad application of pharmacometrics in drug development.* J Clin Pharmacol, 2010. **50**(9 Suppl): p. 31S-46S.
3. Agoram, B., W.S. Woltosz, and M.B. Bolger, *Predicting the impact of physiological and biochemical processes on oral drug bioavailability.* Adv Drug Deliv Rev, 2001. **50 Suppl 1**: p. S41-67.
4. Huang, W., S.L. Lee, and L.X. Yu, *Mechanistic approaches to predicting oral drug absorption.* AAPS J, 2009. **11**(2): p. 217-24.
5. Yu, L.X., et al., *Transport approaches to the biopharmaceutical design of oral drug delivery systems: prediction of intestinal absorption.* Adv Drug Deliv Rev, 1996. **19**(3): p. 359-76.
6. Yu, L.X. and G.L. Amidon, *Saturable small intestinal drug absorption in humans: modeling and interpretation of cefatrizine data.* Eur J Pharm Biopharm, 1998. **45**(2): p. 199-203.
7. Yu, L.X. and G.L. Amidon, *A compartmental absorption and transit model for estimating oral drug absorption.* Int J Pharm, 1999. **186**(2): p. 119-25.
8. Polak, S., et al., *Prediction of the in Vivo Behaviour of Modified Release Formulations of Metoprolol from in Vitro Dissolution Profiles Using the Adam Model (Simcyp V8).* Drug Metabolism Reviews, 2008. **40**: p. 45-46.
9. Darwich, A.S., et al., *Interplay of metabolism and transport in determining oral drug absorption and gut wall metabolism: a simulation assessment using the "Advanced Dissolution, Absorption, Metabolism (ADAM)" model.* Curr Drug Metab, 2010. **11**(9): p. 716-29.
10. Grass, G.M., *Simulation models to predict oral drug absorption from in vitro data.* Advanced Drug Delivery Reviews, 1997. **23**(1-3): p. 199-219.
11. Norris, D.A., et al., *Development of predictive pharmacokinetic simulation models for drug discovery.* Journal of Controlled Release, 2000. **65**(1-2): p. 55-62.
12. Kimura, T. and K. Higaki, *Gastrointestinal transit and drug absorption.* Biological & Pharmaceutical Bulletin, 2002. **25**(2): p. 149-164.
13. Hironaka, T., et al., *Evaluation of Substantial Contribution of PEPT1-Mediated Transport to Oral Absorption of Cephalexin Based on Gastrointestinal Transit Kinetics.* Drug Metabolism Reviews, 2007. **39**: p. 165-166.
14. Yokoe, J., et al., *Analysis and prediction of absorption behavior of colon-targeted prodrug in rats by GI-transit-absorption model.* Journal of Controlled Release, 2003. **86**(2-3): p. 305-313.

15. Kimura, T., et al., *Analysis and prediction of absorption profile including hepatic first-pass metabolism of N-methyltyramine,a potent stimulant of gastrin release present in beer, after oral ingestion in rats by gastrointestinal-transit-absorption model.* Drug Metabolism and Disposition, 2000. **28**(5): p. 577-581.
16. Shen, H., et al., *Impact of genetic knockout of PEPT2 on cefadroxil pharmacokinetics, renal tubular reabsorption, and brain penetration in mice.* Drug Metab Dispos, 2007. **35**(7): p. 1209-16.
17. Jappar, D., et al., *Significance and regional dependency of peptide transporter (PEPT) 1 in the intestinal permeability of glycylsarcosine: in situ single-pass perfusion studies in wild-type and PEPT1 knockout mice.* Drug Metab Dispos, 2010. **38**(10): p. 1740-6.
18. Hu, Y., et al., *Targeted disruption of peptide transporter PEPT1 gene in mice significantly reduces dipeptide absorption in intestine.* Mol Pharm, 2008. **5**(6): p. 1122-30.
19. Abuasal, B.S., et al., *In silico modeling for the nonlinear absorption kinetics of UK-343,664: a P-gp and CYP3A4 substrate.* Mol Pharm, 2012. **9**(3): p. 492-504.
20. Jappar, D., Y. Hu, and D.E. Smith, *Effect of dose escalation on the in vivo oral absorption and disposition of glycylsarcosine in wild-type and PEPT1 knockout mice.* Drug Metab Dispos, 2011. **39**(12): p. 2250-7.
21. Sinko, P.J. and G.L. Amidon, *Characterization of the oral absorption of beta-lactam antibiotics. I. Cephalosporins: determination of intrinsic membrane absorption parameters in the rat intestine in situ.* Pharm Res, 1988. **5**(10): p. 645-50.
22. Sinko, P.J. and G.L. Amidon, *Characterization of the oral absorption of beta-lactam antibiotics. II. Competitive absorption and peptide carrier specificity.* J Pharm Sci, 1989. **78**(9): p. 723-7.
23. Wenzel, U., et al., *Endogenous expression of the renal high-affinity H+-peptide cotransporter in LLC-PK1 cells.* Am J Physiol, 1998. **275**(6 Pt 1): p. C1573-9.
24. Takeda, M., et al., *Interaction of human organic anion transporters with various cephalosporin antibiotics.* Eur J Pharmacol, 2002. **438**(3): p. 137-42.
25. Khamdang, S., et al., *Interaction of human and rat organic anion transporter 2 with various cephalosporin antibiotics.* Eur J Pharmacol, 2003. **465**(1-2): p. 1-7.
26. Ueo, H., et al., *Human organic anion transporter hOAT3 is a potent transporter of cephalosporin antibiotics, in comparison with hOAT1.* Biochem Pharmacol, 2005. **70**(7): p. 1104-13.
27. Granero, L., et al., *Studies on the renal excretion mechanisms of cefadroxil.* Drug Metab Dispos, 1994. **22**(3): p. 447-50.
28. Shen, H., et al., *Localization of PEPT1 and PEPT2 proton-coupled oligopeptide transporter mRNA and protein in rat kidney.* Am J Physiol, 1999. **276**(5 Pt 2): p. F658-65.
29. Shen, H., D.E. Smith, and F.C. Brosius, 3rd, *Developmental expression of PEPT1 and PEPT2 in rat small intestine, colon, and kidney.* Pediatr Res, 2001. **49**(6): p. 789-95.

30. Jones, H.M., et al., *Simulation of human intravenous and oral pharmacokinetics of 21 diverse compounds using physiologically based pharmacokinetic modelling.* Clin Pharmacokinet, 2011. **50**(5): p. 331-47.
31. Watson, K.J., J. Davis, and H.M. Jones, *Application of physiologically based pharmacokinetic modeling to understanding the clinical pharmacokinetics of UK-369,003.* Drug Metab Dispos, 2011. **39**(7): p. 1203-13.
32. de Waart, D.R., et al., *Oral availability of cefadroxil depends on ABCC3 and ABCC4.* Drug Metab Dispos, 2012. **40**(3): p. 515-21.
33. Bolger, M.B., V. Lukacova, and W.S. Woltosz, *Simulations of the nonlinear dose dependence for substrates of influx and efflux transporters in the human intestine.* AAPS J, 2009. **11**(2): p. 353-63.
34. Herrera-Ruiz, D., et al., *Spatial expression patterns of peptide transporters in the human and rat gastrointestinal tracts, Caco-2 in vitro cell culture model, and multiple human tissues.* AAPS PharmSci, 2001. **3**(1): p. E9.
35. Naruhashi, K., et al., *PEPT1 mRNA expression is induced by starvation and its level correlates with absorptive transport of cefadroxil longitudinally in the rat intestine.* Pharm Res, 2002. **19**(10): p. 1417-23.
36. Wenzel, U., et al., *Transport characteristics of differently charged cephalosporin antibiotics in oocytes expressing the cloned intestinal peptide transporter PEPT1 and in human intestinal Caco-2 cells.* J Pharmacol Exp Ther, 1996. **277**(2): p. 831-9.
37. Ganapathy, M.E., et al., *Differential recognition of beta -lactam antibiotics by intestinal and renal peptide transporters, PEPT 1 and PEPT 2.* J Biol Chem, 1995. **270**(43): p. 25672-7.
38. Ries, M., U. Wenzel, and H. Daniel, *Transport of cefadroxil in rat kidney brush-border membranes is mediated by two electrogenic H+-coupled systems.* J Pharmacol Exp Ther, 1994. **271**(3): p. 1327-33.
39. Ocheltree, S.M., et al., *Mechanisms of cefadroxil uptake in the choroid plexus: studies in wild-type and PEPT2 knockout mice.* J Pharmacol Exp Ther, 2004. **308**(2): p. 462-7.
40. Shen, H., et al., *PEPT2 (Slc15a2)-mediated unidirectional transport of cefadroxil from cerebrospinal fluid into choroid plexus.* J Pharmacol Exp Ther, 2005. **315**(3): p. 1101-8.
41. Nakakariya, M., et al., *Predominant contribution of rat organic anion transporting polypeptide-2 (Oatp2) to hepatic uptake of beta-lactam antibiotics.* Pharm Res, 2008. **25**(3): p. 578-85.
42. Englund, G., et al., *Regional levels of drug transporters along the human intestinal tract: co-expression of ABC and SLC transporters and comparison with Caco-2 cells.* Eur J Pharm Sci, 2006. **29**(3-4): p. 269-77.
43. Tsuji, A., et al., *Physicochemical Properties of Amphoteric Beta-Lactam Antibiotics .3. Stability, Solubility, and Dissolution Behavior of Cefatrizine and Cefadroxil as a Function of Ph.* Chemical & Pharmaceutical Bulletin, 1983. **31**(11): p. 4057-4069.
44. Tsuji, A., et al., *Degradation kinetics and mechanism of aminocephalosporins in aqueous solution: cefadroxil.* J Pharm Sci, 1981. **70**(10): p. 1120-8.

45. Tsuji, A., et al., *Intestinal-Absorption Mechanism of Amphoteric Beta-Lactam Antibiotics .1. Comparative Absorption and Evidence for Saturable Transport of Amino-Beta-Lactam Antibiotics by In situ Rat Small-Intestine.* Journal of Pharmaceutical Sciences, 1981. **70**(7): p. 768-772.
46. Marino, E.L. and A. Dominguezgil, *Study of Accelerated Inactivation of Cefadroxil.* International Journal of Pharmaceutics, 1982. **12**(2-3): p. 209-217.
47. Johnson, D. A. and Amidon, G. L. *Determination of intrinsic membrane transport parameters from perfused intestine experiments: a boundary layer approach to estimating the aqueous and unbiased membrane permeabilities.* J Theor Biol, 1988. 131:p. 93-106.